



QA: QA

MDL-WIS-PA-000005 REV00

January 2008

Total System Performance Assessment Model/Analysis for the License Application

Volume I

Prepared for:
U.S. Department of Energy
Office of Civilian Radioactive Waste Management
Office of Repository Development
1551 Hillshire Drive
Las Vegas, Nevada 89134-6321

Prepared by:
Sandia National Laboratories
OCRWM Lead Laboratory for Repository Systems
1180 Town Center Drive
Las Vegas, Nevada 89144

Under Contract Number
DE-AC04-94AL85000

DISCLAIMER

This report was prepared as an account of work sponsored by an agency of the United States Government. Neither the United States Government nor any agency thereof, nor any of their employees, nor any of their contractors, subcontractors or their employees, makes any warranty, express or implied, or assumes any legal liability or responsibility for the accuracy, completeness, or any third party's use or the results of such use of any information, apparatus, product, or process disclosed, or represents that its use would not infringe privately owned rights. Reference herein to any specific commercial product, process, or service by trade name, trademark, manufacturer, or otherwise, does not necessarily constitute or imply its endorsement, recommendation, or favoring by the United States Government or any agency thereof or its contractors or subcontractors. The views and opinions of authors expressed herein do not necessarily state or reflect those of the United States Government or any agency thereof.

**Total System Performance Assessment
Model/Analysis for the License Application**

Volume I

MDL-WIS-PA-000005 REV00

January 2008

INTENTIONALLY LEFT BLANK

ACKNOWLEDGEMENTS

This work was performed in an environment that required close coordination, cooperation, communication, and teamwork. The effort cuts across organizational boundaries, discipline boundaries, geographic boundaries, and cultural boundaries. The team that created and produced the TSPA-LA Model/Analysis for the License Application document consisted of analysts, authors, checkers, reviewers, graphic specialists, technical editors, word processing specialists, reference checkers, and other technical support staff.

The outcome is a direct result of the long and hard hours the team devoted to the development of this product. The dedication demonstrated by the team enabled the production of a high-quality product under very tight deadlines and, therefore, is acknowledged.

Sincere thanks go to the following contributors:

AUTHORS

R. Baca
A. Behie
K. Brooks
B. Bullard
Y. Chen
V. Chipman
T. Dale
N. Deeds
J. Groves
T. Hadgu
C. Hansen
J. Helton
W. Hintze
S. Hommel
K. P. Lee
B. Lester
M. Lord
R. MacKinnon
P. Mattie
J. McNeish
S. Mehta
D. Miller
S. Miller
J. Min
S. Mishra
B. Mukhopadhyay
M. Nutt
L. Pincock
C. Sallaberry
G. Saulnier
S. D. Sevougian
R. Senger
A. Smith
W. Statham
C. Stockman
C. Thom
K. Turnham
P. Vo.
Y. Wang
E. Zwahlen

CHECKERS

R. Zimmerman—Checker Lead
J. Devers—QCS Lead
B. Arnold
C. Beach
S. Darnell
J. Cunnane
R. Dockter
J. Duguid
M. Gross
C. Haukwa
K. Helean
J. Houseworth
G. Keating
J. Lee
J. Leem
P. Mariner
S. Mishra
B. Mitcheltree
W. Mitcheltree
D. Mohr
K. Mon
J. Pickens
B. RamaRao
B. Robinson
D. Sassani
J. Schreiber
A. Smith
R. Spencer
C. Stockman

REVIEWERS

P. Brady (EBS)
N. Brown (WP)
R. Finch (EBS)
S. Finsterle (NS)
D. Franklin (Navy)
E. Hardin (NFE)
C. Ho (NS)
C. Howard (ES)
J. Linhart (DOE-EM)
H. Loo (DOE-EM)
M. Marietta (ITR)
P. Nair (Licensing)
L. Price (FEPs)
R. Quittmeyer (Seismic)

TECHNICAL/MGMT REVIEWERS

K. Knowles
J. McNeish
S. D. Sevougian
P. Swift

SHAREPOINT/FILE MGMT

D. Miller—Document Coordinator
L. Winzer

GRAPHIC COORD/PRODUCTION

D. Miller - Lead
R. Danat
K. Loo
R. McKinley
J. Sandgren
R. Sandgren
J. Scott
D. Young

DOCUMENT PRODUCTION

D. Miller-TSPA Production Lead
C. Beglinger
P. Gibson
V. Kelly
D. Nurse
M. Shrivastava
L. Winzer

CONTENTS

	Page
ACKNOWLEDGMENTS	v
ES1. SCOPE.....	ES-1
ES1.1 Introduction.....	ES-1
ES1.2 Governing Regulations	ES-2
ES2. TOTAL SYSTEM PERFORMANCE ASSESSMENT METHODOLOGY	ES-3
ES3. TSPA-LA MODEL DEVELOPMENT PROCESS	ES-5
ES3.1 Features, Events, and Processes Analysis.....	ES-5
ES3.2 Development of the Scenario Classes.....	ES-6
ES3.3 Incorporation of Uncertainty.....	ES-7
ES3.4 Natural and Engineered Model Components.....	ES-8
ES3.5 Alternative Conceptual Models	ES-8
ES3.6 Configuration Management for the TSPA-LA Model.....	ES-9
ES4. YUCCA MOUNTAIN SITE DESCRIPTION.....	ES-10
ES4.1 Physiographic Setting and Topography.....	ES-10
ES4.2 Climate.....	ES-10
ES4.3 Geology.....	ES-11
ES4.4 Regional Tectonic Setting.....	ES-11
ES4.5 Local Volcanism	ES-11
ES4.6 Hydrology	ES-12
ES5. THE REPOSITORY SUBSURFACE FACILITY AND ENGINEERED BARRIER SYSTEM.....	ES-12
ES5.1 Layout	ES-12
ES5.2 Engineered Barrier System	ES-13
ES6. NATURAL AND ENGINEERED BARRIERS	ES-15
ES6.1 Upper Natural Barrier	ES-16
ES6.2 Engineered Barrier System	ES-17
ES6.3 Lower Natural Barrier.....	ES-20
ES7. GENERAL DESCRIPTION OF THE TSPA-LA MODEL.....	ES-22
ES7.1 Model Components for the Nominal Scenario Class Modeling Case ...	ES-22
ES7.2 Model Components for the Early Failure Scenario Class.....	ES-24
ES7.3 Model Components for the Disruptive Events Scenario Classes.....	ES-26
ES7.4 TSPA Input Database.....	ES-28
ES8. VERIFICATION/VALIDATION OF THE TOTAL SYSTEM PERFORMANCE ASSESSMENT MODEL.....	ES-29
ES8.1 Verification and Validation Strategy	ES-29
ES8.2 Computer Code and Input Verification.....	ES-30
ES8.3 Stability Testing.....	ES-31
ES8.4 Uncertainty Characterization Reviews.....	ES-32
ES8.5 Surrogate Waste Form Validation.....	ES-34
ES8.6 Corroboration of Abstraction Model Results with Validated Process Models.....	ES-34
ES8.7 Auxiliary Analyses.....	ES-35

CONTENTS (Continued)

	Page
ES8.8 Confidence Building: Natural Analogues	ES-37
ES8.9 Summary of Technical Reviews	ES-38
ES9. SYSTEM PERFORMANCE ANALYSES	ES-40
ES9.1. Total Mean Annual Dose to the Reasonably Maximally Exposed Individual for the Repository System	ES-40
ES9.2. Results of the Scenario Class Modeling Case Simulations.....	ES-40
ES9.3 Comparison of Annual Dose with Postclosure Individual and Groundwater Protection Standards	ES-45
ES9.4. Human Intrusion	ES-47
ES10. SUMMARY OF THE RESULTS OF THE TSPA-LA MODEL.....	ES-47
1. PURPOSE	1-1
1.1 INTRODUCTION.....	1-1
1.1.1 Governing Regulations	1-1
1.1.2 Total System Performance Assessment Methodology.....	1-6
1.1.3 Treatment of Uncertainty	1-8
1.2 TSPA-LA MODEL DEVELOPMENT PROCESS	1-8
1.2.1 Features, Events, and Processes Analysis.....	1-9
1.2.2 Development of the Scenario Classes	1-9
1.2.3 Incorporation of Uncertainty.....	1-10
1.2.4 Alternative Conceptual Models	1-11
1.2.5 Configuration Management for the TSPA-LA Model.....	1-11
1.3 YUCCA MOUNTAIN SITE DESCRIPTION	1-13
1.3.1 Physiographic Setting and Topography	1-13
1.3.2 Climate and Precipitation.....	1-14
1.3.3 Geology.....	1-15
1.3.4 Hydrogeology.....	1-17
1.4 DESIGN OF YUCCA MOUNTAIN REPOSITORY SUBSURFACE FACILITIES.....	1-18
1.4.1 Repository Layout.....	1-19
1.4.2 Features of the Engineered Barrier System.....	1-19
1.4.3 Waste Emplacement Approach.....	1-21
1.5 GENERAL DESCRIPTION OF THE TSPA-LA MODEL.....	1-21
1.5.1 Model Components and Modeling Case for the Nominal Scenario Class.....	1-22
1.5.2 Model Components and Modeling Cases for the Early Failure Scenario Class.....	1-24
1.5.3 Model Components and Modeling Cases for the Igneous Scenario Class	1-25
1.5.4 Model Components and Modeling Cases for the Seismic Scenario Class.....	1-27
1.5.5 Model Components for the Human Intrusion Scenario	1-28

CONTENTS (Continued)

	Page
1.6	CONCEPTUAL DESCRIPTION OF PROCESSES RELEVANT TO AN EVALUATION OF POSTCLOSURE PERFORMANCE IN THE ABSENCE OF DISRUPTIVE EVENTS 1-28
1.6.1	Water Movement in the Unsaturated Tuffs above the Repository..... 1-29
1.6.2	Water and Water Vapor Movement around the Repository Drifts 1-30
1.6.3	Water Movement and Radionuclide Transport within and through the Engineered Barrier System 1-32
1.6.4	Water Movement and Radionuclide Transport through the Unsaturated Tuffs below the Repository 1-34
1.6.5	Water Movement and Radionuclide Transport through the Saturated Zone Aquifers to the Biosphere 1-35
1.7	CONCEPTUAL DESCRIPTION OF PROCESSES RELEVANT TO AN EVALUATION OF POSTCLOSURE PERFORMANCE AFTER THE OCCURRENCE OF DISRUPTIVE EVENTS 1-36
1.7.1	Water Movement in the Unsaturated Tuffs above the Repository..... 1-36
1.7.2	Water Movement around the Repository Drifts..... 1-37
1.7.3	Water Movement and Radionuclide Transport within and through the Engineered Barrier System 1-37
1.7.4	Water Movement and Radionuclide Transport through the Unsaturated Tuffs below the Repository 1-39
1.7.5	Water Movement and Radionuclide Transport through the Saturated Zone Aquifers to the Biosphere 1-39
1.7.6	Atmospheric Transport and Redeposition of Radionuclides 1-39
1.8	CONSERVATISMS AND LIMITATIONS RELATED TO THE TSPA-LA MODEL 1-40
1.8.1	Conservatisms Incorporated in the TSPA-LA Model..... 1-40
1.8.2	Limitations of the TSPA-LA Model 1-42
1.9	DESCRIPTION OF THE TOTAL SYSTEM PERFORMANCE ASSESSMENT MODEL/ANALYSIS FOR THE LICENSE APPLICATION..... 1-48
1.10	DOCUMENT ORGANIZATION..... 1-50
1.10.1	Volume I 1-50
1.10.2	Volume II..... 1-51
1.10.3	Volume III..... 1-52
2.	QUALITY ASSURANCE..... 2-1
2.1	CONFIGURATION MANAGEMENT 2-1
2.1.1	Configuration Management of Software..... 2-2
2.1.2	Configuration Management of the Development of the TSPA-LA Model..... 2-2
2.1.3	Configuration Management for the TSPA-LA Model Input 2-6
2.2	MODEL VALIDATION..... 2-7
3.	USE OF SOFTWARE 3-1
3.1	INTRODUCTION..... 3-2

CONTENTS (Continued)

	Page
3.2 ASHPLUME_DLL_LA	3-3
3.2.1 Description of Software	3-3
3.2.2 Relationship to the TSPA-LA Model.....	3-3
3.2.3 Software Documentation.....	3-3
3.2.4 Range of Validation	3-3
3.3 CWD.....	3-4
3.3.1 Description of Software	3-4
3.3.2 Relationship to the TSPA-LA Model.....	3-4
3.3.3 Software Documentation.....	3-4
3.3.4 Range of Validation	3-4
3.4 EXDOC_LA.....	3-4
3.4.1 Description of Software	3-4
3.4.2 Relationship to the TSPA-LA Model.....	3-5
3.4.3 Software Documentation.....	3-5
3.4.4 Range of Validation	3-5
3.5 FAR.....	3-5
3.5.1 Description of Software	3-5
3.5.2 Relationship to the TSPA-LA Model.....	3-5
3.5.3 Software Documentation.....	3-6
3.5.4 Range of Validation	3-6
3.6 FEHM.....	3-6
3.6.1 Description of Software	3-6
3.6.2 Relationship to the TSPA-LA Model.....	3-6
3.6.3 Software Documentation.....	3-6
3.6.4 Range of Validation	3-7
3.7 GETTHK_LA.....	3-7
3.7.1 Description of Software	3-7
3.7.2 Relationship to the TSPA-LA Model.....	3-7
3.7.3 Software Documentation.....	3-7
3.7.4 Range of Validation	3-7
3.8 GOLDSIM.....	3-8
3.8.1 Description of Software	3-8
3.8.2 Relationship to the TSPA-LA Model.....	3-8
3.8.3 Software Documentation.....	3-8
3.8.4 Range of Validation	3-8
3.9 INTERPZDLL_LA	3-9
3.9.1 Description of Software	3-9
3.9.2 Relationship to the TSPA-LA Model.....	3-9
3.9.3 Software Documentation.....	3-9
3.9.4 Range of Validation	3-9
3.10 MFPCP_LA.....	3-10
3.10.1 Description of Software	3-10
3.10.2 Relationship to the TSPA-LA Model.....	3-10
3.10.3 Software Documentation.....	3-10

CONTENTS (Continued)

	Page
3.10.4 Range of Validation	3-10
3.11 MKTABLE AND MKTABLE_LA	3-11
3.11.1 Description of Software	3-11
3.11.2 Relationship to the TSPA-LA Model	3-11
3.11.3 Software Documentation	3-11
3.11.4 Range of Validation	3-11
3.12 MVIEW	3-12
3.12.1 Description of Software	3-12
3.12.2 Relationship to the TSPA-LA Model	3-12
3.12.3 Software Documentation	3-12
3.12.4 Range of Validation	3-12
3.13 PASSTABLE1D_LA	3-12
3.13.1 Description of Software	3-12
3.13.2 Relationship to the TSPA-LA Model	3-13
3.13.3 Software Documentation	3-13
3.13.4 Range of Validation	3-13
3.14 PASSTABLE3D_LA	3-13
3.14.1 Description of Software	3-13
3.14.2 Relationship to the TSPA-LA Model	3-13
3.14.3 Software Documentation	3-14
3.14.4 Range of Validation	3-14
3.15 PREWAP_LA	3-14
3.15.1 Description of Software	3-14
3.15.2 Relationship to the TSPA-LA Model	3-14
3.15.3 Software Documentation	3-14
3.15.4 Range of Validation	3-14
3.16 SCCD	3-15
3.16.1 Description of Software	3-15
3.16.2 Relationship to the TSPA-LA Model	3-15
3.16.3 Software Documentation	3-15
3.16.4 Range of Validation	3-15
3.17 SEEPAGEDLL_LA	3-16
3.17.1 Description of Software	3-16
3.17.2 Relationship to the TSPA-LA Model	3-16
3.17.3 Software Documentation	3-16
3.17.4 Range of Validation	3-16
3.18 SOILEXP_LA	3-17
3.18.1 Description of Software	3-17
3.18.2 Relationship to the TSPA-LA Model	3-17
3.18.3 Software Documentation	3-17
3.18.4 Range of Validation	3-17
3.19 SZ_CONVOLUTE	3-17
3.19.1 Description of Software	3-17
3.19.2 Relationship to the TSPA-LA Model	3-18

CONTENTS (Continued)

	Page
3.19.3 Software Documentation.....	3-18
3.19.4 Range of Validation	3-18
3.20 TSPA_INPUT_DB.....	3-18
3.20.1 Description of Software	3-18
3.20.2 Relationship to the TSPA-LA Model.....	3-18
3.20.3 Software Documentation.....	3-19
3.20.4 Range of Validation	3-19
3.21 WAPDEG.....	3-19
3.21.1 Description of Software	3-19
3.21.2 Relationship to the TSPA-LA Model.....	3-19
3.21.3 Software Documentation.....	3-19
3.21.4 Range of Validation	3-20
3.22 CORROBORATIVE SOFTWARE USED.....	3-20
4. INPUTS.....	4-1
4.1 DIRECT INPUTS.....	4-1
4.2 TSPA-LA MODEL GENERATED PARAMETERS.....	4-2
4.3 PARAMETER ENTRY FORMS.....	4-2
4.4 TRACEABILITY OF INPUTS.....	4-3
4.5 CRITERIA.....	4-4
4.6 CODES AND STANDARDS	4-4
4.7 TSPA INPUT DATABASE.....	4-4
4.7.1 Database Structure	4-5
4.7.2 Database Operation Login	4-5
4.7.3 Parameter Identification Form	4-5
4.7.4 Parameter Documentation Form	4-6
4.7.5 Parameter Value Entry Form	4-6
4.7.6 Parameter Entry Form Information Entry Form	4-6
4.7.7 Parameter Verification Form	4-6
4.7.8 Database Reports.....	4-7
4.7.9 Database Support of GoldSim.....	4-8
5. ASSUMPTIONS.....	5-1
5.1 NOMINAL SCENARIO CLASS.....	5-1
5.1.1 Unsaturated Zone Flow	5-1
5.1.2 Engineered Barrier System Environment	5-2
5.1.3 Waste Form Degradation and Mobilization.....	5-4
5.1.4 Engineered Barrier System Flow and Transport.....	5-4
5.1.5 Unsaturated Zone Transport.....	5-6
5.1.6 Saturated Zone Flow and Transport.....	5-6
5.1.7 Biosphere	5-7
5.2 EARLY FAILURE SCENARIO CLASS	5-7
5.2.1 Drip Shield Early Failure Modeling Case.....	5-7
5.2.2 Waste Package Early Failure Modeling Case	5-8
5.3 IGNEOUS SCENARIO CLASS.....	5-8

CONTENTS (Continued)

	Page
5.3.1	Igneous Intrusion Modeling Case 5-8
5.3.2	Volcanic Eruption Modeling Case 5-9
5.4	SEISMIC SCENARIO CLASS 5-10
5.5	HUMAN INTRUSION SCENARIO 5-11
6.	TSPA-LA MODEL DESCRIPTION 6-1
6.1	CONCEPTUAL DESIGN 6.1-1
6.1.1	Features, Events, and Processes Screening and Scenario Development 6.1.1-1
6.1.2	Calculation of Dose for the TSPA-LA Model 6.1.2-1
6.1.3	Treatment of Uncertainty in the TSPA-LA Model 6.1.3-1
6.1.4	TSPA-LA Model Structure and Design 6.1.4-1
6.1.5	TSPA-LA Model File Architecture 6.1.5-1
6.2	ALTERNATIVE CONCEPTUAL MODELS 6.2-1
6.3	TSPA-LA MODEL FOR THE NOMINAL SCENARIO CLASS 6.3-1
6.3.1	Mountain-Scale Unsaturated Zone Flow 6.3.1-1
6.3.2	Engineered Barrier System Thermal-Hydrologic Environment 6.3.2-1
6.3.3	Drift-Scale Unsaturated Zone Flow 6.3.3-1
6.3.4	Engineered Barrier System Chemical Environment 6.3.4-1
6.3.5	Waste Package and Drip Shield Degradation 6.3.5-1
6.3.6	Engineered Barrier System Flow 6.3.6-1
6.3.7	Waste Form Degradation and Mobilization 6.3.7-1
6.3.8	Engineered Barrier System Transport 6.3.8-1
6.3.9	Unsaturated Zone Transport 6.3.9-1
6.3.10	Saturated Zone Flow and Transport Model Component 6.3.10-1
6.3.11	Biosphere 6.3.11-1
6.4	TSPA-LA MODEL FOR THE EARLY FAILURE SCENARIO CLASS 6.4-1
6.4.1	Drip Shield Early Failure Modeling Case 6.4-2
6.4.2	Waste Package Early Failure Modeling Case 6.4-5
6.4.3	Treatment of Uncertainty 6.4-7
6.4.4	Model Component Consistency and Conservatisms in Assumptions and Parameters 6.4-7
6.5	TSPA-LA MODEL FOR THE IGNEOUS SCENARIO CLASS 6.5-1
6.5.1	Igneous Intrusion Modeling Case 6.5-2
6.5.2	Volcanic Eruption Modeling Case 6.5-10
6.6	TSPA-LA MODEL FOR THE SEISMIC SCENARIO CLASS 6.6-1
6.6.1	TSPA-LA Model Components and Submodels for the Seismic Scenario Class 6.6-2
6.6.2	Interaction of Seismic Scenario Class Submodels with other TSPA-LA Submodels 6.6-31
6.6.3	Model Component Consistency and Conservatisms in Assumptions and Parameters 6.6-35
6.6.4	Alternative Conceptual Model(s) for Seismic Scenario Modeling Cases 6.6-37

CONTENTS (Continued)

	Page
6.7 TSPA-LA MODEL FOR THE HUMAN INTRUSION SCENARIO.....	6.7-1
6.7.1 TSPA-LA Model Components and Submodels for the Human Intrusion Scenario	6.7-2
6.7.2 Evaluation of the Earliest Time of Waste Package Penetration by Human Intrusion	6.7-3
6.7.3 TSPA-LA Model Implementation	6.7-17
6.7.4 Model Component Consistency and Conservatism in Assumptions and Parameters	6.7-22
6.7.5 Alternative Conceptual Model(s) for the Human Intrusion Scenario for TSPA-LA.....	6.7-23

FIGURES

	Page
ES-1. Yucca Mountain Area	FES-1
ES-2. Timeline of Legislative and Regulatory Events: 1980 to 2010	FES-2
ES-3. Structure of the Process of the TSPA-LA	FES-3
ES-4. Major Steps in a Generic Performance Assessment	FES-4
ES-5. Iterative Application of the TSPA Process	FES-5
ES-6. Performance Assessment Pyramid Showing the Steps Involved in Developing a Total System Model	FES-6
ES-7. Schematic of Attributes of Repository Performance	FES-7
ES-8. Schematic Representation of the Development of the TSPA-LA Model, Including the Nominal, Igneous, and Seismic Scenario Classes	FES-8
ES-9. TSPA-LA Principal Model Components and Submodels	FES-9
ES-10. Principal Components of the Yucca Mountain Repository System	FES-10
ES-11. Geographic and Prominent Topographic Features of the Death Valley Region ...	FES-11
ES-12. Topographic Map of the Yucca Mountain Site Showing in Slope Characteristics	FES-12
ES-13. Overall Water Flow Behavior in the Unsaturated Zone, Including the Relative Flux Magnitudes of Fracture and Matrix Flow Components in the Different Hydrogeologic Units	FES-13
ES-14. Distribution of Faults in the Yucca Mountain Site Area and Adjacent Areas to the South and West	FES-14
ES-15. East-West Structure Section across Yucca Mountain Site Area	FES-15
ES-16. Location and Age of Post-Miocene (less than 5.3 million years) Volcanoes (or clusters where multiple volcanoes have indistinguishable ages) in the Yucca Mountain Region	FES-16
ES-17. Regional Map of the Saturated Zone Flow System Showing Direction of Flow and Outline of the 3-D Saturated Zone Site-Scale Flow Model Domain	FES-17
ES-18. Subsurface Facility Layout	FES-18
ES-19. Cross-Section Illustration of the EBS	FES-19
ES-20. Conceptual Drawing of Mountain-Scale Flow Processes	FES-20
ES-21. Illustration of the Four Climate Periods Used in the TSPA-LA Model and the Analogues for the Monsoon and Glacial-Transition Climates	FES-21
ES-22. Schematic Illustration (not to scale) of Thermal-Hydrologic Processes in the Vicinity of the Emplacement Drifts Due to Repository Heating	FES-22
ES-23. General EBS Design Features and Materials, Water Movement, and Drift Degradation	FES-23
ES-24. Conceptual Drawing of Unsaturated Zone Transport Processes	FES-24
ES-25. Conceptualization of Features and Processes Important to Saturated Zone Transport	FES-25
ES-26. Schematic Design of the Drip Shield and Waste Package	FES-26
ES-27. Three Waste Types Grouped into Two Representative Waste Packages: CSNF and CDSP WPs	FES-27
ES-28. Schematic of CSNF Waste Form Degradation Mechanisms at Various Scales ...	FES-28

FIGURES (Continued)

	Page
ES-29. Overview of the Biosphere Groundwater Scenario Showing Groundwater Transport of Radionuclides and Uptake by the RMEI.....	FES-29
ES-30. Schematic Diagram of the Intersection of an Igneous Dike with the Repository and Waste Packages.....	FES-30
ES-31. Schematic Representation of a Volcanic Eruption at Yucca Mountain Showing Transport of Radioactive Waste in a Tephra Plume	FES-31
ES-32. Model Validation Approach for the TSPA-LA Model.....	FES-32
ES-33. Stability of Seismic Ground Motion Modeling Case for 20,000 Years: (a) Comparison of Expected Annual Dose for Three Replicates and (b) Confidence Interval Around Mean Annual Dose.....	FES-33
ES-34. Expected Annual Dose Over 20,000 Years for Seismic Ground Motion Modeling Case Considering Additional Specified Event Times and Damage Fractions	FES-34
ES-35. Annual Dose from a Seismic Ground Motion Event at 1,000 Years with Damage Fraction 10^{-6} for Three Timestep Schemes.....	FES-35
ES-36. Comparison of Ash-Fall Thickness at Cerro Negro with ASHPLUME Simulated Results.....	FES-36
ES-37. Location of Peña Blanca Nopal I Ore Deposit in the Sierra Peña Blanca	FES-37
ES-38. Geologic Characterization of Nopal 1 Ore Body.....	FES-38
ES-39. Uranium Concentration Determined in Groundwater Samples from Wells at and near the Nopal I Ore Deposit	FES-39
ES-40. Total Expected Annual Dose for 10,000 Years after Closure	FES-40
ES-41. Total Expected Annual Dose for 1,000,000 Years after Closure	FES-41
ES-42. Contribution of Individual Radionuclides to Total Mean Annual Dose for 10,000 Years after Repository Closure.....	FES-42
ES-43. Contribution of Individual Radionuclides to Total Mean Annual Dose for 1,000,000 Years after Repository Closure.....	FES-43
ES-44. Annual Dose for the Nominal Scenario Class Modeling Case for the Post-10,000-Year Period.....	FES-44
ES-45. Mean Annual Dose Contributions from Major Radionuclides for the Nominal Scenario Class Modeling Case for the Post-10,000-Year Period	FES-45
ES-46. Expected Annual Dose for the Drip Shield Early Failure Modeling Case for (a) the First 10,000 Years after Repository Closure and (b) Post-10,000-Year Period.....	FES-46
ES-47. Mean Annual Dose Contributions from Major Radionuclides for the Drip Shield Early Failure Modeling Case for (a) the First 10,000 Years after Repository Closure and (b) Post-10,000-Year Period	FES-47
ES-48. Expected Annual Dose for the Waste Package Early Failure Modeling Case (a) the First 10,000 Years after Repository Closure and (b) Post-10,000-Year Period.....	FES-48
ES-49. Mean Annual Dose Contributions from Major Radionuclides for the Waste Package Early Failure Modeling Case for (a) the First 10,000 Years after Repository Closure and (b) Post-10,000-Year Period	FES-49

FIGURES (Continued)

	Page
ES-50. Expected Annual Dose for the Igneous Intrusion Modeling Case for (a) 10,000 Years after Repository Closure and (b) Post-10,000-Year Period.....	FES-50
ES-51. Mean Annual Dose Contributions from Major Radionuclides for the Igneous Intrusion Modeling Case for (a) the First 10,000 Years after Repository Closure and (b) Post-10,000-Year Period.....	FES-51
ES-52. Expected Annual Dose for the Volcanic Eruption Modeling Case for (a) 10,000 Years after Repository Closure and (b) Post-10,000-Year Period.....	FES-52
ES-53. Mean Annual Dose Contributions from Major Radionuclides for the Volcanic Eruption Modeling Case for (a) the First 10,000 Years after Repository Closure and (b) Post-10,000-Year Period	FES-53
ES-54. Expected Annual Dose for the Seismic Ground Motion Modeling Case for (a) 10,000 Years after Repository Closure and (b) Post-10,000-Year Period	FES-54
ES-55. Mean Annual Dose Contributions from Major Radionuclides for the Seismic Ground Motion Modeling Case for (a) the First 10,000 Years after Repository Closure and (b) Post-10,000-Year Period.....	FES-55
ES-56. Expected Annual Dose for the Seismic Fault Displacement Modeling Case for (a) 10,000 Years after Repository Closure and (b) Post-10,000-Year Period	FES-56
ES-57. Mean Annual Dose Contributions from Major Radionuclides for the Seismic Fault Displacement Modeling Case for (a) 10,000 Years after Repository Closure and (b) Post-10,000-Year Period.....	FES-57
ES-58. Total Mean Annual Dose and Median Annual Doses for Each Modeling Case for (a) 10,000 Years after Repository Closure and (b) Post-10,000-Year Period..	FES-58
ES-59. Combined ²²⁶ Ra and ²²⁸ Ra Activity Concentrations, Excluding Natural Background, for Likely Features, Events, and Processes Using Nominal, Early Failure, and Seismic Ground Motion Damage Processes.....	FES-59
ES-60. Combined Activity Concentrations of All Alpha Emitters (including ²²⁶ Ra but without radon and uranium isotopes), Excluding Natural Background, for Likely Features, Events, and Processes Using Nominal, Early Failure, and Seismic Ground Motion Damage Processes.....	FES-60
ES-61. Mean Annual Drinking Water Dose from Combined Beta and Photon Emitters for Likely Features, Events, and Processes using the Nominal, Early Failure, and Seismic Ground Motion Damage Processes	FES-61
ES-62. Expected Annual Individual Dose at the RMEI Location from Human Intrusion 200,000 Years after Repository Closure.....	FES-62
1-1. Performance Assessment Pyramid Showing the Steps Involved in Developing a Total System Model	F1-1
1-2. Performance Assessment Pyramid Showing How Detailed Underlying Information Builds the Technical Basis for the TSPA-LA Model	F1-2
1-3. Schematic Representation of the Development of the TSPA-LA Model, Including the Nominal, Igneous, and Seismic Scenario Classes	F1-3
1-4. Geographic and Prominent Topographic Features of the Death Valley Region	F1-4

FIGURES (Continued)

	Page
1-5. Topographic Map of the Yucca Mountain Site Showing Differences in Slope Characteristics North and South of Drill Hole Wash.....	F1-5
1-6. Overall Water Flow Behavior in the Unsaturated Zone, Including the Relative Flux Magnitudes of Fracture and Matrix Flow Components in the Different Hydrogeologic Units	F1-6
1-7. Distribution of Faults in the Yucca Mountain Site Area and Adjacent Areas to the South and West	F1-7
1-8. East-West Structure Section across Yucca Mountain Site Area.....	F1-8
1-9. Location and Age of Post-Miocene (less than 5.3 million years) Volcanoes (or clusters where multiple volcanoes have indistinguishable ages) in the Yucca Mountain Region	F1-9
1-10. Subsurface Facility Layout	F1-10
1-11. Cross Section Illustration of the Engineered Barrier System	F1-11
1-12. Conceptual Drawing of Mountain-Scale Flow Processes.....	F1-12
1-13. Illustration of the Four Climate Periods Used in the TSPA-LA Model and Analogues for the Monsoon and Glacial-Transition Climates	F1-13
1-14. Schematic Design of the Drip Shield and Waste Package.....	F1-14
1-15. Three Waste Types Grouped into Two Representative Waste Packages: CSNF and CDSP WPs	F1-15
1-16. Schematic of CSNF Waste Form Degradation Mechanisms at Various Scales	F1-16
1-17. General EBS Design Features and Materials, Water Movement, and Drift Degradation.....	F1-17
1-18. Conceptualization of Unsaturated Zone Transport Processes	F1-18
1-19. Overview of the Biosphere Groundwater Scenario Showing Groundwater Transport of Radionuclides and Uptake by the RMEI.....	F1-19
1-20. Schematic Illustration of the Processes Affecting Ambient Drift Seepage	F1-20
1-21. Schematic Illustration (not to scale) of Thermal-Hydrologic Processes in the Vicinity of the Emplacement Drifts Due to Repository Heating.....	F1-21
1-22. Conceptualization of Features and Processes Important to Saturated Zone Transport.....	F1-22
1-23. TSPA-LA Principal Model Components and Submodels	F1-23
2-1. Flowchart Illustrating the Management Control Process for the TSPA-LA Model	F2-1
2-2. Example of the TSPA-LA Model Change Approval Form	F2-2
2-3. Example of the TSPA-LA Model Change Checklist.....	F2-3
2-4. Example of the TSPA-LA Model Implementation Checklist.....	F2-4
2-5. Example of the TSPA-LA Model Concept Checklist.....	F2-7
3-1. Hardware Configuration for TSPA-LA Modeling.....	F3-1
3-2. TSPA-LA Software Architecture.....	F3-2
4-1. Control of Information for TSPA-LA Model Development and Analysis	F4-1
4-2. Development and Revision of Parameter Entry Forms	F4-2

FIGURES (Continued)

	Page
4-3. Structural Framework (Schema) for the TSPA Input Database Showing Relationships between Tables.....	F4-3
4-4. Example of a Parameter Identification Form for the TSPA Input Database	F4-4
4-5. Example of a Parameter Documentation Form for the TSPA Input Database	F4-5
4-6. Example of a Parameter Value Entry Form for a One-Dimensional Data Table in the TSPA Input Database.....	F4-6
4-7. Example of a PEF Information Entry Form in the TSPA Input Database.....	F4-7
4-8. Example of a Parameter Verification Form for the TSPA Input Database.....	F4-8
6-1. TSPA-LA Principal Model Components and Submodels	F6-1
6.1.1-1. Steps in the Features, Events, and Processes Analysis and Scenario Selection Process	F6.1.1-1
6.1.1-2. Schematic Illustration of the Features, Events, and Processes Analysis Method.....	F6.1.1-2
6.1.1-3. Schematic Representation of the TSPA-LA Model Components for the Nominal Scenario Class.....	F6.1.1-3
6.1.1-4. Schematic Representation of the TSPA-LA Model Components for the Early Failure Scenario Class.....	F6.1.1-4
6.1.1-5. Schematic Representation of the TSPA-LA Model Components for the Igneous Intrusion Modeling Case.....	F6.1.1-5
6.1.1-6. Schematic Representation of the TSPA-LA Model Components for the Volcanic Eruption Modeling Case.....	F6.1.1-6
6.1.1-7. Schematic Representation of the TSPA-LA Model Components for the Seismic Scenario Class	F6.1.1-7
6.1.1-8. Schematic Representation of the TSPA-LA Model Components for the Human Intrusion Scenario	F6.1.1-8
6.1.4-1. Information Transfer Between the Model Components and Submodels of the TSPA-LA Nominal Scenario Class	F6.1.4-1
6.1.4-2. Repository Percolation Subregions Used in the TSPA-LA Model (based upon the 10th percentile percolation flux case, glacial-transition climate)	F6.1.4-2
6.1.4-3. Information Transfer Between the Model Components and Submodels of the TSPA-LA Early Failure Scenario Class	F6.1.4-3
6.1.4-4. Information Transfer Between the Model Components and Submodels of the TSPA-LA Igneous Intrusion Modeling Case.....	F6.1.4-4
6.1.4-5. Information Transfer Between the Submodels of the TSPA-LA Volcanic Eruption Modeling Case	F6.1.4-5
6.1.4-6. Information Transfer Between the Model Components and Submodels of the TSPA-LA Seismic Scenario Class.....	F6.1.4-6
6.1.4-7. Information Transfer Between the Model Components and Submodels of the TSPA-LA Human Intrusion Scenario.....	F6.1.4-7

FIGURES (Continued)

	Page
6.1.5-1. Illustrated Overview of all the Various Elements that Make Up the Framework for Initializing and Running the TSPA-LA Model.....	F6.1.5-1
6.1.5-2. Illustration Depicting Elements Required for Loading of Initial Parameter Values and Dynamically Linked Libraries for the TSPA-LA Model.....	F6.1.5-2
6.1.5-3. Illustration Depicting Elements Active When Information from the Multiscale Thermohydrologic Model is Preprocessed by PREWAP_LA	F6.1.5-3
6.1.5-4. Illustration Depicting Elements Active When Preprocessing for the Localized Corrosion Initiation Analysis	F6.1.5-4
6.1.5-5. Illustration Depicting Elements Active when Sampling of Uncertain Unsaturated Zone Parameters and Generation of Input Files	F6.1.5-5
6.1.5-6. Illustration Depicting Elements Active in the Execution of the TSPA-LA GoldSim Model File and the TSPA-LA Volcanic Eruption GoldSim Model File.....	F6.1.5-6
6.1.5-7. TSPA-LA Software Configuration Illustrating Software Run with GoldSim ...	F6.1.5-7
6.1.5-8. Details of the Software Configuration for the Localized Corrosion Initiation Analysis.....	F6.1.5-8
6.1.5-9. Layout of Calculation Containers that Define the Highest Level of Organization of the TSPA-LA Model File	F6.1.5-9
6.1.5-10. Levels of Discretization of Engineered System Representation in the TSPA-LA Model File	F6.1.5-10
6.1.5-11. Schematic of the Five Repository Percolation Subregions Showing the Implementation of the Levels of Discretization Shown on Figure 6.1.5-10....	F6.1.5-11
6.3.1-1. Information Flow Diagram for the Mountain-Scale Unsaturated Zone Flow ...	F6.3.1-1
6.3.1-2. Inputs, Outputs, and Basis for Model Confidence for the Climate Analysis.....	F6.3.1-2
6.3.1-3. Illustration of the First Three Climate States Used in the TSPA-LA Model and the Analogues for the Monsoon and Glacial-Transition Climates.....	F6.3.1-3
6.3.1-4. Inputs, Outputs, and Basis for Model Confidence for the Infiltration Model....	F6.3.1-4
6.3.1-5. Schematic Illustration Showing the Variation of Precipitation and Consequent Infiltration with Respect to Elevation at Yucca Mountain	F6.3.1-5
6.3.1-6. Inputs, Outputs, and Basis for Model Confidence for the Site-Scale Unsaturated Zone Flow Process Model	F6.3.1-6
6.3.1-7. Comparison of Net Infiltration, Percolation Flux at the Repository Horizon, and Percolation Flux at the Water Table in the Tenth Percentile Infiltration Scenario During the Glacial-Transition Climate State	F6.3.1-7
6.3.1-8. General Stratigraphy at the Yucca Mountain Site Observed at Borehole SD-6	F6.3.1-8
6.3.2-1. Information Flow Diagram for the EBS Thermal-Hydrologic Environment Submodel	F6.3.2-1
6.3.2-2. Inputs, Outputs, and Basis for Model Confidence for the Multiscale Thermohydrologic Process Model.....	F6.3.2-2
6.3.2-3. Inputs, Outputs, and Basis for Model Confidence for the EBS Thermal-Hydrologic Environment Submodel	F6.3.2-3

FIGURES (Continued)

	Page
6.3.2-4. The Distribution of the Four Primary Host-Rock Units is Shown for the Repository Layout Considered in the Multiscale Thermohydrologic Model Calculations for the TSPA-LA Model	F6.3.2-4
6.3.2-5. Thermal-Hydrologic Conditions for the PWR1-2 Waste Package Plotted for 10th, 30th, 50th and 90th Percentile Percolation-Flux Cases at a Location near the Center of the Repository	F6.3.2-5
6.3.2-6. Thermal-Hydrologic Conditions for the PWR1-2 Waste Packages Plotted for 10th Percentile Percolation Flux Case at a Location Near the Center of the Repository	F6.3.2-6
6.3.2-7. Repository Percolation Subregions Used in the TSPA-LA Model (based upon the 30th percentile infiltration case, glacial-transition period)	F6.3.2-7
6.3.2-8. Thermal-Hydrologic Time History Parameter Inputs to the TSPA-LA Model.....	F6.3.2-8
6.3.3-1. Information Flow Diagram for the Drift Seepage and Drift Wall Condensation Submodels.....	F6.3.3-1
6.3.3-2. Inputs, Outputs, and Basis for Model Confidence for the Drift Seepage Submodel.....	F6.3.3-2
6.3.3-3. Schematic Illustration (not to scale) of Thermal-Hydrologic Processes in the Vicinity of the Emplacement Drifts Due to Repository Heating.....	F6.3.3-3
6.3.3-4. Schematic Illustration of the Processes Affecting Ambient Drift Seepage	F6.3.3-4
6.3.3-5. Procedure for Probabilistic Calculation of Seepage at Selected Timesteps in the TSPA-LA Model.....	F6.3.3-5
6.3.3-6. Inputs, Outputs, and Basis for Model Confidence for the Drift Wall Condensation Submodel	F6.3.3-6
6.3.3-7. Schematic Illustration of the Processes Affecting Drift-Wall Condensation	F6.3.3-7
6.3.3-8. Schematic Depicting Approximate Locations of Disposal Drifts Chosen for Condensation Analysis.....	F6.3.3-8
6.3.4-1. Information Flow Diagram for the EBS Chemical Environment Submodel	F6.3.4-1
6.3.4-2. Inputs, Outputs, and Basis for Model Confidence for the EBS Chemical Environment Submodel	F6.3.4-2
6.3.4-3. General EBS Design Features and Materials, Water Movement, and Drift Degradation.....	F6.3.4-3
6.3.4-4. Schematic Diagram of EBS Flow Pathways (arrows) and Critical Locations (labels).....	F6.3.4-4
6.3.5-1. Schematic Design of the Drip Shield and Waste Package.....	F6.3.5-1
6.3.5-2. Information Flow Diagram for Waste Package and Drip Shield Degradation ..	F6.3.5-2
6.3.5-3. Inputs, Outputs, and Basis for Model Confidence for the Waste Package and Drip Shield Degradation Submodel	F6.3.5-3
6.3.5-4. Schematic of Waste Package Implementation in the Waste Package Degradation Model Showing a Waste Package in a Dripping Environment	

FIGURES (Continued)

	Page
6.3.5-5.	After a Drip Shield Failure and Patches Degrading from General Corrosion on the Surface of the Waste Package..... F6.3.5-4
6.3.5-5.	Exposure Conditions and Degradation Processes for the Drip Shield and Waste Package F6.3.5-5
6.3.5-6.	Effect of Scaling the General Corrosion Distribution by a Size Factor of Four..... F6.3.5-6
6.3.5-7.	Schematic of Waste Package Closure Lid Design..... F6.3.5-7
6.3.5-8.	Process and Data Flow for the Waste Package and Drip Shield Degradation Model Component F6.3.5-8
6.3.5-9.	Integration of Submodels for Localized Corrosion Initiation Analysis..... F6.3.5-9
6.3.5-10.	Computational Organization of Localized Corrosion Initiation Analysis for Crown Seepage F6.3.5-10
6.3.6-1.	Information Flow Diagram for the EBS Flow Submodel..... F6.3.6-1
6.3.6-2.	Inputs, Outputs, and Basis for Model Confidence for the EBS Flow Submodel F6.3.6-2
6.3.6-3.	Cross Section of Typical Emplacement Drift..... F6.3.6-3
6.3.6-4.	Schematic Diagram of Water Flow Pathways in the EBS..... F6.3.6-4
6.3.7-1.	Information Flow Diagram for Waste Form Degradation and Mobilization..... F6.3.7-1
6.3.7-2.	Inputs, Outputs, and Basis for Model Confidence for Waste Form Degradation and Mobilization F6.3.7-2
6.3.7-3.	Three Waste Types Grouped into Two Representative Waste Packages: CSNF and CDSP WPs F6.3.7-3
6.3.7-4.	Decay Chains of the Actinide Elements F6.3.7-4
6.3.7-5.	Implementation of the In-Package Chemistry Submodel F6.3.7-5
6.3.7-6.	Schematic of CSNF Fuel Waste Form Degradation Mechanisms at Various Scales..... F6.3.7-6
6.3.7-7.	Implementation of the DSNF Degradation Submodel..... F6.3.7-7
6.3.7-8.	Connections between the Dissolved Concentrations Limits Submodel and Other TSPA-LA Submodels F6.3.7-8
6.3.7-9.	Illustration of Type I and Type II Out-of-Bound Conditions Using the Plutonium Solubility Model as an Example F6.3.7-9
6.3.7-10.	Comparison of the Solubility-Limited Dissolved Concentration Model for Plutonium F6.3.7-10
6.3.7-11.	Schematic Representation of Colloid Suspension Stability as a Function of pH and Ionic Strength for (a) Groundwater and Glass Degradation Colloids (montmorillonite), (b) CSNF Residue Colloids (ZrO ₂), (c) Uranium Mineral Colloids (meta-autunite), and (d) Steel Degradation Colloids (hematite)..... F6.3.7-11
6.3.7-12.	Logic Diagram for Computing the Concentration and Stability of All Colloids in the Waste Package..... F6.3.7-12
6.3.8-1.	Information Flow Diagram for the EBS Transport Submodel..... F6.3.8-1

FIGURES (Continued)

	Page
6.3.8-2. Inputs, Outputs, and Basis for Model Confidence for the EBS Transport Submodel.....	F6.3.8-2
6.3.8-3. Cross Section of Idealized Drift Showing EBS Transport Submodel Domains for a CSNF Waste Package	F6.3.8-3
6.3.8-4. Schematic Representation of CSNF Waste Package Showing its Relationship to the Cell Pathway Network Used to Implement the EBS Transport Submodel.....	F6.3.8-4
6.3.8-5. Setup of a Cell Pathways for a CSNF Waste Package Used in the EBS Transport Submodel.....	F6.3.8-5
6.3.8-6. Setup of Cell Pathways for a CDSP Waste Package Used in the EBS Transport Submodel.....	F6.3.8-6
6.3.8-7. Setup of Invert Cell Pathways Used in the EBS Transport Submodel and their Relationship to the Actual Invert Geometry	F6.3.8-7
6.3.8-8. Setup of Dual-Continuum EBS-UZ Interface Cell Pathway Network and its Relationship to the Near-Field Unsaturated Zone	F6.3.8-8
6.3.8-9. Schematic Representation of the Computational Grid for the EBS-UZ Interface Model.....	F6.3.8-9
6.3.8-10. Simple Model Setup Using Cell Pathways with Different Diffusive Areas....	F6.3.8-10
6.3.9-1. Information Flow Diagram for Unsaturated Zone Transport	F6.3.9-1
6.3.9-2. Inputs, Outputs, and Basis for Model Confidence for the Unsaturated Zone Transport Submodel.....	F6.3.9-2
6.3.9-3. Conceptualization of Unsaturated Zone Transport Processes	F6.3.9-3
6.3.9-4. Illustration of Radionuclide Diffusion Into and Out of Matrix Pores.....	F6.3.9-4
6.3.9-5. Illustration of Colloid-Facilitated Transport Processes	F6.3.9-5
6.3.9-6. Location of Repository Release Nodes for Five Percolation Subregions.....	F6.3.9-6
6.3.10-1. Information Flow Diagram for Saturated Zone Flow and Transport.....	F6.3.10-1
6.3.10-2. Inputs, Outputs, and Basis for Model Confidence for the Saturated Zone Flow and Transport Model Component.....	F6.3.10-2
6.3.10-3. Conceptualization of Features and Processes Important to Saturated Zone Transport.....	F6.3.10-3
6.3.10-4. Illustration of Colloid-Facilitated Transport Processes	F6.3.10-4
6.3.10-5. Regional Map of the Saturated Zone Flow System Showing Direction of Flow and Outline of the 3-D Saturated Zone Site-Scale Flow Model Domain.....	F6.3.10-5
6.3.10-6. Source Regions for Radionuclide Release in the Saturated Zone Flow and Transport Abstraction Model.....	F6.3.10-6
6.3.10-7. Map of the 3-D Saturated Zone Model Domain Showing Simulated Particle Paths.....	F6.3.10-7
6.3.10-8. Radionuclide Decay Chains Considered in Saturated Zone Transport Calculations.....	F6.3.10-8
6.3.10-9. Conceptualization of the 1-D Saturated Zone Flow and Transport Abstraction.....	F6.3.10-9

FIGURES (Continued)

	Page
6.3.10-10. Simulated Particle Paths for Different Values of Horizontal Anisotropy in Permeability	F6.3.10-10
6.3.10-11. Flowchart of the Implementation of the Saturated Zone Flow and Transport Submodel in the TSPA-LA Model	F6.3.10-11
6.3.11-1. Information Flow Diagram for the Biosphere Model Component of the TSPA-LA Model.....	F6.3.11-1
6.3.11-2. Inputs, Outputs, and Basis for Model Confidence for the Biosphere Model Component of the TSPA-LA Model.....	F6.3.11-2
6.3.11-3. Overview of the Biosphere Groundwater Exposure Case Showing Groundwater Transport of Radionuclides and Exposure to the Reasonably Maximally Exposed Individual.....	F6.3.11-3
6.3.11-4. Schematic Representation of the Transport of Radioactive Waste in the Volcanic Ash Exposure Case.....	F6.3.11-4
6.3.11-5. Relationship among Biosphere Submodels for the Groundwater Exposure Case.....	F6.3.11-5
6.3.11-6. Relationship among Biosphere Submodels for the Volcanic Ash Exposure Case.....	F6.3.11-6
6.4-1. Schematic Representation of the TSPA-LA Model Components for the Early Failure Scenario Class.....	F6.4-1
6.4-2. Information Flow Diagram for the Early Failure Scenario Class in the TSPA-LA Model.....	F6.4-2
6.4-3. Inputs, Outputs, and Basis for Model Confidence for the Early Failure Scenario Class.....	F6.4-3
6.5-1. Location and Age of Post-Miocene (less than 5.3 million years) Volcanoes (or clusters where multiple volcanoes have indistinguishable ages) in the Yucca Mountain Region	F6.5-1
6.5-2. Schematic Drawing of the Processes Associated with a Dike Intrusion or Eruption through the Repository.....	F6.5-2
6.5-3. TSPA-LA Model Components for the Igneous Intrusion Modeling Case	F6.5-3
6.5-4. Information Flow Diagram for the TSPA-LA Igneous Intrusion Modeling Case	F6.5-4
6.5-5. Inputs, Outputs, and Basis for Model Confidence for the TSPA-LA Igneous Intrusion Modeling Case.....	F6.5-5
6.5-6. Schematic Diagram of the Intersection of an Igneous Dike with the Repository and Waste Packages	F6.5-6
6.5-7. TSPA-LA Model Components for the Volcanic Eruption Modeling Case	F6.5-7
6.5-8. Information Flow Diagram for the TSPA-LA Volcanic Eruption Modeling Case	F6.5-8
6.5-9. Inputs, Outputs, and Basis for Model Confidence for the TSPA-LA Volcanic Eruption Modeling Case.....	F6.5-9

FIGURES (Continued)

	Page
6.5-10. Schematic Diagram of the Intersection of an Igneous Dike and Eruptive Conduit with the Repository	F6.5-10
6.5-11. Number of Waste Packages Hit by Conduits from a Volcanic Eruption.....	F6.5-11
6.5-12. Schematic Representation of a Volcanic Eruption at Yucca Mountain, Showing Transport of Radioactive Waste in a Tephra Plume	F6.5-12
6.5-13. Schematic Diagram of Tephra Redistribution Model.....	F6.5-13
6.5-14. Comparison of Dose to the RMEI for Post-Eruptive Processes and Dose to the RMEI During a Volcanic Eruption	F6.5-14
6.6-1. Schematic Representation of the TSPA-LA Model Components for the Seismic Scenario Class	F6.6-1
6.6-2. Information Flow Diagram for the Seismic Scenario Class in the TSPA-LA Model	F6.6-2
6.6-3. Inputs, Outputs, and Basis for Model Confidence for the Seismic Scenario Class.....	F6.6-3
6.6-4. Schematic Illustration of the Seismic Scenario Class, the Seismic Effects within a Drift, and Subsequent Radionuclide Releases to the Accessible Environment.....	F6.6-4
6.6-5. Schematic Representation of Future Configurations of EBS Components for Seismic Damage Abstraction.....	F6.6-5
6.6-6. Hazard Curve for Seismic Scenario Class	F6.6-6
6.6-7. Comparison of Mean Rockfall Volumes for Lithophysal (a and b) and Nonlithophysal (c and d) Zones.....	F6.6-7
6.6-8. Drip Shield Plate Fragility as a Function of Rockfall Load: (a) 10 Percent, (b) 50 Percent, and (c) 100 Percent.....	F6.6-8
6.6-9. Drip Shield Framework Fragility as a Function of Rockfall Load: (a) 10 Percent, (b) 50 Percent, and (c) 100 Percent.....	F6.6-9
6.6-10. Probability of Damage for a CSNF WP under and Intact Drip Shield: (a) 23 mm OCB with Intact Internals, (b) 23 mm OCB with Degraded Internals, and (c) 17 mm OCB with Degraded Internals	F6.6-10
6.6-11. Probability of Damage for a CDSP WP under an Intact Drip Shield: (a) 23 mm OCB with Intact Internals, (b) 23-mm OCB with Degraded Internals, and (c) 17-mm OCB with Degraded Internals.....	F6.6-11
6.6-12. Quadratic Fit for Mean Damaged Area on a CSNF WP with Degraded Internals under an Intact Drip Shield: (a) 23-mm OCB and (b) 17-mm OCB	F6.6-12
6.6-13. Quadratic Fit for Mean Damaged Area on a CDSP WP under an Intact Drip Shield: (a) 17-mm OCB with Degraded Internals, (b) 23-mm OCB with Degraded Internals, and (c) 23-mm OCB with Intact Internals.....	F6.6-13
6.6-14. Probability of Incipient and Immediate Rupture for (a) CSNF and (b) CDSP WPs under Intact Drip Shields.....	F6.6-14
6.6-15. Probability of Damage for a CSNF WP Surrounded by Rubble: (a) 23-mm and (b) 17-mm.....	F6.6-15

FIGURES (Continued)

	Page
6.6-16. Quadratic Fit for Mean Damage Area on a CSNF WP with Degraded Internals Surrounded by Rubble: (a) 23-mm and (b) 17-mm	F6.6-16
6.6-17. Probability of Puncture for a CSNF WP Surrounded by Rubble.....	F6.6-17
6.7-1. Schematic Representation of the TSPA-LA Model Components for the Human Intrusion Scenario	F6.7-1
6.7-2. Information Flow Diagram for the Human Intrusion Scenario in the TSPA-LA Model.....	F6.7-2
6.7-3. Inputs, Outputs, and Basis for Model Confidence for the Human Intrusion Scenario.....	F6.7-3
6.7-4. Unconfined Compressive Strength versus Young’s Modulus in Tptpll Zone.....	F6.7-4
6.7-5. Conceptualization of the Human Intrusion Scenario for the TSPA-LA and Subsequent Radionuclide Releases to the Accessible Environment.....	F6.7-5
6.7-6. Schematic Depiction of Borehole (map view) with a Bisecting Fracture	F6.7-6
6.7-7. Schematic Illustration of the Implementation of Human Intrusion in TSPA-LA	F6.7-7

TABLES

	Page
1-1. Principal Documents that Support the TSPA-LA Model	T1-1
2-1. Configuration Control Documents for the TSPA-LA Model	T2-1
3-1. TSPA-LA Model Software Codes	T3-1
3-2. ASHPLUME_DLL_LA Software Documents	T3-3
3-3. CWD Software Documents.....	T3-3
3-4. EXDOC_LA Software Documents.....	T3-3
3-5. FAR Software Documents	T3-4
3-6. FEHM Software Documents.....	T3-4
3-7. GetThk_LA Software Documents	T3-4
3-8. GoldSim Software Documents	T3-5
3-9. InterpZdll_LA Software Documents	T3-5
3-10. MFCP_LA Software Documents.....	T3-6
3-11. MKTABLE/MkTable_LA Software Documents	T3-6
3-12. MVIEW Software Documents.....	T3-6
3-13. PassTable1D_LA Software Documents	T3-7
3-14. PassTable3D_LA Software Documents	T3-7
3-15. PREWAP_LA Software Documents	T3-7
3-16. SCCD Software Documents	T3-8
3-17. SEEPAGEDLL_LA Software Documents	T3-8
3-18. SoilExp_LA Software Document	T3-8
3-19. SZ_Convolute Software Documents.....	T3-9
3-20. TSPA_Input_DB Software Documents	T3-9
3-21. WAPDEG Software Documents.....	T3-10
4-1. Direct Inputs.....	T4-1
4-2. TSPA Generated Data Tracking Numbers Referenced by Parameter Entry Forms	T4-10
4-3. Requirements	T4-11
6-1. TSPA-LA Model Discretization	T6-1
6.1.2-1. Effect of Combinations of Scenario Classes on Total Mean Annual Dose	T6.1.2-1
6.1.3-1. Aleatory Uncertainties in the TSPA-LA Model	T6.1.3-1
6.1.3-2. Examples of Epistemic Uncertainties in the TSPA-LA Model	T6.1.3-2
6.1.4-1. Percolation Subregion Information.....	T6.1.4-1
6.1.5-1. Location of Implementation Description in the GoldSim TSPA Model File.....	T6.1.5-1

TABLES (Continued)

	Page
6.2-1. Table of Alternative Conceptual Models	T6.2-1
6.3.1-1. Durations of Climate States in First 10,000 Years	T6.3.1-1
6.3.1-2. Net Infiltration Rates Averaged over the Unsaturated Zone Model Domain and Probability-Weighting Factors for the Infiltration Scenarios.....	T6.3.1-1
6.3.1-3. Alternative Conceptual Models Considered for the Mountain-Scale Unsaturated Zone Flow.....	T6.3.1-2
6.3.2-1. Parameter Distribution for Host-Rock Thermal-Conductivity Uncertainty.....	T6.3.2-1
6.3.2-2. Percolation-Based Probability Subregion Quantile Ranges	T6.3.2-1
6.3.2-3. Probability Weighting for the 12 Percolation Flux and Host-Rock Thermal-Conductivity Combinations	T6.3.2-1
6.3.2-4. List of Thermal-Hydrologic Variables Predicted by the MSTHM Process Model and Used in the TSPA-LA Model	T6.3.2-2
6.3.2-5. Alternative Conceptual Model Considered for the Engineered Barrier System Thermal-Hydrologic Environment.....	T6.3.2-2
6.3.3-1. Spatial Variability and Uncertainty Distributions for l/α for Method A as Defined in the Abstraction of Drift Seepage	T6.3.3-1
6.3.3-2. Spatial Variability and Uncertainty Distributions for Fracture Permeability ($\log(k [m^2])$).....	T6.3.3-1
6.3.3-3. Inputs Passed by the TSPA-LA Model to the Seepage Dynamically Linked Library	T6.3.3-2
6.3.3-4. Drift-Wall Condensation: 1,000 Years; High Dispersion Coefficient, Low Invert Transport Properties, Well-Ventilated Drip Shield.....	T6.3.3-4
6.3.3-5. Parameter Distributions for Drift Wall Condensation Abstraction.....	T6.3.3-5
6.3.3-6. Alternative Conceptual Models Considered for the Drift Seepage and Drift-Wall Condensation Submodels.....	T6.3.3-6
6.3.4-1. Illustration of the Form of the Mean Water-Rock Interaction Parameter Table	T6.3.4-1
6.3.4-2. Illustration of the Form of an In-Drift Precipitated Salts Look-up Table for Each Unique Set of Values of Carbon Dioxide Partial Pressure, P_{CO_2} , and Temperature	T6.3.4-2
6.3.4-3. Illustration of Estimated Model Uncertainty Ranges for In-Drift Precipitated Salts Submodel Outputs of pH and Ionic Strength.....	T6.3.4-4
6.3.4-4. Summary of Chemistry for Seepage and Condensation in the TSPA-LA Model.....	T6.3.4-5
6.3.4-5. Alternative Conceptual Models Considered for EBS Physical and Chemical Environment	T6.3.4-6
6.3.5-1. Drip Shield and Waste Package Degradation Mechanisms and Their Disposition for Implementation in the TSPA-LA Model	T6.3.5-1

TABLES (Continued)

	Page
6.3.5-2. Alternative Conceptual Models Considered for Drip Shield and Waste Package Degradation	T6.3.5-1
6.3.5-3. Uncertain Inputs to the TSPA-LA Model for Generalized Corrosion of the Drip Shield and Waste Package and Stress Corrosion Cracking of the Waste Package	T6.3.5-3
6.3.5-4. Uncertain Inputs to Localized Corrosion Initiation Stand-Alone Model.....	T6.3.5-6
6.3.6-1. The EBS Flow Abstraction within the TSPA-LA Model	T6.3.6-1
6.3.6-2. Drip Shield and Waste Package Flow Splitting Parameters	T6.3.6-2
6.3.6-3. Alternative Conceptual Models Considered for the EBS Flow	T6.3.6-2
6.3.7-1. Waste Package Configurations	T6.3.7-1
6.3.7-2. Radionuclides Included in TSPA-LA	T6.3.7-2
6.3.7-3. Nominal Grams of Radionuclides per Waste Package for Each Type of Waste	T6.3.7-3
6.3.7-4a. Radionuclide Inventory Per Waste Package Showing the Amount of Decay and Ingrowth Experienced During the Preclosure Period	T6.3.7-4
6.3.7-4b. Supplemental Radionuclide Inventory Per Waste Package due to Mixed Oxide Fuel and Lanthanide Borosilicate Waste Showing the Amount of Decay and Ingrowth Experienced During the Preclosure Period	T6.3.7-5
6.3.7-5. Initial Radionuclide Inventories and Initial Radionuclide Activities Per Waste Package Type in the TSPA-LA Model	T6.3.7-6
6.3.7-6. Disposition of Radionuclides for Groundwater Release Modeling Cases: Nominal, Igneous Intrusion, and Seismic	T6.3.7-7
6.3.7-7. Uncertainty Multipliers for Grams per Waste Package of Radionuclides for Each Waste Type.....	T6.3.7-11
6.3.7-8. Summary of In-Package Chemistry Abstraction (Vapor or Liquid Influx).....	T6.3.7-11
6.3.7-9. In-Package Ionic Strength Abstraction for Vapor Influx Case.....	T6.3.7-11
6.3.7-10. In-Package Ionic Strength Abstraction for CSNF Cell 1 of Liquid Influx Case (log I (molal)).....	T6.3.7-12
6.3.7-11. In-Package Ionic Strength Abstraction for CDSP Cell 1A of Liquid Influx Case (log I (molal))	T6.3.7-13
6.3.7-12. In-Package Ionic Strength Abstraction for CDSP Cell 1B of Liquid Influx Case (log I (molal))	T6.3.7-14
6.3.7-13. In-Package Ionic Strength Deviation for CSNF Cell 1 of Liquid Influx Case (log I (molal)).....	T6.3.7-15
6.3.7-14. In-Package Ionic Strength Deviation for CDSP Cell 1A of Liquid Influx Case (log I (molal)).....	T6.3.7-16
6.3.7-15. In-Package Ionic Strength Deviation for CDSP Cell 1B of Liquid Influx Case (log I (molal)).....	T6.3.7-17
6.3.7-16. Maximum pH for CSNF Cell 1 of Liquid Influx.....	T6.3.7-17
6.3.7-17. Maximum pH for CDSP Cell 1A of Liquid Influx.....	T6.3.7-18
6.3.7-18. Maximum pH for CDSP Cell 1B of Liquid Influx	T6.3.7-18
6.3.7-19. Minimum pH for CSNF Cell 1 of Liquid Influx.....	T6.3.7-18
6.3.7-20. Minimum pH for CDSP Cell 1A of Liquid Influx.....	T6.3.7-18

TABLES (Continued)

	Page
6.3.7-21. Minimum pH for CDSP Cell 1B of Liquid Influx.....	T6.3.7-19
6.3.7-22. Maximum pH for CSNF Cell 1 of Vapor Influx.....	T6.3.7-19
6.3.7-23. Maximum pH for CDSP Cell 1A of Vapor Influx.....	T6.3.7-19
6.3.7-24. Maximum pH for CDSP Cell 1B of Vapor Influx.....	T6.3.7-19
6.3.7-25. Minimum pH for CSNF Cell 1 of Vapor Influx.....	T6.3.7-20
6.3.7-26. Minimum pH for CDSP Cell 1A of Vapor Influx.....	T6.3.7-20
6.3.7-27. Minimum pH for CDSP Cell 1B of Vapor Influx.....	T6.3.7-20
6.3.7-28. Log K Temperature Interpolation Functions for Use in the Total Carbonate Concentration Abstraction.....	T6.3.7-20
6.3.7-29. Initial Release Fraction Percentage Distributions.....	T6.3.7-21
6.3.7-30. Linear Regression Model Alkaline Case (pH \geq 6.8).....	T6.3.7-21
6.3.7-31. Linear Regression Model for Acid Case (pH < 6.8).....	T6.3.7-22
6.3.7-32. Dissolution Rate Parameters for High-Level Radioactive Waste Glass.....	T6.3.7-23
6.3.7-33. Solubility-Controlling Solid Phases Used in the Dissolved Concentration Limits Model Abstraction.....	T6.3.7-24
6.3.7-34. Base Americium Solubility Look-Up Table (log[Am], mg/L).....	T6.3.7-25
6.3.7-35. Base Neptunium (Np ₂ O ₅) Solubility Look-Up Table (log[Np], mg/L).....	T6.3.7-26
6.3.7-36. Base Neptunium (NpO ₂) Solubility Look-Up Table (log[Np], mg/L).....	T6.3.7-27
6.3.7-37. Base-Case Plutonium Solubility Look-Up Table (log[Pu], mg/L).....	T6.3.7-28
6.3.7-38. Base Protactinium Solubility Look-Up Table (log[Pa], mg/L).....	T6.3.7-30
6.3.7-39. Base Thorium Solubility Look-Up Table (log[Th], mg/L).....	T6.3.7-31
6.3.7-40. Base Tin Solubility Look-Up Table (log[Sn], mg/L).....	T6.3.7-32
6.3.7-41. Uncertainty in Americium Solubility Model.....	T6.3.7-33
6.3.7-42. Uncertainty in Neptunium (Np ₂ O ₅) Solubility Model.....	T6.3.7-34
6.3.7-43. Uncertainty in Neptunium (NpO ₂) Solubility Model.....	T6.3.7-35
6.3.7-44. Uncertainty in Plutonium Solubility Model.....	T6.3.7-36
6.3.7-45. Uncertainty in Protactinium Solubility Model.....	T6.3.7-36
6.3.7-46. Uncertainty in Thorium Solubility Model.....	T6.3.7-37
6.3.7-47. Uncertainty in Tin Solubility Model.....	T6.3.7-37
6.3.7-48. Multiplication Factor, N(pH), Used to Modify Fluoride Concentration Uncertainty Terms (ϵ_2) for Americium.....	T6.3.7-38
6.3.7-49. Multiplication Factor, N(pH), Used to Modify Fluoride Concentration Uncertainty Terms (ϵ_2) for Neptunium (Np ₂ O ₅).....	T6.3.7-39
6.3.7-50. Multiplication Factor, N(pH), Used to Modify Fluoride Concentration Uncertainty Terms (ϵ_2) for Neptunium (NpO ₂).....	T6.3.7-40
6.3.7-51. Multiplication Factor, N(pH), Used to Modify Fluoride Concentration Uncertainty Terms (ϵ_2) for Plutonium.....	T6.3.7-41
6.3.7-52. Multiplication Factor, N(pH), Used to Modify Fluoride Concentration Uncertainty Terms (ϵ_2) for Thorium.....	T6.3.7-42
6.3.7-53. Uranium Solubility Look-Up Table (log[U], mg/L) for CSNF WPs Breached under Nominal Conditions or by Seismic Activity.....	T6.3.7-43
6.3.7-54. Uncertainty in Log K Values for Base-Case Uranium Solubility Model (CSNF WP Nominal and Seismic Scenario Classes).....	T6.3.7-44

TABLES (Continued)

	Page
6.3.7-55. Multiplication Factor, N(pH), Used to Modify Fluoride Concentration Uncertainty Terms (ϵ_2) for Uranium (CSNF WP, Nominal and Seismic Scenario Classes)	T6.3.7-45
6.3.7-56. Schoepite Controlled Uranium Solubility Look-Up Table (log[U], mg/L) for CDSP WPs Breached Under any Scenario, CSNF WPs Breached in by an Igneous Intrusion, and in the Invert (all locations and scenarios).....	T6.3.7-46
6.3.7-57. Na-Boltwoodite and Na ₄ UO ₂ (CO ₃) ₃ Controlled Uranium Solubility Look-Up Table (log[U], mg/L) for CDSP WPs Breached under Any Scenario, CSNF WPs Breached by an Igneous Intrusion, and in the Invert (all locations and scenarios)	T6.3.7-47
6.3.7-58. Uncertainty in Uranium Solubility Model in CDSP WPs Breached Under Any Scenario, CSNF WPs Breached by an Igneous Intrusion, and in the Invert (all locations and scenarios)	T6.3.7-48
6.3.7-59. Multiplication Factor, N(pH), Used to Modify Fluoride Concentration Uncertainty Terms (ϵ_2) for Uranium in CDSP WPs Breached under Any Scenario, CSNF Waste Packages Breached by an Igneous Intrusion and in the Invert (all locations and scenarios)	T6.3.7-49
6.3.7-60. Actinide Caps (mg/L) Between an Ionic Strength of 3 and 10 Molal for CSNF Packages.....	T6.3.7-50
6.3.7-61. Actinide Caps (mg/L) Between an Ionic Strength of 3 and 10 Molal for CDSP Packages, Cell 1b.....	T6.3.7-50
6.3.7-62. Parameters for TSPA-LA Glass Waste Form Colloid Abstraction	T6.3.7-51
6.3.7-63. Parameters for TSPA-LA CSNF Waste Form Irreversible Colloid Abstraction.....	T6.3.7-54
6.3.7-64. Parameters for TSPA-LA SNF Waste Form Reversible Colloid Abstraction.....	T6.3.7-56
6.3.7-65. Parameters for TSPA-LA Iron Oxyhydroxide Colloid Abstraction	T6.3.7-58
6.3.7-66. Parameters for TSPA-LA Groundwater Colloid Abstraction.....	T6.3.7-60
6.3.7-67. Alternative Conceptual Models Considered for In-Package Chemistry.....	T6.3.7-61
6.3.7-68. Alternative Conceptual Models Considered for CSNF Waste Form Degradation.....	T6.3.7-61
6.3.7-69. Alternative Conceptual Models Considered for High-Level Radioactive Waste Glass Degradation.....	T6.3.7-62
6.3.7-70. Alternative Conceptual Models Considered for Dissolved Concentration Limits	T6.3.7-63
6.3.7-71. Alternative Conceptual Models Considered for Colloids.....	T6.3.7-64
6.3.8-1. Summary of EBS Transport Abstraction	T6.3.8-1
6.3.8-2. Parameters for EBS Transport Abstraction.....	T6.3.8-2
6.3.8-3. Sampled Parameter Ranges and Distributions Used for Kinetic Sorption on Stationary Corrosion Products.....	T6.3.8-8
6.3.8-4. Sampled Model Inputs Used in the EBS Radionuclide Transport Abstraction.....	T6.3.8-10

TABLES (Continued)

	Page
6.3.8-5. Unsaturated Zone Saturation and Flux Inputs Used in the EBS Radionuclide Transport Abstraction.....	T6.3.8-12
6.3.8-6. Summary of CSNF Rind Volume Calculation Parameters for TSPA-LA.....	T6.3.8-13
6.3.8-7. Alternative Conceptual Models Considered for EBS Transport.....	T6.3.8-14
6.3.9-1. Radionuclide Half-Life and Daughter Products Used in the TSPA-LA Model.....	T6.3.9-1
6.3.9-2. Matrix Sorption Coefficient Distributions for Unsaturated Zone Units in the Unsaturated Zone Transport Submodel	T6.3.9-3
6.3.9-3. Species Dependent Free Water Diffusivities Used to Calculate the Effective Matrix Diffusion Coefficients for Unsaturated Zone Transport	T6.3.9-5
6.3.9-4. Parameter Distributions for Tortuosities Used to Calculate the Effective Matrix Diffusion Coefficients for Unsaturated Zone Transport	T6.3.9-6
6.3.9-5. Fracture γ Parameter Distribution for all Rock in the Unsaturated Zone Transport.....	T6.3.9-6
6.3.9-6. Parameter Distributions for Fracture Porosity for Unsaturated Zone Transport.....	T6.3.9-7
6.3.9-7. Parameter Distributions for Fracture Frequency for Unsaturated Zone Transport.....	T6.3.9-8
6.3.9-8. Colloid Size and Concentration Distributions for Unsaturated Zone Transport.....	T6.3.9-8
6.3.9-9. Cumulative Probability Distributions for Colloid Transport at Matrix Interfaces for Unsaturated Zone Transport.....	T6.3.9-9
6.3.9-10. Colloid Size Exclusion Factor Used in the Compliance Model	T6.3.9-10
6.3.9-11. Radionuclide Sorption Coefficients onto Colloids for Unsaturated Zone Transport (revised groundwater colloid mass concentration parameters for TSPA-LA Model).....	T6.3.9-11
6.3.9-12. Colloid Retardation Factors (Colloidal_Retard_Factor_dist) for Unsaturated Zone Transport	T6.3.9-12
6.3.9-13. Lower Triangular Matrix for all Species Except Uranium and Selenium as Generated from the Correlation (Covariance) Matrix by Cholesky Factorization Using MathCad.....	T6.3.9-12
6.3.9-14. Lower Triangular Matrix for Uranium and Selenium as Generated from the Correlation (Covariance) Matrix by Cholesky Factorization Using MathCad.....	T6.3.9-13
6.3.9-15. Alternative Conceptual Models Considered for the Unsaturated Zone Transport Model.....	T6.3.9-13
6.3.10-1. Radionuclides Transported in the Saturated Zone Flow and Transport Submodel	T6.3.10-1
6.3.10-2. Uncertain Model Inputs Used in the 3-D Saturated Zone Flow and Transport Process Model and 1-D Saturated Zone Flow and Transport Abstraction.....	T6.3.10-2
6.3.10-3. Constant TSPA Parameters for Saturated Zone Flow One-Dimensional Transport Model.....	T6.3.10-7

TABLES (Continued)

	Page
6.3.10-4. Flow Path Lengths of Pipe Segments	T6.3.10-7
6.3.10-5. Average Specific Discharge in Flow Path Segments.....	T6.3.10-7
6.3.10-6. Summary of Alpha Concentration Results in Amargosa Valley Groundwater	T6.3.10-8
6.3.10-7. Alternative Conceptual Models Considered for Saturated Zone Flow and Radionuclide Transport.....	T6.3.10-8
6.3.11-1. Pathways for the Groundwater Exposure Case.....	T6.3.11-1
6.3.11-2. Pathways for the Volcanic Ash Exposure Case.....	T6.3.11-1
6.3.11-3. Groundwater BDCF Uncertainty Representation in the TSPA-LA Model, GoldSim Model File for the Present-Day Climate	T6.3.11-2
6.3.11-4. Alternative Conceptual Models Considered for the Biosphere	T6.3.11-4
6.4-1. Early Failure Unconditional Probability Values.....	T6.4-1
6.4-2. Uncertain Inputs Used in the Early Failure Scenario Class.....	T6.4-1
6.5-1. Waste Form Temperatures Inside Intrusive Body	T6.5-1
6.5-2. Annual Frequencies of Intersection of Repository by a Dike for the License Application Footprint	T6.5-2
6.5-3. Cumulative Distribution Function for the Number of Waste Packages Hit by Conduits.....	T6.5-3
6.5-4. Key Parameters for the ASHP LUME Code.....	T6.5-4
6.5-5. Key Input Parameters to the Tephra Redistribution Submodel	T6.5-6
6.6-1. Expected Waste Package Failure Due to Fault Displacement	T6.6-1
6.6-2. Uncertain Inputs Used in the Seismic Scenario Class	T6.6-2
6.6-3. Seismic Ground Motion and Fault Displacement Modeling Cases Using Pre-Specified Parameters	T6.6-5
6.6-4. Alternative Conceptual Models Considered for the Seismic Scenario Class.....	T6.6-6
6.7-1. Waste Package Specification and Design Dimensions.....	T6.7-1
6.7-2. Specifications of Drilling Components.....	T6.7-1
6.7-3. Uniaxial Compressive Strength and Young’s Moduli by Rock Unit	T6.7-2
6.7-4. Material Properties for Drip Shield and Waste Package Fabrication	T6.7-2
6.7-5. Borehole Properties used in UZ Flow and Transport Calculations	T6.7-3
6.7-6. Borehole Fracture Properties used in UZ Flow and Transport Calculations.....	T6.7-4
6.7-7. Fraction of SZ Source Region Nodes in each Percolation Subregion Bin	T6.7-4

INTENTIONALLY LEFT BLANK

EXECUTIVE SUMMARY

ES1. SCOPE

ES1.1 Introduction

Total System Performance Assessment Model/Analysis for the License Application (TSPA-LA) describes the method, structure, validation or confidence building, and application of a computational model of the performance of the repository system. This model, the Total System Performance Assessment Model, was developed to evaluate the safety of the Yucca Mountain repository for the safe disposal of spent nuclear fuel (SNF) and high-level radioactive waste (HLW). The TSPA-LA is one of an iterative series of performance assessments conducted during the progress of the Yucca Mountain Project. The TSPA-LA Model evaluates the ability of the repository to adequately isolate nuclear waste meeting standards for exposure following repository closure, according to the U.S. Nuclear Regulatory Commission (NRC) Proposed Rule.

The NRC Proposed Rule 10 CFR 63, Parts E and L, consists of proposed changes to the existing rule, published as Implementation of a Dose Standard after 10,000 Years (70 FR 53313 [DIRS 178394], pp. 55313 to 55320), and the unrevised portions of the existing rule, published in the Federal Register as Energy: Disposal of High-Level Radioactive Wastes in a Geologic Repository at Yucca Mountain, Nevada (10 CFR Part 63 [DIRS 180319]). General references to the NRC Proposed Rule will cite both 70 FR 53313 [DIRS 178394] and 10 CFR Part 63 [DIRS 180319]. References to specific articles from either the proposed changes to the existing rule (e.g., 10 CFR 63.321 [DIRS 178394]) or to parts of the existing rule that have not changed (e.g., 10 CFR 63.322 [DIRS 180319]) will use, as shown here, only the DIRS reference number that applies. The same convention is followed when referring to the proposed and existing rules from the U.S. Environmental Protection Agency (EPA). The EPA Proposed Rule 40 CFR Part 197, Subpart B, was published as Public Health and Environmental Radiation Protection Standards for Yucca Mountain, NV (70 FR 49014 [DIRS 177357], pp. 49014 to 49065). The existing rule, as published in the Federal Register, is 40 CFR Part 197, Public Health and Environmental Radiation Protection Standards for Yucca Mountain, NV; Final Rule (66 FR 32074 [DIRS 155216], pp. 32074 to 32135).

The NRC Proposed Rule standards apply to the first 10,000 years following repository closure (10 CFR 63.311(a)(1) [DIRS 178394]), and include additional standards within the period of geologic stability (10 CFR 63.311(a)(2) [DIRS 178394]), defined as one million years after repository closure (10 CFR 63.302 [DIRS 178394]). Figure ES-1 shows the Yucca Mountain area and the entrance to the underground facilities, which will become part of the repository after a license to construct the repository is granted. Figure ES-2 shows a timeline of the major legislative and regulatory actions bearing on the Yucca Mountain Project from 1980 to the present. Among the regulatory mandates of NRC Proposed Rule 10 CFR Part 63 ([DIRS 178394] and [DIRS 180319]) is the requirement to demonstrate, by means of risk-informed assessment, the reasonable expectation of waste isolation after closure of the repository (NRC Proposed Rule 10 CFR 63.304 [DIRS 180319]).

The TSPA-LA Model evaluates the performance of engineered and natural components of the Yucca Mountain repository system for the expected natural conditions prevailing at the Yucca

Mountain site (referred to as the Nominal Scenario Class), considers the effect on repository performance of unexpected early failure of the engineered components of the repository system, and evaluates the impact on repository performance due to natural disruptive events, such as igneous activity and seismic events, and evaluates the impact of an inadvertent human intrusion from drilling into the repository. The technical basis for the TSPA-LA Model includes field, laboratory, and natural-analogue data obtained during site characterization investigations at Yucca Mountain and analogue sites. The development of the process models, submodels, and other components included in the TSPA-LA Model can be found in the supporting analysis model reports that are referenced in appropriate sections of this report.

ES1.2 Governing Regulations

The TSPA-LA Model supports evaluations of the performance of the Yucca Mountain repository system under the relevant postclosure regulatory requirements promulgated in NRC Proposed Rule 10 CFR 63, Subparts E and L ([DIRS 178394] and [DIRS 180319]). The TSPA-LA Model was also used to address the criteria related to postclosure performance described in *Yucca Mountain Review Plan, Final Report* (NRC 2003 [DIRS 163274], Section 2.2), and agreement items associated with the NRC's Key Technical Issues (Reamer 2001 [DIRS 158380], Attachment 1). The TSPA-LA Model serves as part of the overall U.S. Department of Energy (DOE) strategy to provide for the safe disposal of SNF and HLW, a process comprising the following five steps, as illustrated by Figure ES-3:

- Step 1: Define the goals and boundary conditions of the TSPA-LA Model according to regulations promulgated by the U.S. government.
- Step 2: Develop the design for the Yucca Mountain repository so that the repository will meet the regulatory standards, including the contributions to repository performance of both natural and engineered barriers to radionuclide migration from the repository.
- Step 3: Identify and evaluate features, events, and processes (FEPs) potentially relevant to the long-term performance of a waste-disposal repository, screen the identified FEPs, and use relevant FEPs to establish scenario classes for use in assessing estimated repository performance.
- Step 4: Develop and use the TSPA-LA Model to estimate repository performance.
- Step 5: Analyze and interpret the results of the model simulations of repository performance with respect to the performance measures established by the regulations.

The TSPA-LA Model addresses Step 4 of that process, as informed by the preceding steps, to provide information for Step 5, which describes the results.

In particular, the TSPA-LA Model calculates estimates of the:

- a. Annual doses to the reasonably maximally exposed individual (RMEI) from releases from the undisturbed Yucca Mountain disposal system (NRC Proposed Rule 10 CFR 63.311 [DIRS 178394])
- b. Annual doses to the RMEI from releases from the Yucca Mountain disposal system resulting from human intrusion (NRC Proposed Rule 10 CFR 63.321 [DIRS 178394])
- c. Annual levels of radioactivity in the representative volume of groundwater of 3,000 acre feet (NRC Proposed Rule 10 CFR 63.331 [DIRS 180319])
- d. Annual doses to the RMEI for early drip-shield (DS) and waste-package (WP) failures
- e. Annual doses to the RMEI for igneous and seismic scenarios (NRC Proposed Rule 10 CFR 63.342(c)(1) [DIRS 178394]).

ES2. TOTAL SYSTEM PERFORMANCE ASSESSMENT METHODOLOGY

The general performance assessment (PA) process adopted by the DOE follows the methodology developed by Cranwell et al. (1990 [DIRS 101234], Sections 2 and 3). Over time, the methodology has been enhanced, including input from the NRC, and applied to numerous projects by various international organizations involved in radioactive waste management. Figure ES-4 shows the major steps in the PA process. Previous PAs and related supplemental analyses of the performance of the Yucca Mountain repository were conducted to meet various regulatory milestones, following the publication of the Nuclear Waste Policy Amendments Act of 1987, Public Law No. 100-203 [DIRS 100016]. The Yucca Mountain PAs have been iterative, with each succeeding PA building on and extending the scope and results of the previous PAs by incorporating both an improved understanding of the processes affecting performance and, through additional field observations and laboratory analyses, better identification and quantification of the parameters used in the TSPAs. Figure ES-5 illustrates the evolution of the PA iterations for the Yucca Mountain Project and identifies the corresponding TSPAs. The most recent TSPA documents were *Total System Performance Assessment for the Site Recommendation* (TSPA-SR) (CRWMS M&O 2000 [DIRS 143665]) and the application of the TSPA-SR Model to *Total System Performance Assessment – Analyses for Disposal of Commercial and DOE Waste Inventories at Yucca Mountain – Input to Final Environmental Impact Statement and Site Suitability Evaluation* (Williams 2001 [DIRS 157307]). The TSPA-LA Model is built on the foundation of those earlier PAs and has been enhanced by updated analyses of the processes affecting Yucca Mountain and the design elements of the repository, including a comprehensive consideration of the FEPs that are relevant to repository system performance.

Figure ES-6 represents the PA process as a pyramid. The foundation of the pyramid consists of a system characterization involving assimilation of the information collected by scientists and engineers involved in site characterization and engineering design. The repository system and site characterization provides information regarding waste properties, facility design, regional geology, regional hydrology, and environmental characteristics of the Yucca Mountain site. The

broad foundation of the pyramid represents the more than 20-year body of knowledge, collected in the field and in the laboratory, regarding the Yucca Mountain repository system. These data were used to identify the set of possible FEPs that may be part of and affect the performance of the repository system. This body of knowledge also provides the basis for the second stage of the PA pyramid.

The second stage of the PA pyramid consists of the development and testing of process models that include the retained FEPs, and their outcomes regarding repository performance. The process models consist of sets of hypotheses, assumptions, simplifications, and idealizations that, together, describe the essential aspects of a system or subsystem of the repository relative to performance. An example of such a process model is one that describes the movement of water and dissolved radionuclides by diffusive flow in rock pores or by advective flow in fracture openings in the unsaturated bedrock surrounding the repository and through the saturated zone (SZ) below the repository. Because the PA methodology deals with future outcomes and includes uncertainty in both descriptions of processes and parameter values, an essential element of the PA methodology is to capture uncertainty in probabilistic analyses that represent likely outcomes, based on the best available values of process model parameters and the processes involved.

The third stage of the PA pyramid involves the development of abstracted models. These abstractions are progressive simplifications of the detailed models of physical and chemical processes to more compact, efficient numerical models. Abstractions consist of statistical or mathematical abstractions, including look-up tables, equations representing response surfaces, probability distributions, linear transfer functions, or reductions of model dimensionality. The abstractions used to analyze the projected evolution through time of the various components of the repository system are compact but still capture the salient features of the process models, along with their associated uncertainties.

The top level of the PA pyramid consists of the integrated total system models. The total system model is a numerical model that is used to simulate the integrated behavior of the entire Yucca Mountain repository system. The TSPA-LA Model incorporates the abstracted detailed models that describe the TSPA-LA Model components, and their submodels, from their development to their implementation, including information from the analysis model reports. The abstractions and associated process models and submodels describing various repository attributes in a series of analysis model reports form the technical basis for the TSPA-LA Model.

The attributes of both natural and engineered systems comprising the total repository system, as illustrated on Figure ES-7, include:

- Limited water entering emplacement drifts and coming into contact with the WPs and, subsequently, the waste forms
- Prolonged lifetimes of WPs and DSs
- Gradual and limited radionuclide mobilization and release from the repository's engineered barrier system (EBS)

- Retarded radionuclide transport by means of retardation and dilution in natural hydrogeologic systems after release from the EBS
- Low mean annual dose to receptors, even considering the potential occurrence of disruptive events.

Use of the TSPA-LA Model to simulate Yucca Mountain repository behavior and project future outcomes is aided by the development of scenario classes to assist in the analysis of repository performance and provide the framework for the TSPA-LA Model analyses. The TSPA-LA Model is structured to address a specific set of scenario classes that span the range of possible FEPs for both expected conditions and disruptive events. The TSPA-LA Model scenario classes include the Nominal Scenario Class, the Early Failure Scenario Class, two disruptive event scenario classes, the Igneous Scenario Class and the Seismic Scenario Class, and a human intrusion scenario.

This document contains references to the supporting analysis model reports for the model abstractions that are included in the TSPA-LA Model. Other information from the documents supporting the process models and their abstractions is included in the electronic GoldSim model file for the TSPA-LA Model, along with additional references to the parameter values and distributions of parameter values that are incorporated in the TSPA-LA Model.

ES3. TSPA-LA MODEL DEVELOPMENT PROCESS

The TSPA-LA Model was developed to support the evaluation of a geologic repository for the safe disposal of SNF and HLW at Yucca Mountain, Nevada, and evaluates the ability of the natural and engineered systems of the Yucca Mountain repository to isolate nuclear waste from the biosphere. The TSPA-LA Model evaluates repository performance for the first 10,000 years following repository closure and for the period of geologic stability, understood at NRC Proposed Rule 10 CFR 63.302 [DIRS 178394] to be one million years after repository closure.

ES3.1 Features, Events, and Processes Analysis

The development of the TSPA-LA Model for the Yucca Mountain repository system began, as is shown on Step 3 of Figure ES-3, with a thorough analysis and screening of the FEPs that could affect repository performance after closure. The results of the FEPs analyses led to the development of process models and abstractions that address the attributes necessary to allow the TSPA-LA Model to assess repository safety and determine whether or not the repository meets regulatory standards. These process models and their abstractions considered FEPs that could affect the Yucca Mountain repository system and, in turn, FEPs that could be affected by the presence of the repository.

Figure ES-8 is a schematic representation of the development of the TSPA-LA Model and describes, for analysis purposes, the repository system divided into individual model components. Each individual model component represents a major process or set of processes of the total repository system. Figure ES-9 shows the model component areas as well as the event scenario classes that are included in the analyses of repository performance. Figure ES-10 shows the principal components and supporting submodels of the Yucca Mountain repository system.

ES3.2 Development of the Scenario Classes

A scenario is a well-defined, connected sequence of FEPs that describes a possible future condition of the repository system. A scenario class is a set of related scenarios that share sufficient similarities that they can usefully be aggregated for the purposes of screening or analysis. The objective of scenario development for the TSPA-LA Model is to define a limited set of scenario classes that are representative of the range of future FEPs that are potentially relevant to the licensing of the facility.

The TSPA-LA approach focuses on a set of scenario classes that are distinguished by initiating events. The Nominal Scenario Class includes all possible future outcomes except those initiated by early failure of the DSs or WPs, igneous or seismic activity, and inadvertent human intrusion into the repository. The Igneous Scenario Class includes all possible future outcomes initiated by igneous activity. The Seismic Scenario Class includes all possible futures initiated by seismic activity. In addition to the analyses of the scenario classes, the TSPA-LA Model also simulates a Human Intrusion Scenario according to the scenario and criteria described in NRC Proposed Rule 10 CFR 63.322 [DIRS 180319].

Modeling cases are used in the TSPA-LA Model to represent scenario classes and to calculate estimates of performance measures for the repository system. The TSPA-LA Model starts with the Nominal Scenario Class, which incorporates all expected FEPs describing the fundamental processes at work under ambient conditions without disruptive events, early failures, or a human intrusion, as well as possible changes to those processes. The Nominal Scenario Class is analyzed with the Nominal Modeling Case.

The Early Failure Modeling Cases, the DS Early Failure Modeling Case and the WP Early Failure Modeling Case, address FEPs that describe early DS and WP failure due to manufacturing and material defects and pre-placement operations, including improper heat treatment of the WPs.

Igneous disruption of the repository is addressed by two modeling cases. The Igneous Intrusion Modeling Case addresses the FEPs for the possibility that magma, in the form of a dike, could intrude into repository drifts, potentially destroying DSs and WPs in those drifts intruded by the magma, exposing the waste forms to percolating water that could mobilize radionuclides from the waste forms and transport the radionuclides through the unsaturated zone (UZ) and SZ to the RMEI. The Volcanic Eruption Modeling Case addresses FEPs that describe a volcanic conduit (or conduits) that invades the repository, destroys WPs, and erupts at the land surface. The volcanic eruption disperses volcanic tephra and entrained waste under atmospheric conditions and deposits the contaminated tephra on land surfaces where the contaminated tephra becomes subject to redistribution by soil and near-surface hydrogeologic processes.

Seismic disruption of the repository is addressed by two modeling cases that analyze possible seismic disruption of the repository and its effect on repository performance. The Seismic Ground Motion (GM) Modeling Case addresses FEPs concerning damage to WPs and DSs due to vibratory ground motion. The Seismic Fault Displacement (FD) Modeling Case includes the effects of fault displacement on WPs and DSs. FEPs that describe localized corrosion of WPs and DSs are also considered in this modeling case because disruption of the DSs could possibly

result in crown seepage that, in turn, could induce localized corrosion. This modeling case includes advection and diffusion of mobilized radionuclides out of the WP breaches.

The TSPA-LA Model considers a Human Intrusion Scenario in a stylized calculation that simulates a future drilling operation in which an intruder drills a land-surface borehole using a drilling apparatus operating under the common techniques and practices currently employed in exploratory drilling for groundwater in the region around Yucca Mountain. During drilling, the drilling apparatus directly intersects a degraded DS and WP causing a release of waste and continues into the SZ underlying Yucca Mountain. The TSPA-LA Model simulated a Human Intrusion Scenario occurring approximately 200,000 years after repository closure.

ES3.3 Incorporation of Uncertainty

Uncertainty in the expected behavior of the Yucca Mountain repository system requires that the TSPA-LA Model analyses be probabilistic in order to capture the full range of potential outcomes.

Uncertainty in the TSPA-LA Model is characterized as either epistemic or aleatory uncertainty where:

- **Epistemic Uncertainty**, also referred to as “reducible” uncertainty, concerns the state of uncertainty in knowledge about a parameter value due to limited data or alternative interpretations of the available data. Epistemic uncertainty can be reduced, in principle, using the results of experimental testing and additional data collection.
- **Aleatory Uncertainty**, also referred to as “irreducible” uncertainty, concerns whether or not there is a chance occurrence of a FEP. No amount of exploratory work will allow determining whether or not a chance event will or will not occur at any given time, but determining a range of likelihoods-of-occurrence for a given timeframe is generally supportable through using various formalized means for combining scientific insights from experts in the field.

The TSPA-LA Model calculates future outcomes for multiple realizations using distributions of values for uncertain parameters that may be important to performance, rather than deterministic or single-value calculations for each parameter in the repository system. The model realizations are performed using various combinations of parameter values obtained from the parameter-value distributions in the TSPA Input Database, which contains parameter values obtained from field observations, laboratory data, data from established technical literature, and process-model analyses as described in Section 6.3. Each of the combinations of parameter values is representative of a subset of the full range of potential outcomes. These probabilistic analyses thus reflect an appropriate range of process behaviors or parameter values, or both, of the inherently variable Yucca Mountain repository system, given that complete knowledge of the system is not attainable.

ES3.4 Natural and Engineered Model Components

The TSPA-LA Model for the Yucca Mountain repository system is based on several natural and engineered model components. These principal model components of the TSPA-LA Model function as follows (Figure ES-9):

- UZ Flow describes fluid flow through the unsaturated welded and nonwelded tuffs above and below the repository.
- The EBS Environment describes the coupled processes in the environment surrounding and within the engineered elements of the repository.
- WP and DS Degradation describes the responses of these engineered systems to heat, humidity, seepage, and the geochemical environment of the EBS.
- Waste Form Degradation and Mobilization describes the degradation and dissolution of the waste forms and the release of radionuclides from the WPs.
- EBS Flow and Transport describes the flow of water and the transport of radionuclides from the repository to the UZ below the repository.
- UZ Transport describes the transport of radionuclides released from the repository through the UZ below the repository to the SZ.
- SZ Flow and Transport describes water flow and radionuclide transport from beneath the repository and downgradient through saturated rocks and alluvium, to the RMEI.
- Biosphere describes the biologic uptake of radionuclides, including inhalation, ingestion, and water consumption by humans at the site of the RMEI. The biosphere model component also includes consumption of bio-accumulated radionuclides in plants and animal food products.

In addition, the TSPA-LA Model considers early DS and WP failures, a human intrusion scenario, and describes the potential effects on the repository and the surrounding environment in response to igneous and seismic events.

ES3.5 Alternative Conceptual Models

A conceptual model is a set of working hypotheses and assumptions that provide an acceptable description of a system for its intended purpose. Because the TSPA process deals with future outcomes and includes uncertainty in both process descriptions and parameter values, there may be alternative conceptual models (ACMs) that provide reasonable descriptions of a particular system or subsystem. Considering ACMs helps build confidence that plausible changes in modeling assumptions or simplifications will not change conclusions regarding subsystem and total-system performance. Each model component and submodel discussion includes a summary evaluation of ACMs. For example, the development of the EBS Physical and Chemical Environment process model included consideration of an alternate initial water chemistry and the potential effect of feldspar equilibrium on seepage water composition, and the potential for

carbonate exchange to affect CO₂ composition in the UZ. All these ACMs were considered during development of the EBS Physical and Chemical Environment process model. Because ACMs must be compatible with all known data and established facts, their number is limited. Typically, when two or more models exist for the same phenomena and data, the more conservative one from a total-system perspective has been chosen for implementation.

ES3.6 Configuration Management for the TSPA-LA Model

The description of the TSPA-LA Model indicates how the supporting parameter values, along with the process-model abstractions representing many different aspects of the Yucca Mountain repository system, were integrated into one comprehensive PA model and used to estimate future repository performance. Appropriate restrictions were built into the TSPA-LA Model during its development to help ensure that the process-model abstractions were used only within their range of applicability.

The numerical abstractions of the process models were integrated in the TSPA-LA Model using software called GoldSim. The GoldSim software implements the TSPA-LA Model and simulates repository performance and calculates potential annual dose to the RMEI. The software used for the TSPA-LA Model is subject to the Yucca Mountain Project Quality Assurance program and controlled through the Software Configuration Management system to ensure that calculations are traceable to controlled software. The TSPA-LA Model simulations are conducted on computers and servers in a controlled environment. The TSPA-LA Model simulations are recorded, and the results are stored in the Yucca Mountain Technical Data Management System.

A number of software codes were implemented to support the development of the TSPA-LA Model. Some of these codes were used to provide supporting information, and some codes were directly implemented in the TSPA-LA Model using the GoldSim simulation software. Supporting software codes, including process models, were developed and operated externally before running the TSPA-LA Model. Software codes directly implemented as dynamically linked libraries (DLLs) in the TSPA-LA Model are generally referred to as abstractions and are run within the TSPA-LA Model. All software codes used to support the TSPA-LA Model are qualified and are under configuration control. Each qualified software code is uniquely identified with the software name, tracking number, version number, hardware platform, and operating system under which the code was qualified. All software documentation, including the software media, is linked to the unique tracking number.

Input parameter values are controlled through the TSPA Input Database. The database supports the TSPA-LA Model by providing the parameter values and distributions of these parameter values necessary for the TSPA analysis of the repository. The TSPA Input Database categorizes, stores, and retrieves fixed and distributed values of the TSPA-LA Model parameters and allows qualified, authorized analysts to review and update parameter values. The TSPA Input Database has strict user controls, featuring read and write access and audit trails that ensure the security, integrity, and traceability of the information used in the TSPA-LA Model analyses.

The TSPA-LA Model handles both the multiple-realization requirement and can accommodate the maximum size of coupled submodels. The GoldSim software fulfills these requirements

using an efficient solver that minimizes run time for each individual realization. The Monte Carlo sampling structure in GoldSim along with GoldSim's distributed processing capability allows the software to simultaneously run multiple realizations, then reassembles the results from these realizations into an ensemble result from the entire probabilistic run. Further, GoldSim acts as a driver, or integration software, that can couple other large pieces of software for those process models and submodels that were not converted to response surfaces, but are run concurrently in the TSPA-LA Model. A separate software code, EXDOC 2.0 (EXDOC_LA V. 2.0. 2007 [DIRS 182102]), uses the GoldSim results to compute mean and median dose histories.

ES4. YUCCA MOUNTAIN SITE DESCRIPTION

The Yucca Mountain repository system consists of natural and engineered systems that together will ensure the safe disposal of radioactive materials. The following provides a brief overview of the Yucca Mountain site and context for the development of the TSPA-LA Model.

The characteristics of the natural systems at Yucca Mountain that affect repository performance include climate, site geology, and site hydrogeology. The characteristics of the site geology and hydrogeology that affect repository performance include groundwater flow through the UZ and SZ, radionuclide transport, and disruptive events caused by igneous and seismic activity. The Yucca Mountain repository system lies in the Great Basin physiographic province. Characteristics of the natural system at Yucca Mountain that aid in repository performance include a semiarid climate, relatively stable site geology, a deep water table, and limited groundwater flow through the UZ and SZ. The Yucca Mountain area has a low incidence of large magnitude seismic activity. Volcanic activity in the Yucca Mountain region has declined through recent geologic time as described in *Igneous Activity at Yucca Mountain: Technical Basis for Decision Making* (NRC 2007 [DIRS 182132], Sections 2 and 3).

ES4.1 Physiographic Setting and Topography

Yucca Mountain is located within a transition zone between the northern boundary of the Mojave Desert and the southern boundary of the Great Basin Desert. The topography in this region is characterized by isolated, long and narrow, roughly north-south-trending mountain ranges and broad intervening valleys (Figure ES-11). The topography in the Yucca Mountain vicinity was shaped by erosional processes on the eastward-sloping ridge of the mountains and along faults and fault scarps that have created a series of washes downcut to varying degrees into different bedrock formations (Figure ES-12).

ES4.2 Climate

Current climatic conditions for the repository site and the Yucca Mountain region are discussed in *Yucca Mountain Site Description* (BSC 2004 [DIRS 169734], Section 6.3). The Yucca Mountain Project environmental program collected site climate and meteorological data using a network of nine automated weather stations (BSC 2004 [DIRS 169734], Section 7.1.3.2). The climate data show that the mountains west of Yucca Mountain cause a rain shadow effect, causing the present-day Nevada climate to be semiarid to arid, with dry winds and low precipitation. The climatic factors that most affect water-transport processes in the Yucca Mountain UZ are solar radiation-intensity flux; diurnal and seasonal temperature cycles; relative

humidity; and precipitation, in the form of either rain or snow as well as extended periods of drought.

ES4.3 Geology

Yucca Mountain is an uplifted, block-faulted ridge of alternating layers of Miocene age welded and nonwelded volcanic tuffs. The major Yucca Mountain geologic units are the volcanic tuff formations of the Paintbrush Group, the Calico Hills Formation, and the Crater Flat Group. For purposes of hydrogeologic studies, including infiltration, *Yucca Mountain Site Description* (BSC 2004 [DIRS 169734], Tables 3-1, 3-5, and 7-1) provides a separate stratigraphic nomenclature based on the degree of welding and hydrologic property distributions. The major hydrogeologic units are divided into the Tiva Canyon welded; the Paintbrush nonwelded, which consists primarily of the Yucca Mountain and Pah Canyon members and interbedded tuffs; the Topopah Spring welded; the Calico Hills nonwelded; and the Crater Flat undifferentiated units (Ortiz et al. 1985 [DIRS 101280], pp. 10 to 14, Table 1). Figure ES-13 shows the spatial relationship of the major hydrogeologic units of the UZ in both perspective and north-south and east-west cross-sectional views.

ES4.4 Regional Tectonic Setting

Igneous Activity at Yucca Mountain: Technical Basis for Decision Making (NRC 2007 [DIRS 182132], Section 2) describes the tectonic setting in terms of the geologic framework or structural geologic configuration (or both) of the different rock masses in the Yucca Mountain vicinity. The overall tectonic setting of the Great Basin physiographic province, including Yucca Mountain, is extensional, generally consisting of fault-bounded basins and mountain ranges that have been modified by volcanic activity during the past 15 million years. Typically, faults in the Great Basin include normal and strike-slip faults that reflect the extensional deformation caused by plate tectonic interactions at the western margin of the North American continent. The structural geology of Yucca Mountain and its vicinity is dominated by north-stretching normal faults with movement down to the west (Figures ES-14 and ES-15). Some of the faults on Figure ES-14 show evidence of quaternary activity (i.e., within the last 1.8 million years). Figure ES-15 shows that Yucca Mountain is a large eastward tilting block bounded by the Solitario Canyon fault to the west and the Bow Ridge fault to the east.

ES4.5 Local Volcanism

Two types of volcanism have occurred in the Yucca Mountain region. An early phase of Miocene silicic volcanism in the southwestern Nevada volcanic field culminated between 11.8 and 12.4 million years ago with the eruption of four voluminous ash-flow tuffs of about 1,000 km³ each (Sawyer et al. 1994 [DIRS 100075], pp. 1311 and 1312). One of the silicic ash-flow tuffs that erupted from the Timber Mountain Caldera Complex (Figure ES-16) is the Topopah Spring Tuff, which forms the repository horizon planned for waste emplacement. Yucca Mountain is an uplifted, erosional remnant of these ash-flow tuff deposits.

Small-volume basaltic volcanism continued into the Quaternary Period. In terms of eruption volume, the 15-million-year history of volcanism in the region is viewed as a magmatic system that peaked between 11 and 13 million years ago, with the eruption of over 5,000 km³ of

ash-flow tuffs. Following this peak of eruptive activity, relatively minor volumes of basalt have erupted in the last 11 million years (BSC 2004 [DIRS 169989], Section 6.1.1.1). Considered in terms of total eruption volume, frequency of eruptions, and duration of volcanism, basaltic volcanic activity in the region, including Yucca Mountain, defines one of the least active basaltic volcanic fields in the western United States (e.g., *Synthesis of Volcanism Studies for the Yucca Mountain Site Characterization Project* (CRWMS M&O 1998 [DIRS 105347], Chapter 2)).

ES4.6 Hydrology

ES4.6.1 Surface Hydrology

Yucca Mountain is located in the Amargosa River drainage basin, which is the major tributary drainage area to Death Valley (Figure ES-11). Stream flow from Yucca Mountain is captured by local drainages to the Amargosa River. The Amargosa River and its tributaries are ephemeral streams that are dry most of the time, with surface water-flow occurring rarely in direct response to precipitation. In some cases, groundwater discharges at springs in stream channels. During episodic flooding, flow occurs along the Amargosa River and flows to and fills much of the Death Valley playa to depths of 0.3 m (1 ft) or more (Miller 1977 [DIRS 105462], p. 18). During periods of cooler and wetter climate periods, such as 140,000 to 175,000 years ago, Death Valley was filled with water to depths of 175 m. Throughout the Yucca Mountain region and the Death Valley basin, perennial flow is only observed downgradient from spring discharges and around the margins of playas, where the groundwater discharges at land surface.

ES4.6.2 Groundwater Hydrology

Yucca Mountain is located in the Death Valley Regional Groundwater System (Figure ES-17). Groundwater below Yucca Mountain and in the surrounding region flows generally south toward discharge areas in the Amargosa Desert and Death Valley. The area around Yucca Mountain is in the central subregion of the Death Valley Regional Groundwater System, which has three groundwater basins: Pahute Mesa-Oasis Valley, Ash Meadows, and Alkali Flat-Furnace Creek. The primary sources of groundwater recharge are infiltration on Pahute Mesa, Rainier Mesa, Timber Mountain, and Shoshone Mountain to the north and the Grapevine and Funeral Mountains to the south (Figures ES-11 and ES-17). Recharge in the immediate Yucca Mountain vicinity is low, consisting of water reaching Fortymile Wash (Figure ES-17) as well as precipitation that infiltrates into the subsurface.

ES5. THE REPOSITORY SUBSURFACE FACILITY AND ENGINEERED BARRIER SYSTEM

ES5.1 Layout

Note: The following information regarding the repository subsurface facility and the EBS describes the design analyzed by the TSPA-LA Model and may be updated. The design layout of the Yucca Mountain repository subsurface facility is illustrated on Figure ES-18 and aspects of the design are described in *Total System Performance Assessment Data Input Package for Requirements Analysis for TAD Canister and Related Waste Package Overpack Physical Attributes Basis for Performance Assessment* (SNL 2007 [DIRS 179394]) and in *Total System Performance Assessment Data Input Package for Requirements Analysis for Subsurface*

Facilities (SNL 2007 [DIRS 179466], Table 4-1, Parameter Number 01-02). The waste emplacement drifts will be excavated to a diameter of 5.5 m and a nominal length of 600 m (actual lengths will range from 300 to 800 m) using a tunnel boring machine. Emplacement drifts will accommodate the 70,000 metric tons of heavy metal waste inventory scheduled for emplacement in the repository and are planned with a uniform spacing of 81 m between their centerlines. Each emplacement drift will have a capacity of approximately 100 WPs. An area in the southern section of the repository will be constructed to allow for contingencies during emplacement. The emplacement drift area will be excavated in the Topopah Spring Tuff upper lithophysal unit, Topopah Spring Tuff middle nonlithophysal unit, Topopah Spring Tuff lower lithophysal unit, and the Topopah Spring Tuff crystal-poor lower nonlithophysal unit of the repository host horizon. Eighty percent of the excavation will be in the lower lithophysal unit. The lithophysal rock units contain numerous cavities (lithophysal) of varying size and, consequently, high porosities. The nonlithophysal rock units are highly fractured and are characterized by fewer cavities, lower porosities, and have longer fractures than the lithophysal rock units.

ES5.2 Engineered Barrier System

The principal features of the EBS are a titanium-alloy DS and a two-layer WP to contain the waste. Figure ES-19 is a cross-section illustration of an emplacement drift and the major components of the EBS. The EBS includes ground support, a corrosion-resistant waste-emplacement supporting pallet, and an invert at the base of the drift filled with crushed welded tuff, which will have a steel infrastructure.

ES5.2.1 Ground Support

The repository subsurface ground-support system will be used to maintain drift stability in lithophysal and nonlithophysal rocks. Ground support will consist of friction-type, nongrouted rock bolts and a perforated steel sheet covering the upper 240 degrees of the drift-wall circumference above the invert. The perforations in the steel-sheet liner will provide flexural strength and allow air circulation for moisture removal behind the perforated sheet. Cementitious materials will not be used for the emplacement drifts ground support because of uncertainties related to potential chemical effects on the long-term performance of the repository. However, cement may be used in the turnouts from the access ways to the emplacement drifts. Analyses of the effects of the corrosion of ground support materials indicate only a negligible effect on the composition of seepage waters (SNL 2007 [DIRS 177412], Section 6.8).

ES5.2.2 Drip Shield

The emplacement drifts will be equipped with titanium interlocking DSs designed to reduce the effects of rockfall and seepage dripping on the WPs. The linked DSs will form a single continuous barrier for the entire length of each emplacement drift. The DSs will be fabricated from Titanium Grade 7 plates, with Titanium Grade 29 for structural support, and Alloy 22 for the base plates, which will prevent direct contact between titanium and the steel members of the invert.

ES5.2.3 Waste Package

The WPs will consist of an outer shell and an inner shell. The 25-mm-thick outer shell will be composed of corrosion-resistant Alloy 22. The 50-mm-thick stainless-steel inner shell will serve three functions: (1) the inner shell will provide structural strength to resist rockfall, support the internal waste form components, allow the WPs to be supported by the emplacement pallets, and facilitate handling; (2) the inner shell will provide radiation shielding to reduce the exterior surface contact dose rate; and (3) the inner shell will provide limited containment for the radioactive waste inside the WPs, although the TSPA-LA Model analyses do not consider this containment. The commercial spent nuclear fuel (CSNF) reference WPs also contain a stainless steel transport aging and disposal canister that is 25 mm thick and designed to hold a 21 pressurized water reactor or 44 boiling water reactor SNF assemblies. The co-disposal (CDSP) WP is designed to contain five defense HLW glass canisters surrounding a central canister of DOE-owned spent nuclear fuel (DSNF).

ES5.2.4 Emplacement Pallet

An emplacement pallet will support each WP placed in the repository. The emplacement pallets will prevent the WPs from coming in contact with the invert and any invert moisture. The emplacement pallet will be constructed of Alloy 22, a material that will provide long-term corrosion resistance and is the same material as the WP outer shell.

ES5.2.5 Invert

The invert will provide support for the WP emplacement pallets and the DSs. The invert will consist of a steel support structure and a crushed welded tuff ballast derived from the repository host rock. The ballast will be placed in and around the steel invert infrastructure to an elevation just below the top of the pallets' longitudinal and transverse support beams. The invert ballast will be compacted to prevent long-term settlement.

ES5.2.6 Waste Form

CSNF is composed of irradiated uranium oxide contaminated with fission and neutron induced activation products and their daughters. DSNF consists of a variety of uranium and plutonium compounds, including oxides, metals, and carbides packaged in seal-welded canisters. HLW will be mixed and solidified in a high-temperature, borosilicate glass for storage in stainless-steel canisters. Following breaching of the CSNF WPs and CDSP WPs and exposure of the waste to water infiltrating the WPs, the waste forms will be subject to aqueous dissolution and release of radionuclides. All waste forms will release radionuclides at different rates depending on their integrity and the solubility of the constituents of the waste.

ES5.2.7 Waste Form Cladding

SNF generally is encased in a metallic protective cladding. After the cladding is breached, the waste forms can degrade and release radionuclides to the EBS environment. The TSPA-LA Model takes no barrier credit for CSNF cladding. In addition, DSNF cladding is considered to be failed upon receipt. Therefore, the TSPA-LA Model does not take credit for waste-form cladding.

ES5.2.8 **Emplacement Drift**

The WPs will be placed in 5.5-m diameter, circular emplacement drifts that will serve to enhance the role of the natural barriers and the EBS. The presence of the circular underground drifts will result in the formation of a capillary barrier at the drifts' walls during the thermal and ambient postclosure periods. In addition, the decay heat from the waste in the WPs will lead to the development of a dry-out zone around the drifts that will help to prevent percolation from entering the repository and contacting the waste forms during the thermal period. The effectiveness of the drifts in providing a barrier will depend on the strength of the capillary pressure close to the drifts, host-rock permeability, the local percolation flux above the drifts, the temperature of the rock near the walls of the drifts, and the shape of the drift openings. An analysis of the presence of ground support and rock bolts indicated that these elements of the repository construction will not alter the role of the capillary barrier (SNL 2008 [DIRS 181244], Section 6.4.2.5).

ES5.2.9 **Internal Waste Package Components**

The WPs will have internal steel components and stainless-steel inner WP liners. These internal steel components are expected to degrade to iron oxyhydroxides following WP failure. These iron oxyhydroxides degradation products could potentially sorb radionuclides released from the degradation of the waste forms.

ES5.2.10 **Thermal Loading and Waste Package Spacing**

The WPs will be placed in the emplacement drifts in a line-load configuration with a WP-to-WP spacing of approximately 10 cm and a line-averaged heat load of 1.45 kW/m. Preclosure forced ventilation will be active from the start of emplacement, continuing until 50 years after the last WP is emplaced.

ES6. **NATURAL AND ENGINEERED BARRIERS**

The repository horizon is a minimum of 200 m beneath the land surface with a mean depth from the surface of approximately 300 m. The waste forms are solids (with minor gaseous constituents). Unless there is a volcanic eruption, the means for the radioactive constituents of the waste to reach the biosphere will be along groundwater pathways. The waste forms will pose risks to humans if, and only if, all of the following processes were to occur:

- Breaching of the DSs
- Breaching of the WPs
- Exposure of the waste forms to water
- Dissolution of the waste forms releasing radionuclides into the water
- Release of dissolved or colloid-associated radionuclides from the repository, through the UZ, and subsequent aqueous and colloidal transport of radionuclides through the SZ
- Natural or pumped discharge of radionuclide-containing water from the SZ

- Biosphere uptake of released radionuclides by humans or any part of the food chain.

Sections 7.1.8 and 7.3.1.2 describe other pathways to the biosphere as part of the volcanic eruption modeling case.

Three repository subsystems constitute barriers to radionuclide transport from the repository to the natural environment. The engineered components and natural processes of the Yucca Mountain repository system that are expected to combine to provide long-term waste isolation and act as barriers to radionuclide release, flow, and transport are:

- The Upper Natural Barrier—Limits water movement in the UZ above the repository
- The EBS—Limits water movement, radionuclide release, and radionuclide transport within and through the repository
- The Lower Natural Barrier—Reduces rate of water movement and delays radionuclide transport through the UZ below the repository and radionuclide transport through the SZ, and delays subsequent uptake by the biosphere.

ES6.1 Upper Natural Barrier

Figure ES-20 illustrates the key concepts associated with water movement in the UZ at Yucca Mountain. The source of water in the UZ at the repository horizon is precipitation at the land surface (SNL 2007 [DIRS 184614], Section 6.1.4). Climate controls the range of precipitation and land surface temperature conditions. Three potential climates, present-day, monsoon, and glacial-transition, are identified as likely during the first 10,000 years after repository closure, as illustrated on Figure ES-21. The durations of the 10,000 year climate periods used in the TSPA-LA Model were based on the most reasonable sedimentation rates at analogue climate sites as described in Section 6.3.1.2. The present-day climate is characterized by the relatively warm temperate conditions now observed at Yucca Mountain. The monsoon climate is characterized by hot summers with higher summer rainfall relative to the present-day climate. The glacial-transition climate has cooler and wetter summers and winters relative to the present-day climate. The climate durations used in the TSPA-LA Model for simulating the next 10,000 years at Yucca Mountain are the present-day climate for 600 years, followed by a warmer and wetter monsoon climate for 1,400 years, followed by a cooler and wetter glacial-transition climate for the remaining 8,000 years (Section 6.3.1.2). The climate from 10,000 years after repository closure to the period of geologic stability, defined as 1,000,000 years in NRC Proposed Rule 10 CFR 63.302 [DIRS 178394], is based on specifications regarding deep percolation rates provided in NRC Proposed Rule 10 CFR 63.342(c)(2) [DIRS 178394].

Precipitation on the surface of Yucca Mountain that does not run off, evaporate, or transpire infiltrates downward through the soil horizon and into the matrix and fractures in the bedrock as described in the site-scale UZ flow submodel. Net infiltration is spatially and temporally variable and higher on side slopes and ridge tops where bedrock is exposed. The net infiltration flowing downward to the UZ, the percolation flux, provides the water for groundwater flow and transport that could allow radionuclide transport from the repository to the water table. Flow at the repository horizon is included in the TSPA-LA Model using the drift seepage and drift-wall

condensation submodels. Flow into the repository is modeled with consideration of the capillary effect resulting from the presence of the repository underground opening.

ES6.2 Engineered Barrier System

The EBS includes the engineered components and the physical and chemical environment surrounding and within the engineered elements of the repository. Figure ES-19 illustrates the primary components of the EBS that are the WPs containing the waste, the DSs that protect the WPs from dripping water and falling rocks, and the crushed-tuff invert and support structures beneath the WPs and DSs. The barrier functions of the EBS are to isolate the waste forms from migrating water and chemical conditions leading to mobilization of the radionuclides in the waste forms. The EBS helps divert water from the UZ above the repository to the invert and to the UZ below the repository. The WP and DS Degradation Model Component simulates the response of these engineered systems to heat, humidity, seepage, geochemical environment, and moisture. The Waste Form Degradation and Mobilization Model Component simulates the dissolution of the waste forms and the amount of water released from breached WPs. The EBS Flow and Transport Model Component simulates the flux of fluid and radionuclides from the repository to the UZ below the repository.

ES6.2.1 Water Movement and Radionuclide Transport Within and Through the Engineered Barrier System

Figure ES-22 illustrates the key concepts associated with thermal-hydrologic (TH) processes affecting the EBS, including water vapor movement around the drifts, in the postclosure environment. WP and DS temperatures will be elevated, and some WPs and DSs may approach the boiling point of water immediately after emplacement. However, the heat output from the SNF and HLW will decline continuously because of radioactive decay. Heat output from the WPs will be at a maximum during the nominally 50-year preclosure period, but the emplacement drifts will be ventilated to remove most of the heat (SNL 2007 [DIRS 181383], Section 6.1.3). However, the warming of ventilation air will ensure that preclosure conditions will have relatively low humidity. At permanent closure of the repository, ventilation will cease, and a small zone of boiling to above boiling conditions is expected to form. At the same time, a condensation zone is expected to develop outside the boiling zone, resulting in continuous drainage of condensate and percolation in the near-drift region (SNL 2007 [DIRS 181383], Sections 6.1.3 and 6.1.4). However, the end-to-end WP spacing, coupled with the nonuniform heat output from the relatively hotter CSNF WPs and the relatively cooler CDSP WPs, which contain DSNF and HLW glass, makes it likely there will be direct heat flow toward cooler areas and around the drifts rather than through the drifts. In the drifts, vaporized water will tend to move away from hotter regions within the drifts and condense at cooler locations on the drift walls. The condensed water would then be available to drip directly onto an underlying DS (SNL 2007 [DIRS 181383], Section 6.3.11).

The titanium DSs will provide exceptional structural strength and corrosion resistance in saline environments that may evolve on the DS surfaces. The DSs will shield the WPs from damage due to rockfall as the emplacement drifts degrade over time. The titanium DSs are expected to degrade by general corrosion, which is a slow process. Except for a limited number of early

failures, the first DS failure is not projected to occur until between 200,000 and 310,000 years after repository closure.

The temperature of the WP surfaces, the chemistry of the water in contact with the WP surfaces, and the degradation characteristics of Alloy 22 will affect the degradation rates of the WPs. Degradation of the WPs because of general corrosion is not expected during the preclosure period. During the postclosure dry-out period, drift-wall temperatures are expected to be greater than the boiling point of seepage water. During this time, potential high-temperature modes of degradation include stress corrosion cracking (SCC), dry oxidation, and localized corrosion in response to deliquescence formed by hygroscopic minerals in dust deposited on the WPs and DSs as described in *Engineered Barrier System: Physical and Chemical Environment* (SNL 2007 [DIRS 177412], Section 6.10). Three main types of WP degradation were considered under nominal conditions—general corrosion, SCC, and seepage induced localized corrosion. An additional corrosion process, microbially induced corrosion, was considered to provide enhanced general corrosion on the WPs. The TSPA-LA Model also included mechanical failure of the DSs and WPs in the Seismic Scenario Class. Failure mechanisms that the analyses considered included collapse of DSs, SCC, and rupture of DSs and WPs. Under nominal conditions, the time of the first breach of a WP ranges from 100,000 years to one million years, with breaches caused by SCC in the weld of the outer closure lid. General corrosion failures would occur after 400,000 years.

Liquid water can enter WPs by advection when WP failure is by general corrosion or rupture. Water vapor is present at equilibrium with the relative humidity after all modes of WP failure. Degradation will begin after water contacts the waste forms. Following degradation and the start of dissolution of the waste forms, the concentrations of dissolved radionuclides in the water in the WPs will depend on their solubility limits. In case of high solubility limits, the concentration will depend on the waste form degradation rate. In addition, some radionuclides may attach to mobile colloids in the water. Radionuclides released from the solid waste forms into the solution will be available for transport. Figure ES-23 illustrates radionuclide transport through the EBS as either dissolved species or adsorbed onto colloidal particles. Radionuclide transport through the EBS will depend upon the distribution of water on the waste form surfaces and between the waste form surfaces and the outer edges of the degraded WPs. If water has dripped into the WPs through general corrosion breach, there could be advective transport of radionuclides to the edges of the WPs. If water has not dripped into the WPs then diffusive radionuclide transport could occur in an assumed continuous, interconnected water film.

Radionuclides may be transported through the invert by advection if there is mobile seepage water or by diffusion through the water into the pores of the invert materials. The radionuclides transported through the invert would ultimately be released to the fractures and matrix of the UZ below the repository, as shown on Figure ES-23. The dissolved and colloiddally attached radionuclides will then be available for transport through the matrix and fractures in the UZ rock and ultimately released to the SZ.

The TSPA-LA Model simulates the release of radionuclides from the repository, depending on:

- The degradation rates of the components of the engineered barrier

- The dissolution rates of the waste forms
- The solubilities of the radionuclides
- Whether or not the released radionuclides are dissolved or attached to colloids
- Whether or not the radionuclides are sorbed onto corrosion products or inert material, or both
- The rate and volume of water flowing through the engineered barrier system
- The assumed existence of continuous water-film pathways allowing diffusion.

ES6.2.2 Water and Water-Vapor Movement around the Engineered Barrier System

The heat generated by the decay of waste (SNL 2007 [DIRS 181383], Section 6.1.2, Figure 6.1-1) will result in elevated rock temperatures for thousands of years after emplacement. For the TSPA-LA repository design concept, these temperatures will be high enough, in most locations, to cause boiling conditions in the vicinity of the drifts, thus giving rise to local water redistribution and altered groundwater flow paths in the UZ. As water approaches within a distance of one to several meters above the ceiling or crown of an emplacement drift, changing conditions may affect the amount of water that can drip into the drifts. In the early postclosure period, the water in the vicinity of the drifts will first encounter a dry-out zone. Under boiling conditions, water reaching the dry-out zone will vaporize, thus preventing liquid water from reaching the drifts. Vaporized water in the host rock will tend to move away from the drifts and through the permeable fracture network, driven primarily by the altered pore pressure conditions caused by boiling. In cooler regions away from the drifts, the water vapor will condense in the cooler fractures, where it will have the potential to drain either toward the heat source from above or migrate around the drifts to the UZ below the heated drifts. In addition, water percolating through the repository horizon will be partly diverted around the repository drifts, reducing the amount of liquid water available to enter the drifts and the development of a capillary barrier in the rocks around the drifts may prevent dripping into the drifts.

There may be considerable spatial and temporal variability of the TH conditions in and around the repository (SNL 2007 [DIRS 181383], Section 8.1). The spatial variability will be caused by heterogeneity in the rock properties and variations in the ambient percolation flux. In addition, differences in the thermal output of different WPs may cause a range of TH conditions in the repository. For example, cooler regions are expected along the edges of the repository and near low-thermal output WPs. The temporal variability in water movement around the drifts is caused, in the short-term, by the thermal output of the waste. Eventually, the waste heat output will decline, resulting in hundreds of years of drying and several thousand years of cooling and rewetting of the bedrock surrounding the drifts. Percolation encountering the dry-out zone could still be prevented from dripping into the drifts because of the capillary conditions in the bedrock matrix. The rate of water dripping into an emplacement drift is expected to be considerably less than the local percolation rate because the dry-out zone around the drift is expected to reduce liquid water flow, potentially preventing water from reaching the drift walls for a considerable period. The modeling approach to these phenomena in the long-term repository safety

calculations is conservative, however, and percolation is allowed to reach and even enter drifts soon after the boiling front is no longer in the rock. The uncertainty and variability in TH conditions is included in the parameter value distributions as part of the stochastic simulations conducted with the TSPA-LA Model.

ES6.3 Lower Natural Barrier

ES6.3.1 Flow and Transport in the Unsaturated Zone below the Repository

Figures ES-23 and ES-24 illustrate radionuclide transport of the dissolved or colloiddally attached radionuclides released from the EBS to the UZ beneath the repository. Radionuclide transport within the UZ is expected to be principally by advection, but matrix diffusion and colloid-facilitated transport are considered as well. The effectiveness of these transport mechanisms will depend on sorption/desorption and radioactive decay that are included in the TSPA-LA Model. In the welded tuff units, advection of liquid water through fracture networks is expected to dominate radionuclide transport. Advection is also an important mechanism for transport between fractures and the rock matrix, especially at interfaces between nonwelded and welded tuff units, where there will likely be transitions between dominant advective fracture flow and dominant diffusive matrix flow. Dominant fault-and-fracture flow in welded tuffs will provide relatively short transport times through these units, whereas dominant matrix flow in the vitric nonwelded tuffs will result in much longer transport times. Mass transfer between fractures and the tuff matrix may play an important role in transport within Yucca Mountain and the transfer of radionuclides from fractures to the matrix may retard the overall transport of radionuclides to the water table. Also, the TSPA-LA Model includes variable flow paths, such as through perching horizons, which may affect the direction, distance, and time of radionuclide transport.

Sorption describes the combination of chemical interactions between dissolved solutes and solid phases such as immobile rock matrix or colloids, including adsorption, ion exchange, and surface complexation. Radionuclide transport in the UZ will also likely involve colloid-facilitated transport. Radioactive decay will lead to changes in radionuclide concentrations with time. In simple parent-progeny decay, the activity of the parent radionuclide will decrease with time. Chain decay will add additional complexity to the mix of transported material because of the ingrowth of radionuclide daughter products created from the decay of parent radionuclides. Further, some daughter products may have different sorption characteristics than their parent radionuclides and may have different transport characteristics.

Because the characteristics of the natural environment, along with the processes controlling transport, are variable in space and time, radionuclide transport will also be variable. Part of the temporal variability may involve long-term climatic changes that will not only change the percolation flux but could also cause the water table beneath Yucca Mountain to rise due to wetter climates or fall in response to drier climates.

ES6.3.2 Flow and Radionuclide Transport through the Saturated Zone to the Biosphere

Radionuclides transported through the UZ below the repository will be released to the SZ beneath the repository. Figure ES-25 illustrates the key concepts associated with flow and transport in the SZ beneath and downgradient from the Yucca Mountain site, as well as the pathways by which dissolved radionuclides may come into contact with the biosphere, including potential human uptake of and exposure to radionuclides.

Radionuclides reaching the SZ will be subject to flow and transport processes in the general direction of groundwater flow to the southeast, and then to the south and southwest. The groundwater flow processes determine the rate of water movement within the SZ and the flow paths through which groundwater is likely to travel. The groundwater flow paths extend from where the radionuclides may enter the SZ through volcanic tuff and alluvium to the boundary of the accessible environment and beyond.

Advective transport will be determined by the rate of groundwater flow and the effective porosity of the media through which the flow occurs and processes that relate to interactions between the dissolved or colloidal radionuclides and the aquifer materials. Dispersive processes will be affected by the effective porosity of the host rock and by small-scale velocity heterogeneities that allow some dissolved constituents to travel faster or slower than the average advective transport time.

Dissolved radionuclide transport may be retarded by diffusion from fractures into the rock matrix. The effectiveness of matrix diffusion in retarding radionuclide transport will depend on the diffusive properties of the matrix and the degree of spacing between the flowing fracture zones.

Some radionuclides that are potentially important to repository performance may be sorbed by the matrix of the SZ rocks. Carbon, technetium, and iodine do not sorb (SNL 2008 [DIRS 183750], Sections 6.5.3.1, 6.6.2, 6.6.2[a], 6.7.1, and 6.7.1[a]) and are modeled considering only advection, dispersion, and matrix diffusion processes. Other radionuclides, such as neptunium, uranium, and plutonium, will be sorbed to varying degrees onto colloids, which could subsequently diffuse into the matrix pores of fractured tuffs and alluvium (SNL 2008 [DIRS 183750], Sections 6.5.3.1, 6.7.1, 6.7.1[a], and 8.1). The stronger the sorption, the longer the radionuclide transport time when compared with advective-dispersive transport times.

The time for radionuclides to reach any specified point in the SZ downgradient from the repository, such as the boundary of the controlled area, described as 18 km in the primary direction of groundwater flow (10 CFR Part 63 (66 FR 55732 [DIRS 156671], III Public Comments and Responses, 3.5, p. 55750)), will depend primarily on the groundwater velocity and the potential retardation of radionuclides by sorption on the mineral surfaces within the bedrock or alluvial aquifers of the SZ.

Radionuclides in the SZ downgradient from the repository could enter biosphere pathways, including uptake by the local human population. The principal biosphere pathways to humans consist of the following:

- Direct consumption of water containing dissolved radionuclides
- Consumption of crops produced using water containing dissolved radionuclides
- Consumption of meat or dairy products from livestock watered with contaminated water or fed with contaminated crops, or both
- Direct exposure to contaminated soil
- Inhalation of dust that may contain attached radionuclides.

ES7. GENERAL DESCRIPTION OF THE TSPA-LA MODEL

The development of the TSPA-LA Model began with the identification and screening of the relevant FEPs that could affect the performance of the repository. The FEPs that were screened in were used to develop scenario classes for the TSPA-LA Model analyses. Figure ES-8 is a schematic representation of the development of the TSPA-LA Model showing the individual model components of the repository system. Figure ES-9 shows the hierarchy of the abstractions and submodels of the TSPA-LA Model. Each of the following individual model components represents a major aspect of the total repository system.

ES7.1 Model Components for the Nominal Scenario Class Modeling Case

The Nominal Scenario Class modeling case for the TSPA-LA Model encompasses all screened-in FEPs except those FEPs related to early failure, human intrusion, and igneous or seismic activity. The Nominal Scenario Class modeling case includes the potentially important effects and system perturbations caused by climate change and repository heating that are projected to occur after repository closure. In addition, the Nominal Scenario Class modeling case considers that the WPs and DSs will be subject to EBS environments and will degrade with time until they are breached and expose the waste forms to percolating groundwater. The degraded waste forms will release and mobilize radionuclides for transport out of the emplacement drifts. Radionuclides released from the emplacement drifts will be transported through the UZ below the repository by percolating groundwater and ultimately released to the SZ where they will be available for groundwater flow and transport to the accessible environment. The TSPA-LA Model's calculated annual dose to the RMEI also includes FEPs associated with the biosphere.

ES7.1.1 Unsaturated Zone Flow

The UZ Flow Model Component of the TSPA integrates five processes that contribute to flow in the UZ as shown on Figures ES-8 and ES-9: climate, infiltration, site-scale UZ flow, drift seepage, and drift-wall condensation. The UZ Flow Model Component defines the temporal and spatial distribution of water flow from the ground surface through the unsaturated tuffs above and below the repository horizon and the temporal and spatial distribution of seepage into the

waste emplacement drifts. Figure ES-20 provides a conceptual illustration of the mountain-scale flow processes at Yucca Mountain. Water at the repository horizon is derived from precipitation in the form of rainfall and snow at the land surface above the repository. Long-term temporal variability is included in the TSPA-LA Model by specifying four successive climate states: present-day, monsoon, glacial-transition, and a long-term climate based on specifications regarding deep percolation rates provided in NRC Proposed Rule 10 CFR 63.342(c)(2) [DIRS 178394] (Figure ES-21).

ES7.1.2 Engineered Barrier System Environment

The EBS Environment Model Component encompasses environments that may affect the performance of the EBS, including the mountain-scale TH environment and the chemical environment within the emplacement drifts as shown on Figures ES-8, ES-9, and ES-10. These environments are important to repository performance because they help determine the degradation rates of the EBS components, quantities, and species of mobilized radionuclides, as well as the transport of radionuclides and fluids through the emplacement drifts and into the UZ below the repository. Figure ES-20 shows the position of the repository drifts and WPs with respect to the Yucca Mountain flow system. Water percolating into the repository environment will be affected by heat from the emplaced waste and waste heat, and geochemical processes and conditions will determine the chemical environment of the EBS.

ES7.1.3 Waste Package and Drip Shield Degradation

The WPs and DSs will be the primary engineered components of the EBS (Figure ES-26). The WP and DS Degradation Model Component describes the degradation of the WPs and DSs as a function of time, presence of water, and repository location (Figures ES-8, ES-9, and ES-10). The WP and DS Degradation Model Component simulates general corrosion of the WPs and DSs, general corrosion and localized corrosion of the WP outer surface, SCC of the DSs and WPs, microbially influenced corrosion (MIC) on the WP outer surface, and early WP failure.

ES7.1.4 Waste Form Degradation and Mobilization

The Waste Form Degradation and Mobilization Model Component simulates waste-form degradation and the release of CSNF, DSNF, and HLW radionuclide inventories (Figure ES-27). Figure ES-28 illustrates the mechanisms related to the degradation of CSNF, as well as the release of dissolved and colloidal radionuclides from the waste forms to the EBS Transport Submodel. The Waste Form Degradation and Mobilization Model Component accounts for in-package water chemistry; matrix degradation rates for CSNF, DSNF, and HLW waste forms; radionuclide solubilities; and the types and concentrations of waste form and in-drift colloids.

ES7.1.5 Engineered Barrier System Flow and Transport

The EBS Flow and Transport Model Component calculates the rate of radionuclide release from the EBS to the UZ, which is determined by seepage into the emplacement drifts, condensation on the drift walls, WP and DS degradation, the presence of water films on in-package internals, waste-form degradation, and the TH environment of the EBS. The EBS Flow and Transport Model Component simulates the rate of water flow through the EBS, diffusive and advective transport, sorption, and colloid-facilitated transport.

ES7.1.6 Unsaturated Zone Transport

The UZ Transport Model Component describes the migration of radionuclides from the EBS and through the UZ to the water table. Consistent with the Mountain-Scale UZ Flow Submodel, the conceptual model for UZ transport (Figure ES-24) simulates coupled advective and diffusive transport through fracture and matrix continua using a dual-continuum approach. The UZ Transport Model Component simulates advective, dispersive and diffusive transport; sorption; colloid retardation, filtration, and exclusion; radioactive decay and ingrowth; and changes in water-level elevation.

ES7.1.7 Saturated Zone Flow and Transport

The SZ Flow and Transport Model Component simulates the transport of radionuclides from their introduction at the water table below the repository to the regulatory boundary 18 km downgradient from the Yucca Mountain repository (66 FR 55732 [DIRS 156671], III Public Comments and Responses, 3.5, p. 55750). Radionuclides are transported through the SZ either as solutes or sorbed to colloids. The SZ Flow and Transport Model Component simulates advection, dispersion, and diffusion in fractures; matrix diffusion; colloid retardation and exclusion; and sorption (Figure ES-25).

ES7.1.8 Biosphere

The Biosphere Model Component simulates radionuclide transport in the biosphere and the resulting exposure of the RMEI to radionuclides released from the repository after closure (Figure ES-29). The TSPA-LA Model includes the two dominant mechanisms of radionuclide release to the biosphere: (1) release through the SZ via groundwater, and (2) release through the air by ash dispersal from a volcanic eruption.

ES7.2 Model Components for the Early Failure Scenario Class

The Early Failure Scenario Class addresses FEPs that describe the potential for DS and WP early failure in the absence of disruptive events. The early-failure scenarios include DSs and WPs that fail prematurely due to material defects or improper manufacturing conditions or pre-emplacement operations and practices, such as improper heat treatment or welding flaws. Early DS and WP failures are analyzed using the Drip Shield Early Failure (EF) Modeling Case and the Waste Package EF Modeling Case. The DS and WP Early Failure Modeling Cases address FEPs that describe the potential for DS and WP early failure that could affect repository performance in the absence of disruptive events. The Drip Shield EF Modeling Case analyzes the possibility that DSs could fail prematurely, thus failing to protect the underlying WPs from seepage and possible localized corrosion. The Waste Package EF Modeling Case analyzes WPs that fail prematurely due to material defects, manufacturing errors, or pre-emplacement operations and practices, such as improper heat treatment or welding flaws that could affect WP performance and longevity.

ES7.2.1 Drip Shield Early Failure Modeling Case

Analysis of Mechanisms for Early Waste Package/Drip Shield Failure (SNL 2007 [DIRS 178765], Section 6.1.6) identified numerous potential mechanisms that could result in the

early failure of DSs. The following mechanisms were identified as potentially leading to early DS failure in TSPA-LA Model analyses:

- Improper heat treatment
- Base metal selection flaws
- Improper weld filler material
- Emplacement errors.

The probabilities of occurrence for the four DS early failure mechanisms were combined to develop a probability distribution for the rate of occurrence of undetected defects in DSs where an undetected defect was assumed to result in the early failure of a DS. The occurrence of undetected defects is assumed to be independent between DSs and, therefore, DS early failure is also independent between DSs. The Drip Shield EF Modeling Case considers DSs as associated with the waste forms in CSNF and CDSP WPs. Also, the TSPA-LA Model uses the simplifying assumption that each DS early failure affects a single WP and removes the overlying DS as a barrier to seepage at the time of repository closure, thus allowing the full volume of seepage to contact the affected WP. The TSPA-LA Model then assumes that a WP beneath an early failed DS experiences localized corrosion if it is contacted by seepage, completely compromising the WP outer barrier at the time of repository closure, thus allowing both advective and diffusive transport of radionuclides.

ES7.2.2 Waste Package Early Failure Modeling Case

Analysis of Mechanisms for Early Waste Package/Drip Shield Failure (SNL 2007 [DIRS 178765], Section 6.1.6) identified numerous potential mechanisms that could result in the early failure of WPs. The following mechanisms were identified as potentially leading to early WP failure in TSPA-LA Model analyses:

- Weld flaws
- Improper heat treatment of the outer corrosion barrier
- Improper heat treatment of outer corrosion barrier lid
- Improper stress relief of outer corrosion barrier lid (low plasticity burnishing)
- WP mishandling damage
- Improper base metal selection
- Improper weld filler material.

The TSPA-LA Model calculates the characteristics of weld flaws using distributions for the size and number of potentially undetected weld flaws based on industrial analogue studies, which are then used to form the per WP closure weld volume and weld thickness. The TSPA-LA Model simulates the critical flaw orientation probability and an applicable depth factor to model where undetected flaws might remain and might result in SCC that could penetrate the WP closure welds.

The analysis of the other early WP failure mechanisms determined that the occurrence of an undetected defect could result in early failure of a WP. The probability distribution for the rate of occurrence of undetected defects is equivalent to a probability distribution for the rate of WP

early failures. The occurrence of undetected defects is assumed to be independent between WPs; therefore, WP early failure is also independent between WPs regardless of the type of WP.

ES7.3 Model Components for the Disruptive Events Scenario Classes

Igneous events and seismic activity are possible sources of repository disruption. The TSPA-LA Model assumes that igneous activity will cause EBS damage from magma intersecting and intruding into the repository drifts and/or from an eruption from a volcanic vent passing through the repository. Seismic activity in the form of vibratory ground motion and/or fault displacement will disrupt DSs resulting and allow dripping water to contact WPs, and that could lead to localized corrosion of the WP outer barrier.

The modeling cases described below do not mention the likelihood of these events. Rather, these descriptions indicate how such an event is considered in the TSPA-LA Model if it were to occur.

ES7.3.1 Igneous Scenario Class Modeling Cases

ES7.3.1.1 Igneous Intrusion Modeling Case

The Igneous Intrusion Modeling Case describes the performance of the repository system if igneous activity disrupts the repository. The Igneous Intrusion Modeling Case assumes that a dike intersects the repository and destroys DSs and WPs in those drifts intruded by magma, exposing the waste forms to percolating water and mobilizing radionuclides for transport out of the repository, down through the UZ to the SZ, and then to the accessible environment as shown on Figure ES-30. The Igneous Intrusion Modeling Case uses the following model components to simulate repository performance following an igneous intrusion:

- UZ Flow
- EBS Environment
- WP and DS Degradation
- Waste Form Degradation and Mobilization
- EBS Flow and Transport
- UZ Transport
- SZ Flow and Transport
- Biosphere.

ES7.3.1.2 Volcanic Eruption Modeling Case

The Volcanic Eruption Modeling Case simulates the fraction of igneous events in which a volcanic eruption through the repository also occurs. In this case, waste from WPs intersected by flowing magma is transported to the land surface through one or more eruptive conduits, and tephra and entrained waste are discharged into the atmosphere, transported by wind currents, and deposited at the land surface as shown on Figure ES-31. The Volcanic Eruption Modeling Case also evaluates the hillslope and fluvial redistribution of the contaminated tephra deposited on the land surface using the code FAR (FAR V. 1.2. 2007 [DIRS 182225]).

The TSPA-LA Model uses the following processes and model components to calculate repository system performance for the Volcanic Eruption Modeling Case:

- Volcanic interaction with the repository
- Atmospheric transport
- Tephra redistribution
- Biosphere.

ES7.3.2 Seismic Scenario Class Modeling Cases

The Seismic Scenario Class evaluates repository performance for seismic activity that disrupts the repository drifts and the EBS and uses the same TSPA-LA Model components as the Nominal Scenario Class to evaluate the mobilization and transport of radionuclides exposed to seeping water, release from the EBS, transport in the UZ, and transport in the SZ to the location of the RMEI. The effects of seismic events are taken into account in the EBS but not in the natural system. The Seismic Scenario Class modeling cases simulate damage to DSs and WPs as a function of the magnitude of a seismic event, including Seismic GM and Seismic FD Modeling Cases using mean hazard curves for peak ground velocity (PGV) and fault displacement. Each mean hazard curve is defined as the mean estimate or average of a distribution of hazard curves and typically represents the 80th or greater percentile of the distribution because the average is dominated by the larger values of the distribution.

The Seismic Scenario Class modeling cases use the following model components to estimate total system performance:

- UZ Flow
- EBS Environment
- WP and DS Degradation
- Waste Form Degradation and Mobilization
- EBS Flow and Transport
- UZ Transport
- SZ Flow and Transport
- Biosphere.

ES7.3.2.1 Ground Motion Modeling Case

The Seismic GM Modeling Case includes WPs that fail solely due to ground motion damage from a seismic event. The Seismic GM Modeling Case uses nominal processes because nominal corrosion processes can affect the repository's susceptibility to damage during a seismic ground motion event.

The TSPA-LA Model simulates the effects of vibratory ground motion on both lithophysal and nonlithophysal rock using rockfall analyses. The large rock blocks that could be ejected from the nonlithophysal units of the repository horizon during vibratory ground motion, could fill emplacement drifts during the period of geologic stability. The drifts in the lithophysal zone are predicted to collapse into small fragments with particle sizes of centimeters to decimeters, whereas the large blocks in nonlithophysal zones may be shaken loose from the drift walls and

fall onto DSs. Drift collapse could lead to increased temperature and relative humidity of the outer surface of WPs in lithophysal regions, where rubble filling the collapsed drift could form a thermal blanket covering the WPs. Drift collapse could also affect seepage flux and drift-wall condensation in the emplacement drifts in the lithophysal zones.

ES7.3.2.2 Fault Displacement Modeling Case

The Seismic FD Modeling Case includes only those WPs that fail due to fault displacement damage from known and hypothetical faults in the repository. The projected number of WPs that could fail due to fault displacement is a small fraction of the total number of WPs in the repository. A fault displacement that occurs in an emplacement drift may cause one portion of a drift to be displaced vertically or horizontally relative to an adjacent section, possibly causing shearing of an overlying WP and DS if the fault displacement exceeds the available clearance in the EBS. The TSPA-LA Model simulates direct shear failure of a WP if fault displacement exceeds one-quarter of the outer diameter of the WP OCB (about 0.4 meters to 0.5 meters), allowing advective flow through the sheared WPs. If a WP is sheared, the TSPA-LA Model also assumes that the overlying DS is failed

ES7.3.2.3 Human Intrusion Scenario Modeling Case

The Human Intrusion Modeling Case simulates a single drilling intrusion at 200,000 years that intersects a single waste package, creating a pathway for water flow into the waste and for radionuclide movement out of the EBS. The Human Intrusion Modeling Case uses the following model components to estimate total system performance:

- UZ Flow
- EBS Environment
- WP and DS Degradation
- Waste Form Degradation and Mobilization
- EBS Flow and Transport
- UZ Transport (stylized to represent presence of a borehole)
- SZ Flow and Transport
- Biosphere.

ES7.4 TSPA Input Database

The TSPA Input Database provides the parameter values and distributions of parameter values necessary for the TSPA-LA Model. All input data, including the parameter values and their distributions, are stored and controlled. The TSPA-LA Model was developed concurrently with the supporting models and analyses and tracks and ensures traceability of data and data sources. The TSPA Input Database also categorizes and stores fixed and distributed values of the TSPA-LA Model parameters under strict user controls that ensure the security, integrity, and traceability of the information used in the TSPA-LA Model analyses using signed and catalogued Parameter Entry Forms.

ES8. VERIFICATION/VALIDATION OF THE TOTAL SYSTEM PERFORMANCE ASSESSMENT MODEL

Procedures IM-PRO-003, *Software Management*, Section 6.9.12, and SCI-PRO-006, *Models*, Section 6.3, respectively, were utilized to support verification and validation of the TSPA-LA Model, providing confidence that the TSPA-LA Model adequately represents the physical processes in the repository system and properly transfers outputs between the TSPA-LA Model modules and submodels. Figure ES-32 provides an illustration of the major activities conducted for TSPA-LA Model validation. The model validation activities provide confidence in the TSPA-LA Model and its results. Using these activities ensures that the TSPA-LA Model is valid for its intended use of calculating mean annual dose and other performance measures with respect to radionuclide releases from the repository and compliance with NRC Proposed Rule 10 CFR Part 63, Subparts E and L ([DIRS 178394] and [DIRS 180319]).

ES8.1 Verification and Validation Strategy

TSPA-LA Model verification activities were designed to establish confidence that the calculated results were achieved properly using the modeling tools, submodels, and a given set of controlled inputs. TSPA-LA Model verification included verification of the integrated TSPA-LA Model software (GoldSim), verification of DLL implementations within the TSPA-LA Model, verification of model inputs entered into the TSPA Input Database, and verification of the implementation of the submodel abstractions within the TSPA-LA Model. Coupling between submodels within the TSPA-LA Model was verified by ensuring that information generated by one submodel was fed correctly to successive submodels.

A typical model validation compares the model's results with experimental measurements and/or field observations. However, such measurements are impossible to obtain for the TSPA-LA Model at the temporal and spatial scales of interest for postclosure repository performance. Therefore, the TSPA-LA Model was validated using corroboration, technical review, and natural analogues.

The TSPA-LA Model inputs were checked, controlled, and documented to maintain traceability and transparency. Confidence in the methodology of and inputs to the TSPA-LA Model is provided through:

- Selection of input parameters and/or input data from validated supporting analysis model reports
- Model calibration activities and/or evaluation of the initial boundary conditions for the TSPA-LA Model, establishing model convergence
- Evaluation of the impacts of uncertainties on model results.

These three activities demonstrate that: (1) the TSPA-LA Model's input parameter values from source documents, as well as those parameter values that are calculated by the TSPA-LA Model, are correctly propagated throughout the model; (2) the TSPA-LA Model is stable in terms of the number of realizations, the length of model timesteps, and spatial discretization; and (3) that the

uncertainty in model inputs is propagated through and correctly accounted for in the TSPA-LA Model.

The following post-development methods were used to demonstrate TSPA-LA Model validation with respect to intended use and desired level of confidence:

- Corroboration of TSPA-LA Model results with analogue studies or other relevant observations not previously used to develop or calibrate the model
- Confidence building through incorporation of the recommendations and observations provided by technical reviews conducted by external experts regarding the TSPA-VA, the TSPA-SR, and a draft version of the TSPA-LA
- Corroboration of abstraction or submodel results to the results of the validated mathematical models from which the abstraction or submodel was derived
- Corroboration of TSPA-LA Model results with the results obtained from auxiliary analyses as a means of providing additional confidence.

ES8.2 Computer Code and Input Verification

The verification of computer codes from outside sources and model inputs used in the TSPA-LA Model included: (1) verification of the integrated system software, GoldSim, the software platform on which the TSPA-LA Model is based; (2) verification of DLLs from source documents and DLLs that are generated within the TSPA-LA Model; and (3) verification of model inputs from the TSPA Input Database. Submodels from source analysis and/or model reports were verified by comparing submodel results calculated by the TSPA-LA Model with the results in the analysis and/or model reports. Coupling between submodels was examined by verifying that the information generated by one submodel was input correctly to successive submodels and that the information never exceeded the applicable range of validity of the next successive submodel. The following model verification activities apply and demonstrate that incorporation of information and submodels from other sources into the TSPA-LA Model has not altered the validity of the information, the submodels, or both:

- The TSPA-LA Model software, GoldSim, was qualified per a well defined process following program procedure SCI-PRO-003.
- Outputs from DLLs from other sources, including analysis/model reports and data tracking numbers, were correctly replicated in the TSPA-LA Model.
- Outputs from DLLs calculated within the TSPA-LA Model were found to be within established acceptance criteria.
- Individual submodels were validated in their respective analysis/model reports.
- Results from submodels within the TSPA-LA Model were compared to results contained in analysis/model reports and were found to agree within selected acceptance criteria.

- Feeds from one submodel to another submodel were found to be correctly transferred, and these feeds either did not exceed the valid range of the successive submodel or the values used were fixed within the range or at the upper bound of the range of the successive submodel.
- Inputs from the TSPA Input Database were verified to correspond with source data.

ES8.3 Stability Testing

The stability of the model was evaluated in the following areas:

- Statistical stability of mean and median annual dose
- Numerical accuracy of expected dose calculations
- Adequacy of temporal discretization
- Adequacy of spatial discretization
- Stability of the FEHM UZ transport submodel

The uncertainties represented in the TSPA-LA Model are characterized as either epistemic or aleatory uncertainty, and the numerical evaluation of repository performance treats the two categories of uncertainty separately. This technical approach follows advice given by the NRC and the EPA in their publications, and reflects an internationally accepted way to conduct complex, long-term analyses of this type as indicated by the acceptance of the TSPA methodology by an International Peer Review (*An International Peer Review of the Yucca Mountain Project TSPA-SR* (OECD/IAEA 2002 [DIRS 158098]). Appendix E contains summary comments and recommendations provided by the International Peer Review.

For each modeling case, the TSPA-LA Model calculates a distribution of expected annual doses for each epistemic realization, where the expectation is over the aleatory uncertainty in the modeling case. For brevity these quantities are simply termed expected annual dose. The mean and median of the distribution of expected annual dose is termed the mean annual dose and median annual dose, respectively. Section 6.1.2 provides a formal definition of these quantities and describes the calculations for each modeling case.

The stability of the mean and median annual dose is demonstrated for each modeling case by means of replicated sampling. Three sets of calculations were performed for three independent samples of epistemic uncertainty, termed replicates. Each set of calculations results in estimates of the mean and median annual dose, along with the 95th and 5th percentiles of expected annual dose. Comparison of these statistics resulting from each replicate demonstrates that the sample size is sufficient to obtain statistically stable estimates of mean and median annual dose. Figure ES-33a shows the three estimates of mean annual dose, median annual dose, along with the 95th and 5th percentiles of expected annual dose, for the Seismic GM Modeling Case for 10,000 years postclosure. Figure ES-33a demonstrates that there is very little variation between the results for each replicate, therefore, the results are statistically stable. The three estimates for the mean annual dose for each replicate were then used to calculate a confidence interval (Figure ES-33b). Figure ES-33b shows that the true value of the mean annual dose is contained in the narrow confidence interval for the values of the calculated mean annual dose for each replicate.

In general, these calculations involve numerical evaluation of one or more integrals. Because each modeling case addresses different aleatory uncertainties, the methods of calculating expected annual dose differ for each modeling case. Figure ES-34 illustrates numerical accuracy of the calculated expected annual dose for the Seismic GM Modeling Case for 10,000 years postclosure. Figure ES-34 shows that the expected annual dose does not change when the numerical integration is refined by considering additional specified event times and damage fractions. Therefore, the TSPA-LA Model provides a sufficiently accurate value of expected annual dose. Section 7.3.2 demonstrates that the calculation of expected annual dose is sufficiently accurate for each modeling case.

The temporal discretization of the TSPA-LA Model affects its ability to estimate the future behavior of water and radionuclide movement. Timestep size was evaluated for the Waste Package EF, Igneous Intrusion, Seismic GM and Human Intrusion Modeling Cases, which collectively span the range of processes and events that influence repository performance. The analyses demonstrate that the TSPA-LA Model results are stable with respect to the temporal discretization employed. The degree of stability shown in the graphical comparisons of the results of the stability analysis, see Figure ES-35, indicated that a statistical comparison of timestep changes was not necessary.

The TSPA-LA Model deals with the variability associated with spatial discretization of the various model domains which operate at different scales with spatially dependent information. The TSPA-LA Model also represents variability in environmental conditions among WP by means of representative WPs. The spatial discretization utilized in the TSPA-LA Model accounts for the variable scales of the submodels while avoiding undue computational burdens. Analyses were conducted to examine the effect on TSPA-LA Model results of representing large populations of WPs by a few select WPs. The analyses demonstrate that the TSPA-LA Model results are not sensitive to the use of representative WPs. Therefore, the spatial variability in the environmental conditions among WPs is adequately represented.

Additional stability analyses were conducted for the FEHM UZ Transport Submodel. The FEHM UZ Transport Submodel employs a particle-tracking technique to determine transport of radionuclides through the UZ. Stability was examined by varying the number of particles used to simulate radionuclide transport. The analyses demonstrate that TSPA-LA Model results are not sensitive to the number of particles used. Therefore, the UZ Transport Submodel produces stable results.

ES8.4 Uncertainty Characterization Reviews

10 CFR 63.114 (a)(2) [DIRS 178394] requires that a repository PA include an appropriate treatment of the uncertainty and variability of the values of uncertain parameters. The Lead Laboratory conducted a risk-informed review of the parameters used in the TSPA-LA Model, including sensitivity analyses that focused on the effects of the uncertainty and variability in these parameters on the results provided by the TSPA-LA Model. Fifteen formal reviews were performed to scrutinize the uncertainty characterizations of the values of 40 TSPA-LA Model input parameters and their associated abstractions. The technical reviews focused on: (1) confirming that the values of TSPA-LA Model parameters appropriately reflect the major sources of uncertainty and/or variability in those values; (2) verifying that the probability

distributions were derived using sound statistical methods and interpretations; and (3) ensuring that model parameter probability distributions are reasonable and defensible and do not underestimate dose risk. One result of the reviews was that fifteen probability distributions were subsequently corrected, modified, or independently derived to improve their treatment of uncertainty and variability. The approach of the uncertainty characterization and propagation was generally based on *Guidelines for Developing and Documenting Alternative Conceptual Models, Model Abstractions, and Parameter Uncertainty in the Total System Performance Assessment for the License Application* (BSC 2002 [DIRS 158794]).

The reviews included a risk-based ranking of TSPA-LA Model scenario classes and modeling cases to focus the reviews on the most important component model abstractions for the Nominal Scenario Class, the Early Failure Scenario Class, the Igneous Scenario Class, and the Seismic Scenario Class. The Human Intrusion Scenario was excluded from the ranking because the relevant model parameters (for release, flow, and transport) are addressed in the Nominal Scenario Class.

Based on insights and results from previous TSPAs, the following ranking (from highest to lowest) of the scenario modeling cases was obtained:

1. Seismic Scenario Class, Seismic GM Modeling Case
2. Igneous Scenario Class, Igneous Intrusion Modeling Case
3. Igneous Scenario Class, Volcanic Eruption Modeling Case
4. Early Failure Scenario Class, Waste Package and Drip Shield EF Modeling Cases
5. Seismic Scenario Class, Seismic FD Modeling Case
6. Nominal Scenario Class, Nominal Modeling Case.

The magnitudes of the projected dose risk indicated that the first three modeling cases dominated the projected total dose. The analysis provided a list of key TSPA-LA Model parameters whose uncertainty or variability was anticipated to have the greatest influence on the mean and variance of the dose distribution.

Sensitivity analyses were performed during the development of the TSPA-LA Model to investigate the propagation of uncertainty throughout the TSPA-LA Model and to identify uncertain inputs that may be important to the uncertainty in the calculated results. The during-development sensitivity analyses generally confirmed that the uncertainty reviews of the TSPA-LA Model had identified the key uncertain inputs, confirmed that important uncertain inputs were propagated appropriately in the process models and submodels, demonstrated that the effects of these uncertainties were consistent with underlying physical principles, and identified implementation inaccuracies that were subsequently resolved.

Appendix K presents sensitivity analyses performed with the TSPA-LA Model that were used to identify the dominant sources of uncertainty in total expected dose to the RMEI, and in the contributions to the expected dose from key radionuclides such as ^{239}Pu , both dissolved and sorbed to colloids, ^{237}Np , and ^{99}Tc . The post-development TSPA-LA Model sensitivity analyses also investigated uncertainty in selected process model results such as the time of DS failure and the chemical environment in the repository drifts. These sensitivity analyses confirm that uncertain inputs have been appropriately propagated through the TSPA-LA Model consistent

with physical principles, and the analyses are illustrated using selected causal explanations of the relationships between the input and output variables.

ES8.5 Surrogate Waste Form Validation

The waste forms included in the TSPA-LA Model are CSNF (stainless steel and zirconium-based Zircaloy cladding), DSNF, and HLW. Because all waste forms have some amount of variability in form and radionuclide inventory, the CSNF, DSNF, and HLW waste forms are analyzed in the TSPA-LA Model using surrogates that are generally represented by mean characteristic values. For example, DSNF has 11 categories of DSNF and their individual representation in the TSPA-LA Model would dramatically increase simulation time. The naval spent fuel (Category 1) in the TSPA-LA Model is represented by Zircaloy-clad CSNF. The remaining DSNF (Categories 2 through 11) is represented by a single DOE surrogate spent fuel that has a radionuclide inventory that is the weighted average of the radionuclide inventories of Categories 2 through 11. The dissolution rate of the DOE surrogate spent fuel is instantaneous, based on the rapid dissolution of Category 7 DSNF (i.e., uranium metal) under in-package chemistry conditions. The results of all the analyses show that the use of surrogates to represent naval spent nuclear fuel, as well as CSNF, HLW, and the remaining DSNF is appropriate.

ES8.6 Corroboration of Abstraction Model Results with Validated Process Models

Development of the TSPA-LA Model required the abstraction of process models to provide submodels as well as parameter values for direct input to the TSPA-LA Model. Corroboration of the results provided by the abstractions used in the TSPA-LA Model with their respective process models provides confidence that the direct input parameters implemented in the TSPA-LA Model are technically sound for their intended purpose.

The consistency between the TSPA-LA Model and submodels and the source process models is achieved by ensuring that the individual abstractions are validated for their intended use in the TSPA-LA Model, performing input-verification activities during their implementation in the TSPA-LA Model and performing TSPA-LA Model stability-testing activities during development. Certain post-development validation and confidence building activities unrelated to the TSPA-LA Model development activities need to be performed in order to determine that the TSPA-LA Model is appropriate for its intended use. These confidence-building activities were performed after ensuring the integrity of the underlying process models through abstraction validation and TSPA-LA Model implementation processes, and after the abstractions were shown to be functioning correctly when applied together as TSPA-LA Model components. These activities ensure the stability of the TSPA-LA Model, and they constitute the first steps towards defining and executing follow-up post-development validation and confidence-building activities.

To corroborate the abstraction models with the validated process models, the abstraction results were qualitatively and quantitatively compared with the results obtained by the respective process models. The corroboration was performed for the process models and analyses that served as and provided direct inputs to the TSPA-LA Model. The results demonstrate that the process model abstractions are validated and corroborated with their underlying process models (Section 7.6). The results of the corroboration analysis confirm that the abstractions

implemented in the TSPA-LA Model corroborate qualitatively and quantitatively with their underlying validated process models and analyses.

ES8.7 Auxiliary Analyses

Auxiliary analyses were used to assist in validating the TSPA-LA Model. The auxiliary analyses helped to determine the reasonableness of and provide confidence in the results calculated by the TSPA-LA Model. Four different auxiliary analyses were performed: (1) single realization analysis; (2) comparison of the results of the TSPA-LA Model with a Simplified TSPA Analysis; (3) comparison of the results of the TSPA-LA Model with the TSPA independently developed by the Electric Power Research Institute (EPRI); and (4) a Performance Margin Analysis (PMA) of the TSPA-LA Model's modeling cases.

Single Realization Analysis

Single realization analyses (Section 7.7.1) demonstrate proper functioning of TSPA-LA Model and coupling of its submodels. Single realization analyses were performed on four modeling cases that cover the range of WP failure mechanisms considered in the TSPA-LA Model, and highlight the processes affecting and controlling radionuclide releases under varying thermal-physical-chemical conditions: (1) the Waste Package EF Modeling Case; (2) the Drip Shield EF Modeling Case; (3) the Igneous Intrusion Modeling Case; and (4) the Seismic GM Modeling Case. The Drip Shield and Waste Package EF Modeling Cases emphasize the transport at early times when the repository is at an elevated temperature, as well as the effects of climate change on the intact DSs. The Igneous Intrusion and Seismic GM Modeling Cases show the effects of late-time processes when the DSs have been breached and there is variable damage to the WPs.

The single realizations represent unique combinations of epistemic and aleatory uncertainty. The aleatory uncertainty for each modeling case represents (1) spatial location in the Waste Package and Drip Shield EF Modeling Cases, (2) timing of an event in the Igneous Intrusion Modeling Case, and (3) randomly generated seismic events of varying magnitudes in the Seismic GM Modeling Case. The single realization analyses qualitatively and quantitatively illustrate mass transport of various selected radionuclides with respect to the upper natural barrier, the EBS, and the lower natural barrier.

These analyses help explain the relationship between DS and WP failure mechanisms and failure openings, waste-form degradation under varying thermal-physical-chemical conditions, the partitioning of the released mass between the UZ fractures and UZ matrix at the EBS-UZ boundary, and the transport characteristics of the EBS, UZ, and SZ, including sorption, radioactive decay, decay-chain ingrowth, dispersion, and dilution. In all modeling cases analyzed, early-time release following the WP failure is dominated by non-sorbing and non-solubility limited radionuclides such as ^{99}Tc and ^{129}I , whereas late-time release is dominated by solubility-limited radionuclides that undergo sorption such as ^{242}Pu , ^{237}Np , and ^{239}Pu .

Comparison with Simplified TSPA Analysis

TSPA-LA Model results were compared to results calculated using a stand-alone Simplified TSPA Analysis of the Yucca Mountain repository (Section 7.7.2 and Appendix L) that was

developed to corroborate the TSPA-LA Model using a higher level abstraction than that used in the TSPA-LA Model. The simplification involved removing detail from the TSPA-LA Model to capture spatial and temporal variability, and treating the repository system using a more average representation of processes and parameter values. Although the Simplified TSPA Analysis is different than the TSPA-LA Model in both its structure and computational method, the simplified model has identical technical bases. The Simplified TSPA Analysis simulated: (1) the Nominal Modeling Case; (2) the Waste Package EF Modeling Case; (3) the Seismic GM Modeling Case; and (4) the Igneous Intrusion Modeling Case.

The results of the Simplified TSPA Analysis show that for the Seismic GM and Igneous Intrusion Modeling Cases, the total mean annual dose and the mean annual dose from individual radionuclides are similar in magnitude to those obtained for the corresponding modeling cases using the TSPA-LA Model. The Simplified TSPA Analysis of the Waste Package EF Modeling Case calculated a higher mean annual total and individual radionuclide doses than those calculated with the TSPA-LA Model. The Simplified TSPA Analysis for the Seismic GM Modeling Case indicated a similar trend in the mean annual dose for the key radionuclides, although the magnitude of their mean annual doses were slightly different. The Simplified TSPA Analysis for the Igneous Intrusion Modeling Case indicates that the total probability-weighted mean annual dose is similar in magnitude to that obtained for the nominal scenario simulated over a 1,000,000-year period with the TSPA-LA Model, with minor differences in radionuclide concentrations.

Comparison with EPRI TSPA Analysis

The TSPA-LA Model results were compared to results obtained with the EPRI TSPA analyses obtained using the EPRI Integrated Multiple Assumptions and Release Code (IMARC). Section 7.7.3 and Appendix M describe the similarities and differences between the EPRI TSPA Analysis and the TSPA-LA Model. The EPRI TSPA Analysis used data available in the analysis model reports that were primarily used for preparation of the TSPA for the Site Recommendation (TSPA-SR), and did not use the information used in the TSPA-LA Model. The EPRI Analysis does not explicitly consider aleatory uncertainty, whereas the TSPA-LA Model considers both epistemic and aleatory uncertainty. Compared to the TSPA-LA Model, the EPRI Analysis represents a more simplified implementation of the various process models and their associated uncertainties. To help understand the basis for the doses obtained with the EPRI TSPA Analysis and TSPA-LA Model, the EPRI TSPA nominal modeling case was compared to the corresponding TSPA-LA nominal modeling case. Also, the TSPA-LA Model mean annual doses for the Nominal Modeling Class and Waste Package EF Modeling Case were compared with the corresponding mean annual doses obtained with the EPRI model.

A comparison of the calculated results between those from the EPRI model and those from the TSPA-LA Model indicates similar values of dose and similar radionuclides that contribute most to dose. Although both models predict a similar increase in dose after 100,000 years, after about 1,000 years postclosure, the TSPA-LA Model calculates a greater increase in dose due to early-failure. The early-failure increase in dose occurs later in the EPRI TSPA Analysis. The maximum annual dose calculated by the EPRI TSPA Analysis at one-million years postclosure is about 0.02 mrem/yr as compared to the approximately 0.4 mrem/yr at one million years calculated by the TSPA-LA Model. The differences in the respective results can broadly be

accounted for by differences in: (1) seepage rates through the repository; (2) the representations of early-failure of EBS components; (3) waste form and radionuclide inventory; and (4) solubility limits and sorption characteristics in the UZ and SZ.

Performance Margin Analysis

The Performance Margin Analysis (PMA) (Section 7.7.4 and Appendix C) was used to quantitatively evaluate conservatisms in the TSPA-LA Model to (1) confirm that they are conservative with respect to the calculated mean annual dose; (2) quantify the extent to which the conservatisms, individually and collectively, overestimate the mean annual dose; and (3) assess whether or not the conservatisms introduce any inappropriate risk dilution. The PMA addressed a select set of TSPA-LA modeling cases for both 10,000-year and 1,000,000-year time periods, and utilized modified representations of selected TSPA-LA Model submodels and selected sets of conservative parameter values. The PMA results for peak mean annual dose for the 10,000 year and 1,000,000 year are lower than the doses calculated for the same modeling cases using the TSPA-LA Model. The largest mean annual doses calculated using the PMA are more than an order of magnitude lower for the 10,000 years postclosure period, and are lower by a factor of two for the 1,000,000 years postclosure period. Also, for the PMA results, different modeling cases contribute most to the total mean annual dose than indicated by TSPA-LA Model results. When compared to the total mean annual dose calculated with the TSPA-LA Model, the lower total mean annual dose calculated by the PMA demonstrates that the conservatisms incorporated in the TSPA-LA Model do not introduce risk dilution.

ES8.8 Confidence Building: Natural Analogues

Corroboration of the results of the TSPA-LA Model can be gained, in part, through comparison with natural analogues. Natural analogue results were used in the validation process for the model components and submodels for several of the analysis model reports supporting the TSPA-LA Model. The natural analogues relevant to the Yucca Mountain repository are discussed in *Natural Analogue Synthesis Report* (BSC 2004 [DIRS 169218]) and include natural analogues to materials intended for use in the Yucca Mountain repository as well as the results of some investigations of analogues to geologic processes. The information from natural analogues has contributed to the understanding of drift stability, degradation of the waste forms and elements of the EBS, seepage, UZ flow and transport, coupled processes, SZ transport, the biosphere, and disruptive events, such as volcanism and seismic events. Natural analogue information was used in the development of the supporting submodels of the TSPA-LA Model as provided by the analysis/model reports. The use of natural analogues helps ensure that these submodels are grounded in reality and provides confidence that the TSPA-LA Model provides reasonable results. In addition to the confidence provided in general by the examples of natural analogues on a qualitative basis, performance comparisons with two selected analogues, the Cerro Negro volcanic eruption and the Nopal I uranium mine at Peña Blanca, provide additional confidence in the TSPA-LA Model.

The ASHPLUME software was used to simulate ash-fall thickness from the 1995 eruption of the Cerro Negro volcano. The results show that ASHPLUME can reasonably predict the spatial distribution of ash-fall thickness from the eruption of a basaltic cinder cone volcano similar to Cerro Negro (Figure ES-36). The Cerro Negro ash-fall calculation method was used to simulate

eruptive releases of ash from volcanic vents in the vicinity of the Yucca Mountain repository or from a volcanic vent passing through the repository and resulting in WP destruction and aerial distribution of waste particles containing radionuclides.

Radionuclide transport by groundwater is the most likely off-site transport pathway for the Yucca Mountain repository. The Peña Blanca natural analogue site (Figure ES-37) offers a unique opportunity to examine the groundwater flow and transport of uranium and some of its daughter products in a climatic and geologic setting very similar to that of Yucca Mountain. Both the Peña Blanca and Yucca Mountain sites are set in volcanic tuff in an oxidizing UZ and are in similar desert environments. Figure ES-38 shows the geologic structure at the Nopal I mine, the position of the ore deposit above the water table, and the low westerly to easterly groundwater gradient. The Nopal I mine at Peña Blanca was originally comprised of uraninite, which is chemically similar to nuclear fuel. The Nopal I deposit was analyzed using a modified version of the metal-fuel dissolution submodel used in the TSPA-LA Model. The observed uranium concentrations at observation wells PB1, PB2, PB3, clustered within 50 m of the ore deposit, and PB4, approximately 0.75 km downgradient from the ore deposit shown on Figure ES-39. The concentration values of uranium in the groundwater downgradient from the Nopal I ore deposit indicate that radionuclides released from the deposit appear to have been retarded by the natural geologic system. The relatively high uranium concentrations shown on Figure ES-39 are due to the disturbance caused by drilling the observation wells PB1, PB2, and PB3 in 2002. Successive well cleaning and sampling removed the excess uranium from these wells and uranium concentrations returned to values similar to the concentrations observed in PB4. The results of field investigations at the Nopal I mine and analyses of rock and water samples demonstrate the ability of natural systems to provide a sink for radionuclides released from the deposit.

ES8.9 Summary of Technical Reviews

Technical reviews of PA models form an important part of model validation. During the past decade, the Yucca Mountain Project has developed successive TSPA models as well as accompanying input process models, all of which have been subject to technical reviews by external experts as part of their validation. Each milestone PA for the Yucca Mountain repository was subject to external reviews. The Total System Performance Assessment for the Viability Assessment (TSPA-VA) was the subject of a peer review as described in Section 7.9.1. An International Review Team (IRT) conducted an evaluation of the Total System Performance Assessment for the Site Recommendation (TSPA-SR), and the accompanying TSPA-SR performance-assessment model. Appendix E summarizes the comments provided by the IRT review of the TSPA-SR Model, and the responses to those comments. An Independent Validation Review Team (IVRT) reviewed a draft version of the TSPA-LA Model and the accompanying IVRT report provided comments as described in Section 7.9. The comments from the IVRT technical review of the draft TSPA-LA Model were addressed, and the TSPA-LA Model incorporates the material contained in the responses to those comments.

TSPA-VA Peer Review

The TSPA-VA peer provided a two-year, formal, independent evaluation and critique of the development and completion of the TSPA-VA. The TSPA-VA peer review panel's key

conclusions were as follows. (1) The peer review found that TSPA-VA utilized an overall sound approach for assessing the postclosure performance of the Yucca Mountain repository. (2) The peer review found that the TSPA-VA's descriptions of the long-term probable behavior of the Yucca Mountain repository was not supported by adequate evidence that the TSPA-VA Model represented the systems, components, and processes that they were designed to represent. The peer review found that because the TSPA-VA Model contained both conservative and non-conservative submodels, decisions based on the TSPA-VA Model results should be made cautiously. (3) The peer review concluded that the TSPA-VA was a necessary and useful step in the evolving understanding of the performance of the Yucca Mountain repository. The panel also felt that the TSPA-VA provided valuable insights into the performance of the various repository components and helped identify issues where additional data and analyses could improve the understanding of repository performance. (4) The peer review noted the inherent difficulty in the ability of the TSPA-VA Model to predict the repository behavior during the postclosure regulatory period mandated at that time. (5) The peer review noted that the planned future activities at Yucca Mountain would provide valuable information for confirming, calibrating, and/or validating the process models describing repository performance.

The Yucca Mountain Project fully implemented the recommendations provided by the peer review, resulting in major revisions to the components of the TSPA-VA Model. Using expanded site-scale test data, revisions to the TSPA-LA Model resulted in the TSPA-SR Model, and the associated analyses that supported the Final Environmental Impact Statement.

International Review Team Peer Review

The IRT review provided an independent assessment of the methodology used in the TSPA-SR. The IRT review was based on international standards and guidance. The IRT made several recommendations regarding the application of the TSPA-SR Model and its methodology to the development of the TSPA-LA. The IRT's key conclusions were as follows. (1) The TSPA-SR Model's methodology was sound and implemented in a competent manner. (2) The performance assessment approach provided an adequate basis for suggesting likely compliance with the 10,000 years regulatory standard, and, thereby, for the site recommendation decision. (3) The IRT stated that future TSPA iterations should emphasize that the understanding of the repository system and its performance and provides for safety both during and beyond the postclosure regulatory period. The IRT provided 27 specific recommendations for future improvements to be included in the preparation and submission of the LA (Appendix E).

IVRT Technical Review

The IVRT review scope was defined by the then available TSPA Technical Work Plan for the draft TSPA-LA Model according to two model validation goals: (1) describe the postclosure performance of the repository system for the Nominal, Igneous, and Seismic Scenario Classes; and, (2) produce an estimate of mean dose (and other performance measures, as appropriate) consistent with the degree of conservatism representative of the component abstraction models and parameters values and their uncertainty. The IVRT provided seven recommendations that were implemented in the current TSPA-LA Model (Sections 7.9.3.2 and 7.9.3.3).

ES9. SYSTEM PERFORMANCE ANALYSES

The TSPA-LA Model was used to conduct a PA of the Yucca Mountain repository system. The analyses provide mean and median annual dose to the RMEI for the first 10,000 years after repository closure and for the period of geologic stability (one million years) specified in NRC Proposed Rule 10 CFR 63.303 [DIRS 178394]. The TSPA-LA Model calculated evaluated modeling cases representing nominal conditions, early DS and WP failures, and disruptive events. The TSPA-LA Model analyses also address both the individual and groundwater protection requirements of NRC Proposed Rule 10 CFR 63.311 [DIRS 178394] and 10 CFR 63.331 [DIRS 180319], respectively.

The analyses account for uncertainties in the representations of FEPs that could affect the annual dose. The PA analyses address the effect of alternative parameters, submodels, and approaches to FEPs. The calculations are probabilistic in the sense that the results are for multiple realizations, carried out using sampled values from the probability distributions for the values of the uncertain model parameters.

ES9.1. Total Mean Annual Dose to the Reasonably Maximally Exposed Individual for the Repository System

Figure ES-40 displays the total expected annual dose for first 10,000 years after repository closure and shows that the greatest mean annual dose for this period is less than 0.23 millirem. Figure ES-41 displays the total expected annual dose for the postclosure period from 10,000 to one-million years after repository closure and shows that the greatest median annual dose for this period is less than 1 millirem. These total expected annual dose values represent the sum of the expected dose calculations for each of six scenario class modeling cases considered for the TSPA-LA Model. Figures ES-40 and ES-41 show the distribution of the doses calculated from multiple realizations of the TSPA-LA Model and thus display the uncertainty in the total expected dose resulting from epistemic uncertainty about the repository system.

Figure ES-42 shows the radionuclides that contribute most to the estimate of mean annual dose and indicates that ^{99}Tc , ^{14}C , ^{129}I , and ^{239}Pu dominate the estimated mean annual dose during the first 10,000 years after repository closure. In a similar manner, Figure ES-43 shows that ^{239}Pu , ^{129}I , and ^{226}Ra generally dominate the mean annual dose for the first 100,000 years of the postclosure period; and that ^{226}Ra , ^{242}Pu , and ^{237}Np generally dominate the mean annual dose for the postclosure period from 100,000 to one-million years.

ES9.2 Results of the Scenario Class Modeling Case Simulations

Following are descriptions of the results provided by the scenario class modeling cases used to simulate repository performance. Figures ES-44 through ES-57 present the expected annual dose calculated for the individual modeling cases. The following describes these results by modeling case.

ES9.2.1 Nominal Scenario Class Modeling Case

The results for this modeling case show zero mean annual dose for the first 10,000 years because no WPs are estimated to fail (by general corrosion, localized corrosion, or SCC) in this period.

The first WP failure (by nominal SCC) would occur at approximately 30,000 years, and the DSs would begin to fail by general corrosion at approximately 260,000 years. As shown on Figure ES-44, the estimated maximum mean and median annual doses for the postclosure period from 10,000 to one-million years would be 0.5 and 0.3 millirem, respectively. Figure ES-45 shows the radionuclides that dominate the estimate of mean annual dose for the Nominal Scenario Class Modeling Case. The main contributors to mean annual dose would be the highly soluble and mobile radionuclides ^{129}I and ^{99}Tc .

ES9.2.2 Early Failure Scenario Class Modeling Cases

The Early Failure Scenario Class Modeling Cases include FEPs that relate to early WP and DS failure due to manufacturing, material defects, or pre-encapsulation operations that would include improper heat treatment. Radionuclide mobilization and transport for the Early Failure Scenario Class is similar to the Nominal Scenario Class, but differs from the Nominal Scenario Class in that the Early Failure Scenario Class considers only WPs affected by early DS and WP failures.

ES9.2.2.1 Drip Shield Early Failure Modeling Case

The defective DSs were modeled as being failed at the time of repository closure, and WPs underlying any failed DSs and exposed to seepage are conservatively considered as failed. Figure ES-46 shows the expected annual dose histories for the first 10,000 years after closure and the postclosure period from 10,000 to one-million years. The expected annual doses account for aleatory uncertainty about the number of early failed DSs, types of WPs under failed DSs, and their locations in the repository. The mean, median, and 5th and 95th percentile curves in this plot show the uncertainty in the expected annual dose due to epistemic uncertainty from incomplete knowledge of the behavior of the repository system. The calculations for the first 10,000 years show a projected mean annual dose of approximately 0.0003 millirem at 2,000 years after repository closure. The mean annual dose then decreases steadily and is less than 0.0002 millirem during the postclosure period from 10,000 to one-million years.

Figure ES-47a shows the radionuclides contributing most to the total mean annual dose during the first 2,000 years after repository closure are soluble and mobile radionuclides, in particular ^{99}Tc , ^{129}I , and ^{14}C . During the postclosure period from 10,000 to one-million years, Figure ES-47b shows that ^{239}Pu , ^{242}Pu , ^{226}Ra , and ^{237}Np dominate the mean annual dose.

ES9.2.2.2 Waste Package Early Failure Modeling Case

The WPs are assumed to be failed at the time of repository closure. However, intact DSs overlying early failed WPs will degrade by general corrosion after repository closure. Figure ES-48 shows the expected annual dose histories for the first 10,000 years after repository closure and for the postclosure period from 10,000 to one-million years. The expected annual dose accounts for aleatory uncertainty about the number of early failed WPs, types of early failed WPs, and their locations in the repository. The mean, median, and 5th and 95th percentile curves on Figures ES-48a and ES-48b reflect the epistemic uncertainty in the expected annual dose.

Figure ES-48a shows that the calculated mean annual dose is about 0.004 millirem at about 9,800 years. The mean annual dose during the first 10,000 years postclosure results from early failed CDSP WPs. The relative humidity in the CDSP WP emplacement locations tends to be

higher and forms an aqueous layer suitable for radionuclide diffusion earlier than in the CSNF WPs. Because the CDSP WPs contain DOE SNF and the TSPA-LA Model does not take credit for the canister, cladding, or fuel matrix, diffusive transport of radionuclides can start as soon as the humidity in the breached CDSP WPs is greater than 95 percent (Section 8.2.2.2). The increase in mean annual dose at about 9,800 years postclosure, as shown on Figure ES-48a, is due to the beginning of diffusive transport from early-failed CSNF WPs. Figure ES-48b shows that the estimated mean and median annual doses are about 0.02 and 0.006 millirem, respectively, before 15,000 years, and the doses gradually decrease thereafter until about 300,000 years postclosure. At about 300,000 years postclosure, the DSs begin to fail from general corrosion, and the expected annual dose increases during the period from 300,000 to 400,000 years postclosure because of advective transport of radionuclides through failed WPs.

Figure ES-49a shows that in the first 10,000 years after closure, the more soluble and mobile radionuclides, ^{99}Tc , ^{129}I , and ^{14}C , dominate the estimate of mean annual dose. Figure ES-49b shows that during the postclosure period from 10,000 to one-million years, ^{239}Pu , ^{242}Pu , ^{226}Ra , and ^{237}Np dominate the expected mean annual dose.

ES9.2.3 Igneous Scenario Class Modeling Cases

The Igneous Scenario Class addresses the set of FEPs that describe igneous events that could affect repository performance. The Igneous Scenario Class is represented by: (1) the Igneous Intrusion Modeling Case that represents a magma dike that intrudes into the repository causing subsequent release of radionuclides to the groundwater in the UZ, and (2) the Volcanic Eruption Modeling Case that represents a hypothetical volcanic eruption from a volcanic conduit that passes through the repository and emerges at the land surface with the release of radionuclides to the atmosphere.

ES9.2.3.1 Igneous Intrusion Modeling Case

After a magmatic dike intersects the repository, radionuclide release and transport away from the repository would be similar to the Nominal Modeling Case. All of the DSs and WPs would be damaged, exposing the waste forms to percolating groundwater with subsequent degradation, radionuclide mobilization, and transport through the UZ to the SZ. The Igneous Intrusion Modeling Case considers that the remnants of the DSs, WPs, or cladding do not divert any water from the waste.

Figure ES-49 shows calculated expected annual dose histories that account for aleatory uncertainty in igneous intrusions such as the number of future events and the time at which they may occur. The mean, median, and 5th and 95th percentile curves on Figure ES-50 indicate epistemic uncertainty in expected annual dose resulting from incomplete knowledge of the behavior of the physical system during and after the disruptive event. The calculated mean annual dose for the first 10,000 years postclosure is less than 0.06 millirem, and 1.3 millirem during the postclosure period from 10,000 to one-million years. The median projected annual dose for during the postclosure period from 10,000 to one-million years is less than 0.4 millirem.

Figure ES-51a shows that ^{99}Tc and ^{129}I dominate the estimate of the expected mean annual dose for the first 4,000 years, and ^{239}Pu , ^{99}Tc , and ^{240}Pu dominate the estimate of the mean annual

dose for the first 10,000 years postclosure. Figure ES-51b shows that ^{239}Pu dominates the estimate of the mean for the next 170,000 years, and ^{226}Ra , ^{242}Pu , and ^{237}Np dominates expected mean annual dose for the during the postclosure period from 10,000 to one-million years.

ES9.2.3.2 Volcanic Eruption Modeling Case

Volcanic eruptions may occur at Yucca Mountain if an igneous dike rises through the Earth's crust, intersects one or more repository drifts, and forms an eruptive conduit. WPs in the direct path of the conduit would be destroyed, and the waste in those packages would be entrained in the eruption. Contaminated volcanic ash would be erupted, transported in the atmosphere, deposited at land surface, and subject to potential redistribution by hillslope and fluvial processes. The RMEI could receive a radiation dose from exposure to the contaminated ash.

Figure ES-52 shows the expected annual dose for first 10,000 years after closure and the post-10,000-year period. The expected annual dose considers aleatory uncertainty in the numbers and times of eruptions, the number of WPs intersected by the eruption, the fraction of waste that is ejected, eruptive power, the duration of the eruption, wind direction, and wind speed. The distribution of the expected annual dose is due to epistemic uncertainty with respect to incomplete knowledge of the behavior of the repository system during and after an eruption. The mean annual dose for the first 10,000 years postclosure is less than 0.0002 millirem, and decreases to less than 0.0001 millirem for the postclosure period from 10,000 to one-million years.

Figure ES-53a shows that for the first 1,000 years postclosure, the mean annual dose is dominated by ^{241}Am . Between 1,000 and 10,000 years postclosure, the radionuclides that dominate the mean annual dose are ^{239}Pu and ^{240}Pu . Figure ES-53b shows that ^{239}Pu , ^{240}Pu , and ^{226}Ra are the dominant contributors until approximately 100,000 years after closure when ^{226}Ra and ^{229}Th , ^{126}Sn , and ^{237}Np are the primary dose contributors for the postclosure period from 100,000 to one-million years.

ES9.2.4 Seismic Scenario Class Modeling Cases

The Seismic Scenario Class represents the direct effects of vibratory ground motion and fault displacement associated with seismic activity affecting repository performance. The Seismic Scenario Class modeling cases include seismic-related changes in seepage, the performance of WPs and DSs, and flow in the EBS. The Seismic Scenario Class is represented by the Seismic GM Modeling Case and the Seismic FD Modeling Case.

ES9.2.4.1 Ground Motion Modeling Case

The Seismic GM Modeling Case considers the possible failures of DSs and WPs due to mechanical damage associated with seismic vibratory ground motion, including: accumulation of rockfall on DSs; collapse of the DS framework; SCC of WPs; and rupture or puncture of WPs. Figure ES-54 presents calculated expected annual dose histories for the Seismic GM Modeling Case for the first 10,000 years after closure and the postclosure period from 10,000 to one-million years. The distribution of the expected annual dose takes into account aleatory uncertainty associated with the number of seismic ground motion events, the time and magnitude of each event, and the effects of each event on WPs, DSs, and the emplacement drifts.

The mean, median, and 5th and 95th percentiles of the distribution of expected annual dose shown on Figure ES-54 reflect epistemic uncertainty due to incomplete knowledge of the behavior of the repository system during and after seismic events. Figure ES-54 shows that the largest mean annual dose for first 10,000 years after closure is approximately 0.2 millirem. The median annual dose for the postclosure period from 10,000 to one-million years is less than 0.5 millirem. The smoothness of the plot of the expected annual doses shown on Figure ES-54a is due to the use of a quadrature method to numerically integrate over the aleatory uncertainty for the first 10,000 years after repository closure. Alternatively, the uneven plot shown on Figure ES-54b is due to the use of a Monte Carlo method to numerically integrate over aleatory uncertainty for the postclosure period from 10,000 to one-million years, as well as the inclusion of general corrosion in the Seismic GM Modeling Case.

The results on Figure ES-55a show that ^{99}Tc , ^{14}C , ^{129}I , and ^{239}Pu dominate the estimate of the mean for the first 10,000 years after closure. Figure ES-55b shows that radionuclides ^{99}Tc and ^{129}I , with lesser contributions from ^{79}Se and ^{239}Pu and ^{226}Ra , and ^{135}Cs , dominate the calculated expected mean annual dose during most of the postclosure period from 100,000 to one-million years, with ^{242}Pu and ^{237}Np increasingly prominent after 800,000 years postclosure. The expected mean annual dose due to ^{14}C decreases completely within the first 100,000 years postclosure because of radioactive decay. The CDSP WPs would be the primary WPs damaged during the first 10,000 years after closure because the CSNF WPs are stronger and more failure-resistant. The CSNF WPs will be more robust than CDSP WPs because they include two inner stainless-steel vessels instead of one: the inner vessel and its lid similar to the CDSP WPs, and the CSNF WPs are placed in an outer, tightly fitting stainless-steel transportation, aging, and disposal (TAD) canister. The stainless steel, waste-containing canisters in the CDSP WPs do not fit as tightly and could move more freely under the influence of ground motion. The predominant mechanism that would cause damage to CDSP and CSNF WPs is SCC resulting in diffusive releases of radionuclides.

ES9.2.4.2 Fault Displacement Modeling Case

The Seismic FD Modeling Case includes disruption of WPs and DSs by the displacement of faults. Figure ES-56 shows the expected annual dose histories for the Seismic FD Modeling Case for the first 10,000 years after closure and for the postclosure period from 100,000 to one-million years. The expected annual dose accounts for aleatory uncertainty about the number, type, and locations of disrupted DSs and WPs. The mean, median, and 5th and 95th percentile curves on Figure ES-56 show uncertainty in the distribution of expected annual dose, due to epistemic uncertainty regarding the behavior of the repository system during and after fault displacement events. These figures show that the mean annual dose for the first 10,000 years after closure is less than 0.002 millirem, and less than 0.02 millirem for the postclosure period from 10,000 to one-million years. The median projected dose for the postclosure period from 10,000 to one-million years is approximately 0.01 millirem.

Figure ES-57a shows that ^{99}Tc , ^{239}Pu , and ^{129}I dominate the estimate of the mean annual dose for the first 10,000 years after closure. Figure ES-57b shows that ^{239}Pu dominates the mean annual dose up to 100,000 years postclosure, and ^{242}Pu , ^{226}Ra , and ^{237}Np dominate the mean for the remainder of the postclosure period from 100,000 to one-million years.

ES9.2.5 Total Mean Annual Dose to the Reasonably Maximally Exposed Individual for the Repository System

Figure ES-58 shows the contribution to the total mean annual dose histories for the Drip Shield EF, Waste Package EF, Igneous Intrusion, Volcanic Eruption, Seismic GM, and Seismic FD Modeling Cases. Figure ES-58 shows that the Seismic GM and Igneous Intrusion Modeling Cases provide the largest contributions to the total mean annual dose for the postclosure period from 10,000 to one-million years. The Seismic GM Modeling Case includes general corrosion processes for the postclosure period from 10,000 to one-million years. Figure ES-58 shows that the events that most affect repository performance are seismic ground motion, igneous intrusions, and WP failure due to general corrosion.

ES9.3 Comparison of Annual Dose with Postclosure Individual and Groundwater Protection Standards

ES9.3.1 Individual Protection Standard

The results provided by the TSPA-LA Model include calculations of the total mean annual dose to the RMEI in any year during the next 10,000 years after repository closure (NRC Proposed Rule 10 CFR 63.303(a)) and the total median annual dose to the RMEI in any year from 10,000 years after repository closure through the period of geologic stability (NRC Proposed Rule 10 CFR 63.303(b)). Per NRC Proposed Rule 10 CFR 63.311 [DIRS 178394] the postclosure individual protection standard is 15 millirem up to 10,000 years postclosure and 350 millirem after 10,000 years, but within the period of geologic stability (one million years). The TSPA-LA Model results, shown on Figure ES-40 and ES-41, which refer to distribution of total expected annual dose, show that the highest projected total mean and total median annual doses to the RMEI are estimated to be about 0.23 millirem (Figure ES-40) and 0.99 millirem (Figure ES-41), respectively. These results demonstrate that the total mean annual dose to the RMEI in any year during the next 10,000 years after repository closure is less than the individual protection standard of 15 millirem per NRC Proposed Rule 10 CFR 63.311(a)(1) [DIRS 178394]. In addition, the highest projected dose values, mean or median, throughout the period of geologic stability are more than two orders of magnitude below the individual protection limit of 350 millirem per 10 CFR 63.311(a)(2) [DIRS 178394].

Uncertainty/Sensitivity Results

For different time frames in the analysis, different epistemic parameters emerge as important to the overall uncertainty in the results. Table ES-1 lists summary results of the sensitivity analysis. The important parameters listed on Table ES-1 are as follows:

- *IGRATE*. This parameter is the probability of an igneous event, expressed as the annual frequency of an intersection of the repository by a volcanic dike. Uncertainty in this parameter arises from epistemic uncertainty about igneous activity that may affect the repository.
- *SCCTHRP*. This parameter is the residual stress threshold for the Alloy-22 WP outer barrier, expressed as a percentage of the yield strength. If the residual stress in the WP

outer barrier exceeded this threshold value, stress corrosion cracks could form, which could allow radionuclides to migrate from the WP. The primary causes of residual stresses in the WP outer barrier would be high-peak ground velocity seismic ground motions, which may cause impacts from WP to WP, from WP to emplacement pallet, and from WP to DS. These impacts could cause dynamic loads that could dent the WP, resulting in structural deformation with residual stresses that could make the material susceptible to SCC.

- *WDGCA22*. This parameter relates to the temperature dependence of the Alloy 22 WP outer barrier general corrosion rate. This uncertainty parameter determines the magnitude of this temperature dependence and directly influences the short-term and long-term general corrosion rates of the Alloy 22. Larger values of *WDGCA22* result in earlier, higher general corrosion rates during the thermal period, and lower long-term corrosion rates when the repository temperatures are near the ambient in-situ temperature.

The parameters in Table ES-1 that most affect the total uncertainty in the TSPA-LA Model are factors that govern degradation of the WPs, the occurrence of damage from seismic events, and the frequency with which igneous intrusions occur.

Table ES-1. Top-Ranking Uncertainty Importance Parameters

Time After Closure (years)	Two Most Important Parameters	
3,000	SCCTHRP	IGRATE
5,000	SCCTHRP	IGRATE
10,000	SCCTHRP	IGRATE
125,000	IGRATE	SCCTHRP
250,000	WDGCA22	IGRATE
500,000	IGRATE	WDGCA22
1,000,000	IGRATE	WDGCA22

Source: Output DTN: MO0709TSPAPLOT.000_R0 [DIRS 183010].

ES9.3.2 Groundwater Protection Standard

The groundwater protection standard in NRC Proposed Rule 10 CFR 63.331 [DIRS 180319] stipulates that the releases of radionuclides in groundwater at the location of the RMEI should not cause the level of radioactivity in the representative water volume of 3,000 acre-feet of water (10 CFR 63.332(a)(3) [DIRS 180319]) to exceed the groundwater protection standard. The regulation does not require that evaluation of the groundwater protection standard include very unlikely events. Therefore, igneous and seismic events are not included in applying this standard.

Figure ES-59 shows the estimates of groundwater protection performance measures taken from the simulation for the Early Failure Modeling Cases and the Seismic GM Modeling Case. The first groundwater protection performance measure is the annual maximum concentration of ^{226}Ra and ^{228}Ra in the representative volume of 3,000 acre-ft of water. The second groundwater protection performance measure is gross alpha activity (excluding radon and uranium) in that volume (Figure ES-60). The third is the dose from beta- and photon-emitting radionuclides in

the groundwater, expressed in terms of annual dose to the whole body or any organ of a human receptor resulting from drinking two liters of this water per day (Figure ES-61). The TSPA-LA Model results show that releases from the repository will meet the groundwater protection standard.

ES9.4. Human Intrusion

The TSPA-LA Model was used to simulate a Human Intrusion Scenario in order to address the second requirement of the human intrusion standard (10 CFR 63.321(b) [DIRS 178394]). To calculate dose for all environmental pathways per 10 CFR 63.321(c) [DIRS 178394], the TSPA-LA Model used a probabilistic approach analogous to that used to evaluate conformance with the individual protection and groundwater protection standards.

The estimates of WP degradation suggest that, using current technology, a degraded WP could not be penetrated by drilling before about 200,000 years postclosure. Consequently, the analysis considered the effects of a drilling intrusion at 200,000 years. Figure ES-62 shows the expected annual dose that could result from a drilling intrusion 200,000 years after repository closure. The expected annual dose accounts for aleatory uncertainty about the type of WP intersected by the drill and location of the intersected WP. The mean, median, and 5th and 95th percentiles of the distribution of expected annual dose reflect epistemic uncertainty due to incomplete knowledge of the behavior of the physical system during and after the drilling intrusion.

The values on Figure ES-62 represent the dose from a single WP and are not combinations of releases from other WPs that may fail due to other processes. The mean and median annual doses from human intrusion are estimated to be less than 0.01 millirem. These results indicate that releases from a human intrusion would result in doses well below the human-intrusion individual protection standard of 350 millirem annual individual dose to the RMEI during the postclosure period from 10,000 to one million years.

ES10. SUMMARY OF THE RESULTS OF THE TSPA-LA MODEL

The TSPA-LA Model was applied to the assessment of total system performance of the Yucca Mountain repository based on FEPs that could affect total system performance. The TSPA-LA analyses incorporate uncertainty in input data and submodel performance and use the validated TSPA-LA Model.

The TSPA-LA Model simulation/analysis periods cover 10,000 years after repository closure and the 1,000,000-year period of geologic stability. The 10,000-year simulations were extended an additional 10,000 years to assess whether or not the trends present at the end of 10,000 years continue. The results of the analyses showed that the period between 10,000 years to 20,000 years after repository closure did not display any significant changes to the trends observed from 0 to 10,000 years, providing confidence in the conclusions reached regarding the 10,000-year period.

The TSPA-LA Model results demonstrate that the projected highest mean dose to the RMEI in any year during the next 10,000 years after repository closure is less than the individual protection standard in NRC Proposed Rule 10 CFR 63.311(a)(1) [DIRS 178394], which describes the limits on radionuclides in the representative volume. The TSPA-LA Model

analyses also indicate the performance of the repository system provides significant protection to groundwater. The results show concentrations in the groundwater are likely to be well below the groundwater protection standard in NRC Proposed Rule 10 CFR 63.331 [DIRS 180319] and its Table 1. Likewise, the results suggest the mean annual drinking water dose to any organ and to the whole body from beta- and photon-emitting radionuclides is likely to be well below the applicable standards in the proposed rule.

The physiographic setting, topography, climate, area geology, and soil characteristics at the site of the Yucca Mountain repository are favorable for restricting the amount of infiltration of precipitation into the subsurface. The reduced infiltration along with rock characteristics, ambient and perturbed subsurface environmental conditions, and the geometry of emplacement drifts will further limit the amount of liquid water available to enter the drifts. Features of the waste form and other components of the EBS, together with limitations due to the solubility of radionuclides and the subsurface geology and hydrology, will limit the release, rate of release, and transport of radionuclides to the SZ beneath the repository. Only a small fraction of the radionuclide inventory is projected to be released from the EBS, move down through the UZ beneath the repository, and enter the SZ. Sorption and diffusion of radionuclides into the UZ will further reduce the concentrations of radionuclides entering the SZ. After the migrating radionuclides enter the SZ, the TSPA-LA Model results indicate that the characteristics of the rock, soil, and the hydrologic and geochemical environmental factors in the SZ will combine to retard radionuclide transport and reduce the rate of radionuclide transport to the accessible environment. Including the disruptive events such as igneous and seismic phenomena, the TSPA-LA Model analysis indicates that the repository will, with a high degree of confidence, perform in a manner that protects the natural environment and future human populations in the area.

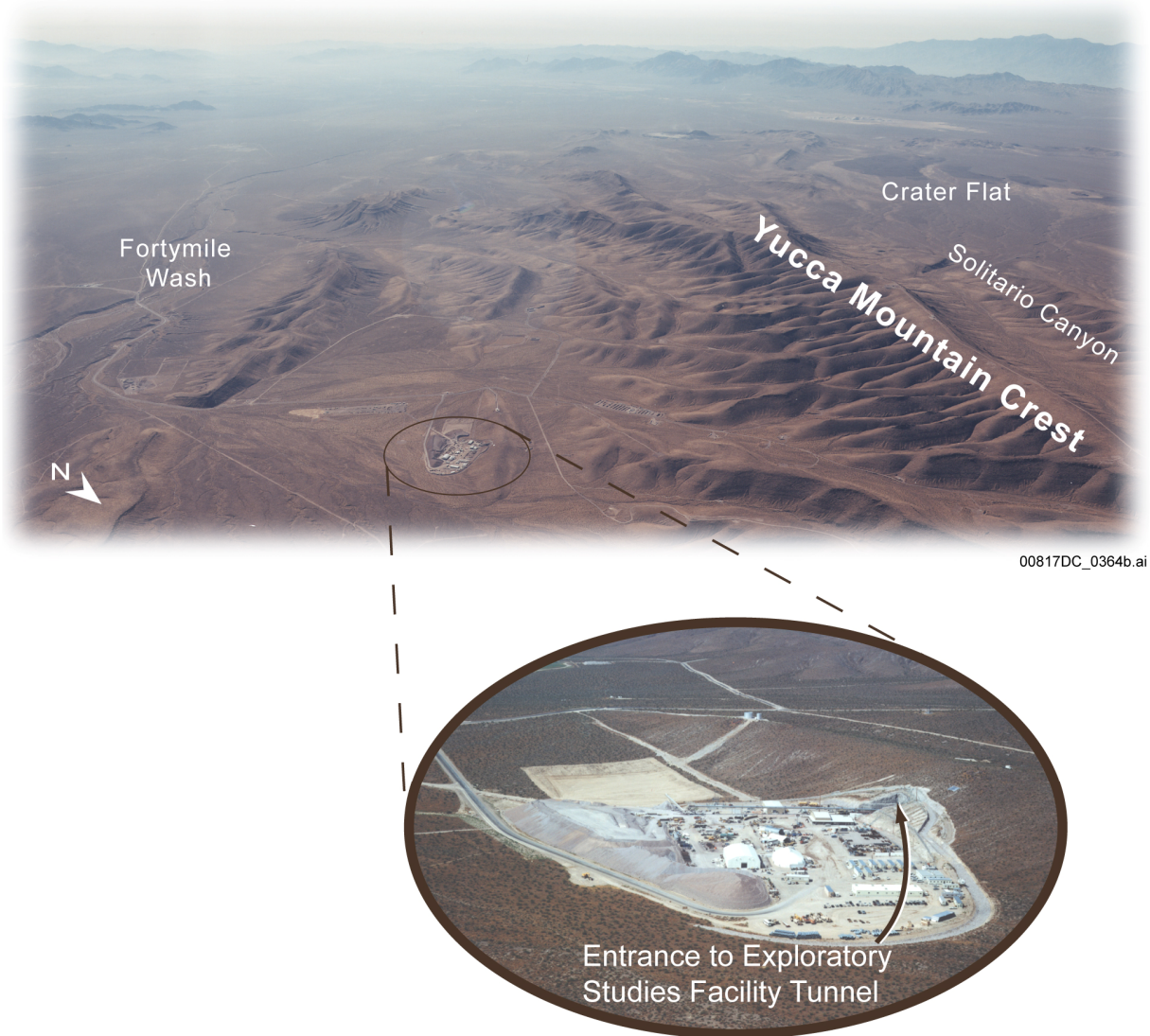
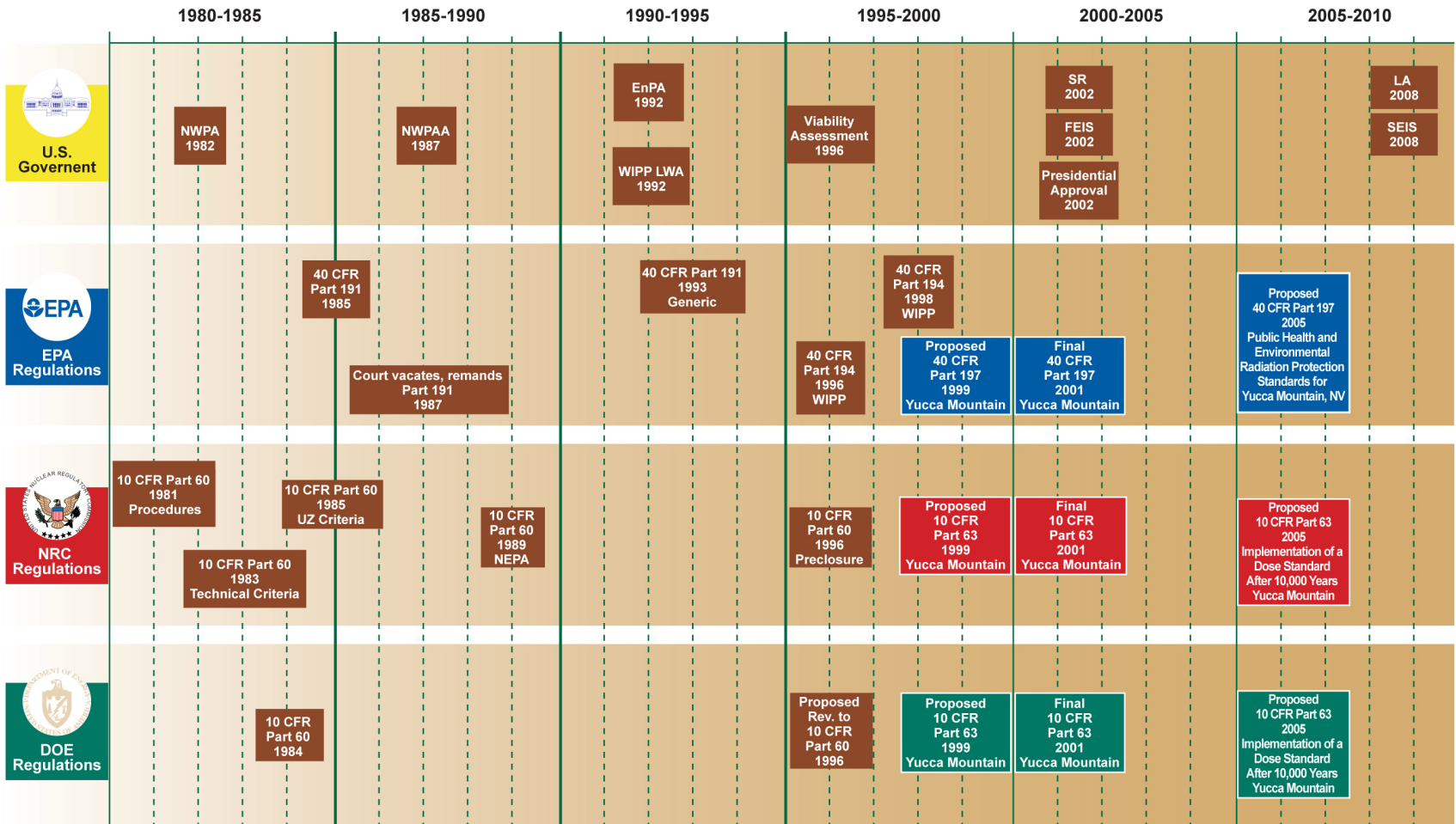
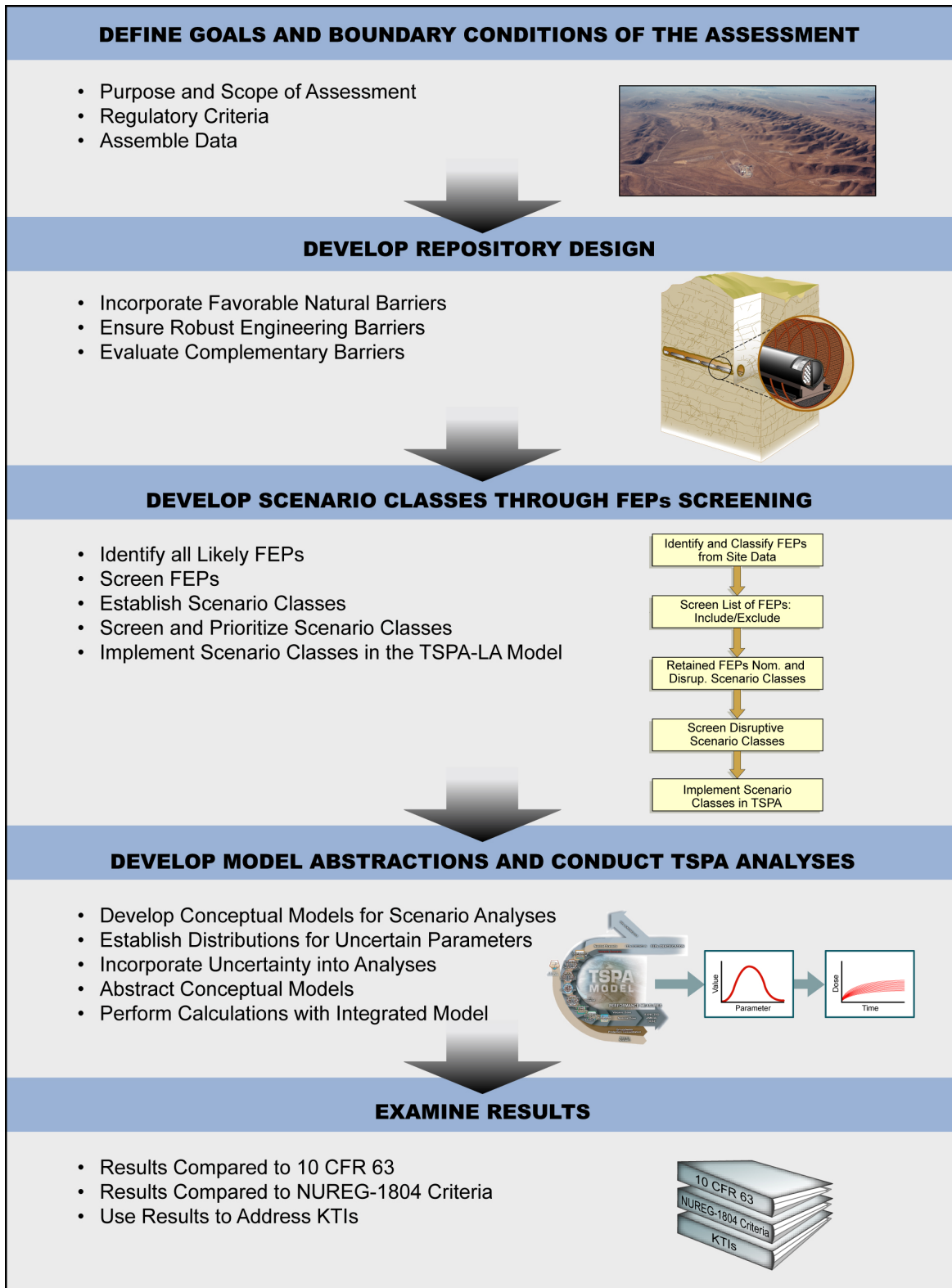


Figure ES-1. Yucca Mountain Area



00817DC_0365b.ai

Figure ES-2. Timeline of Legislative and Regulatory Events: 1980 to 2010



00817DC_0366.ai

Figure ES-3. Structure of the Process of the TSPA-LA

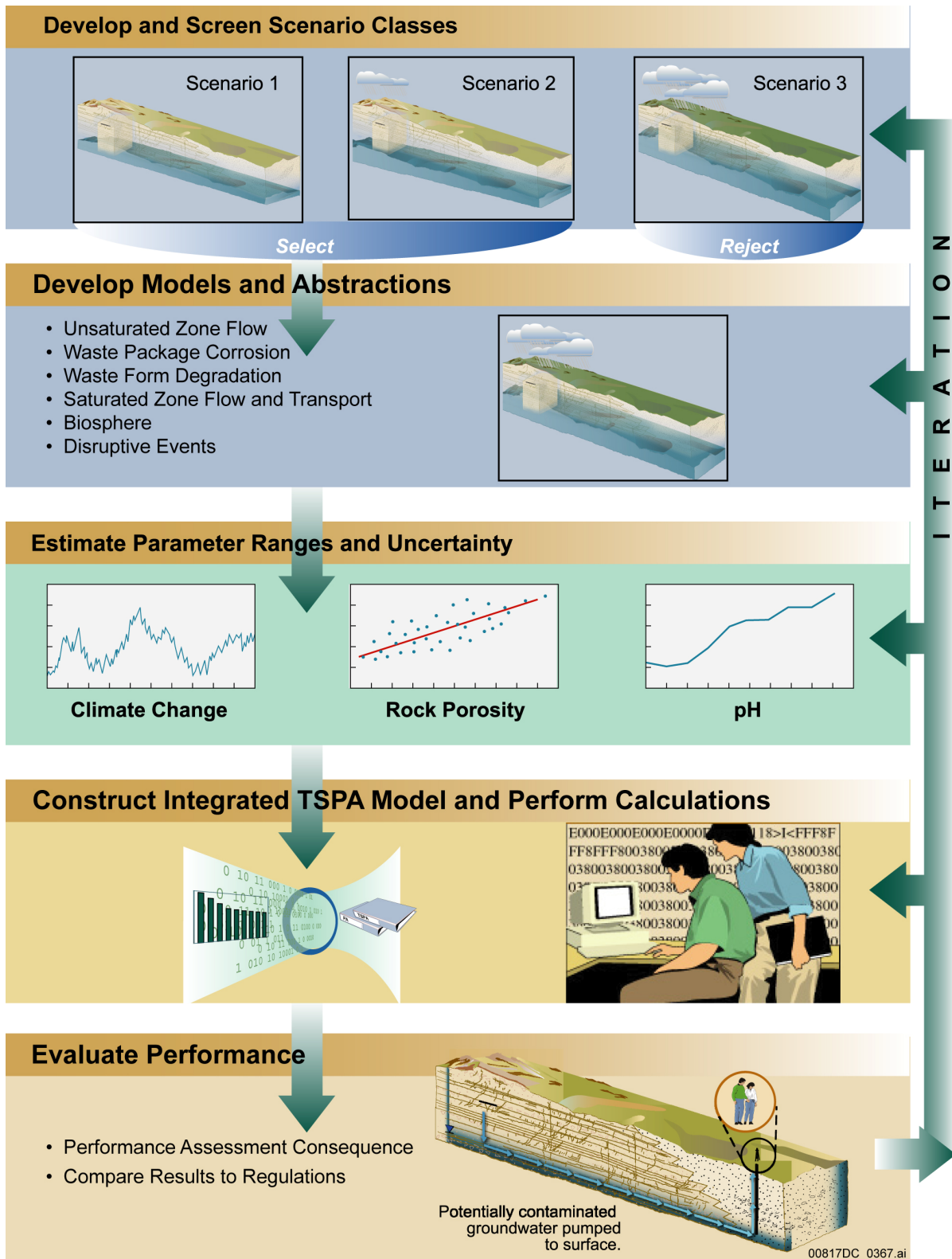
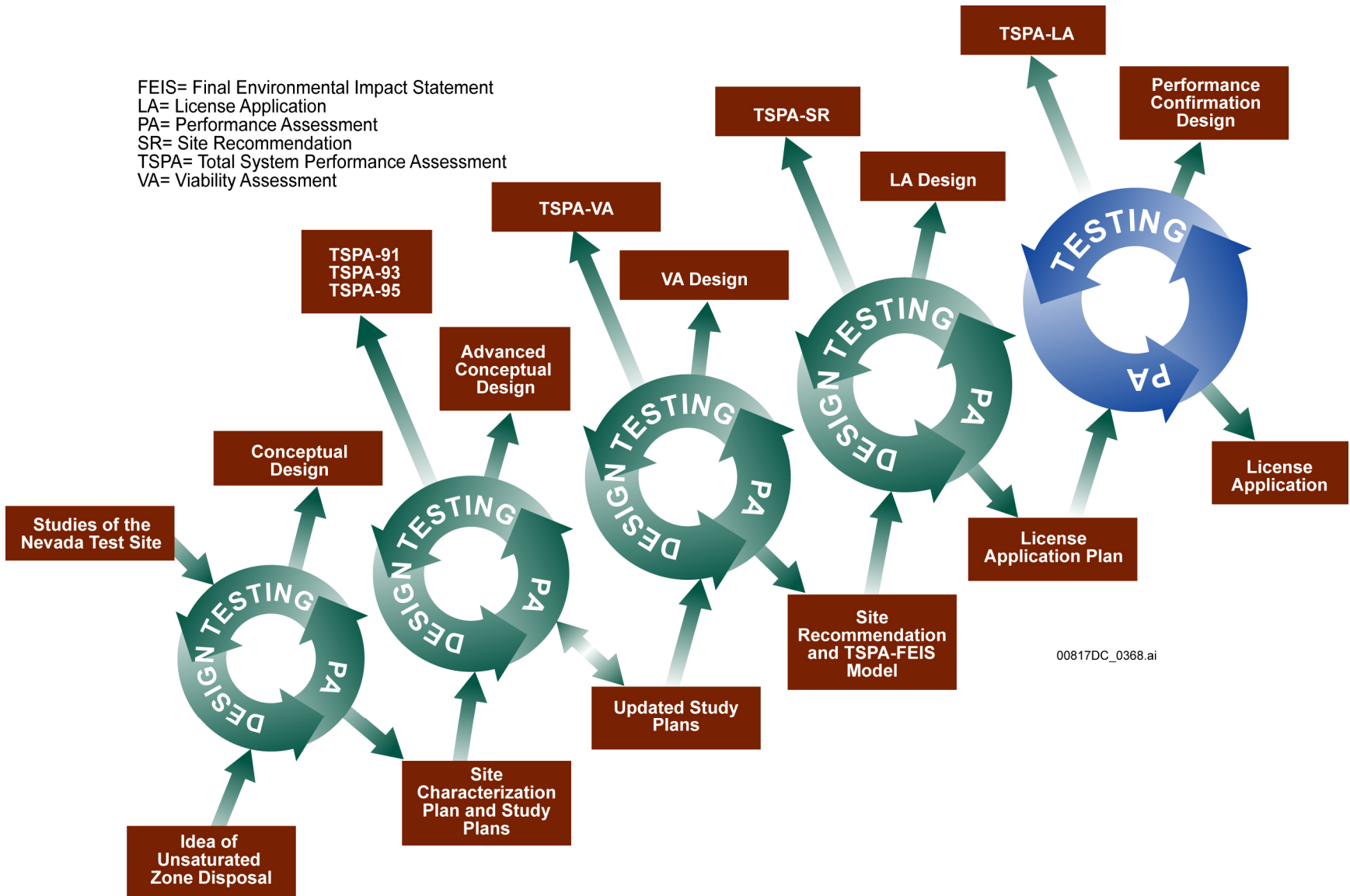


Figure ES-4. Major Steps in a Generic Performance Assessment



00817DC_0368.ai

Figure ES-5. Iterative Application of the TSPA Process

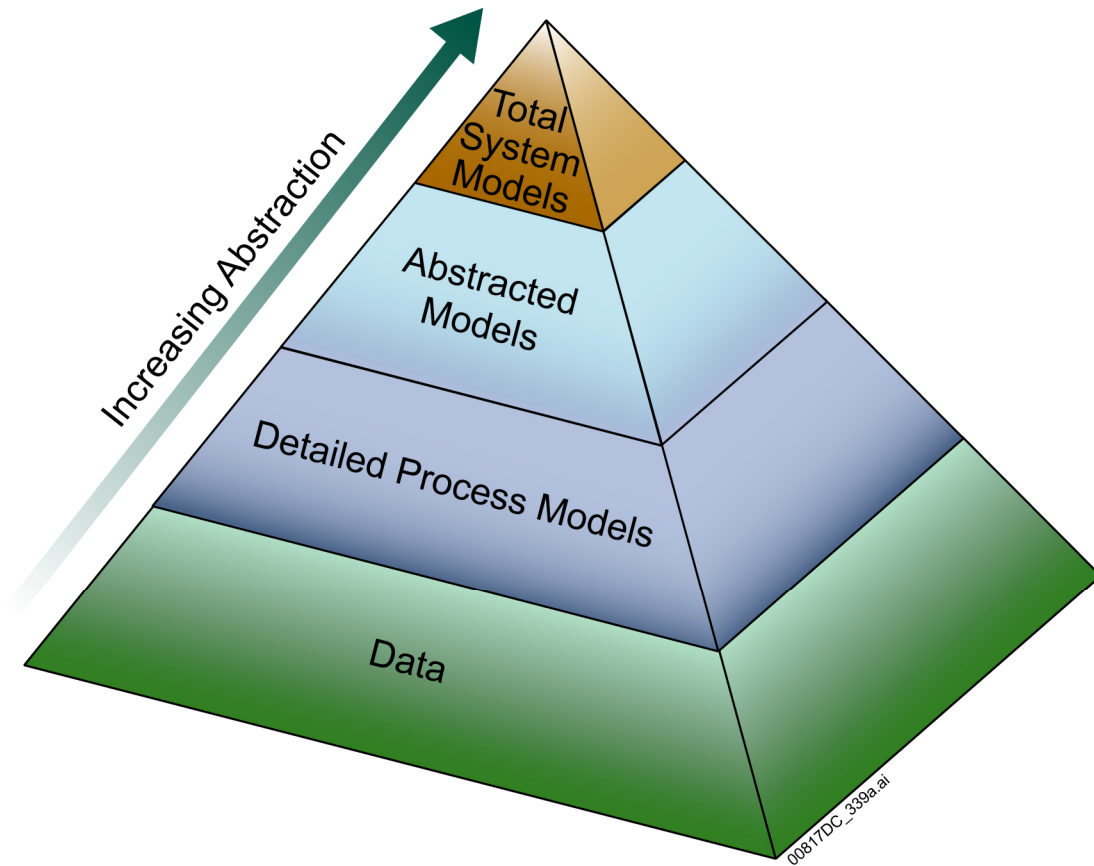


Figure ES-6. Performance Assessment Pyramid Showing the Steps Involved in Developing a Total System Model

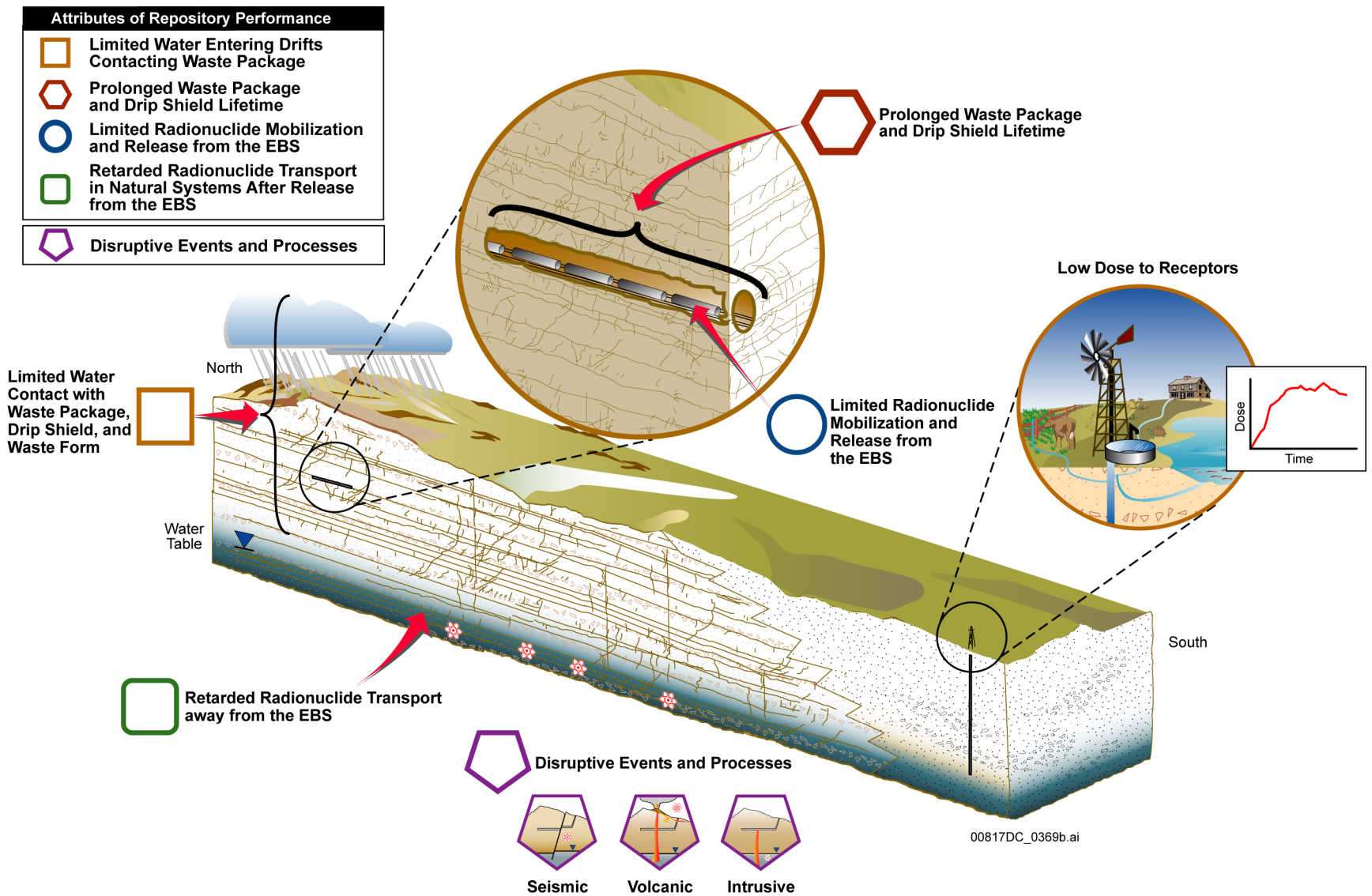


Figure ES-7. Schematic of Attributes of Repository Performance

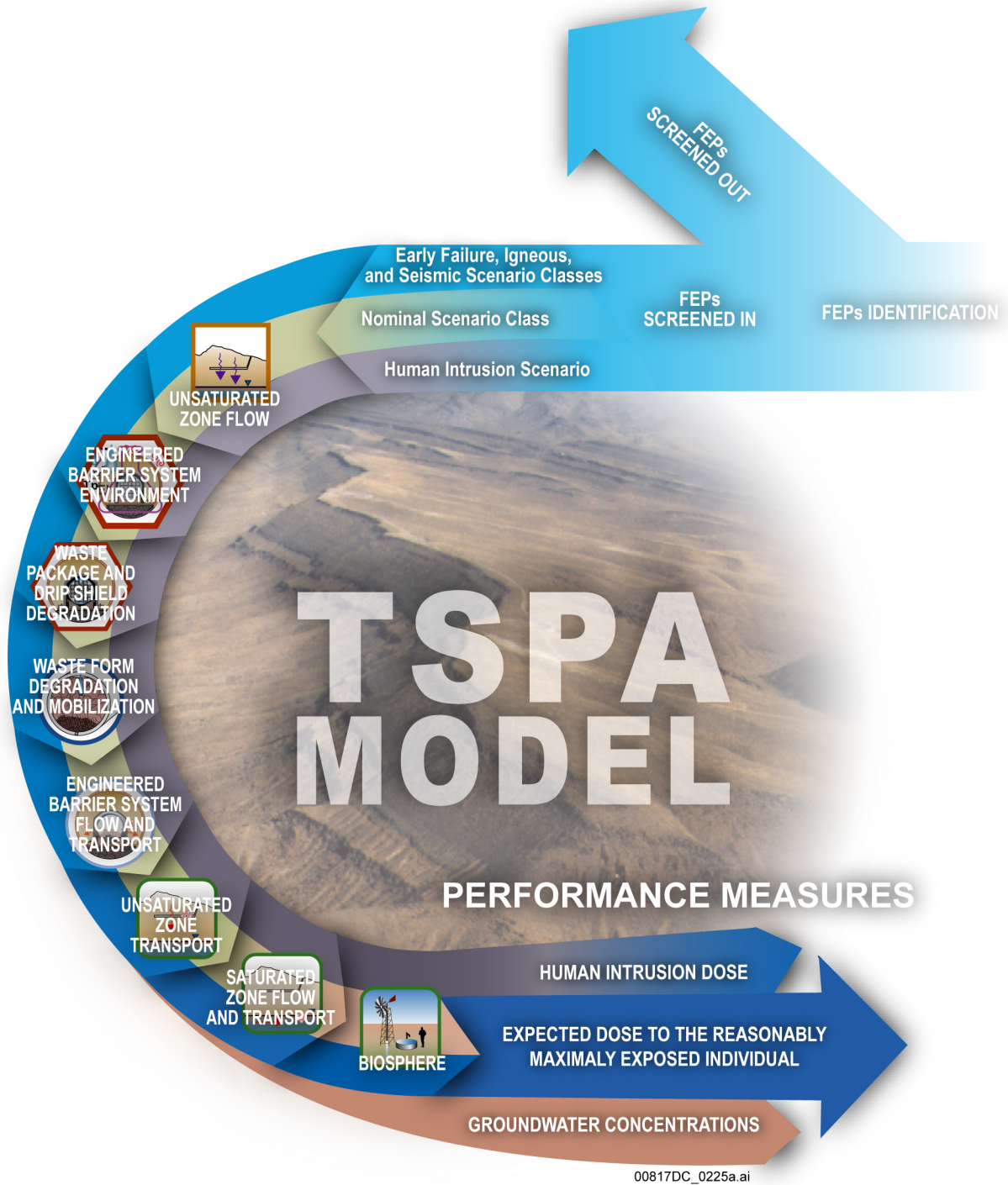
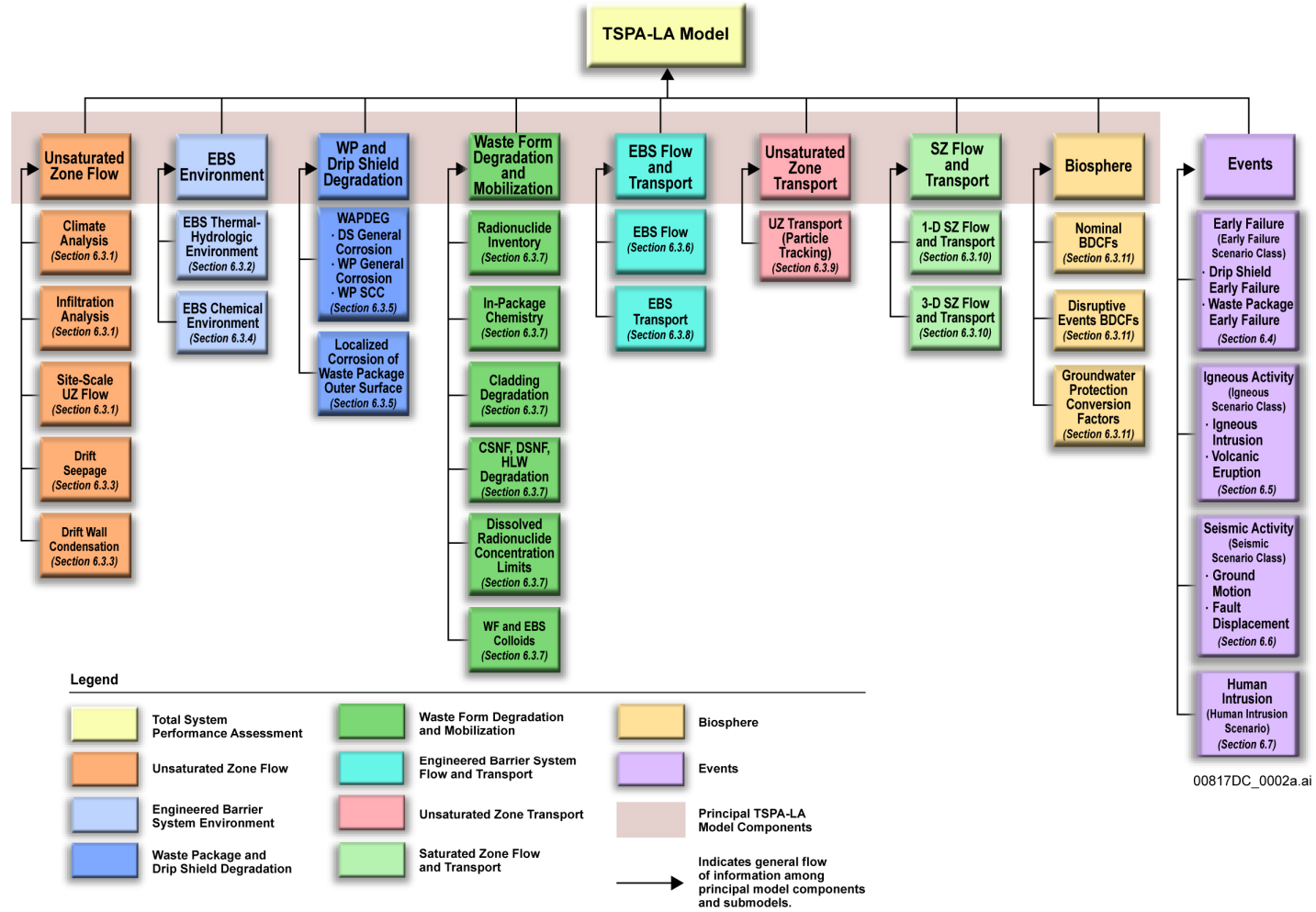


Figure ES-8. Schematic Representation of the Development of the TSPA-LA Model, Including the Nominal, Igneous, and Seismic Scenario Classes



00817DC_0002a.ai

Figure ES-9. TSPA-LA Principal Model Components and Submodels

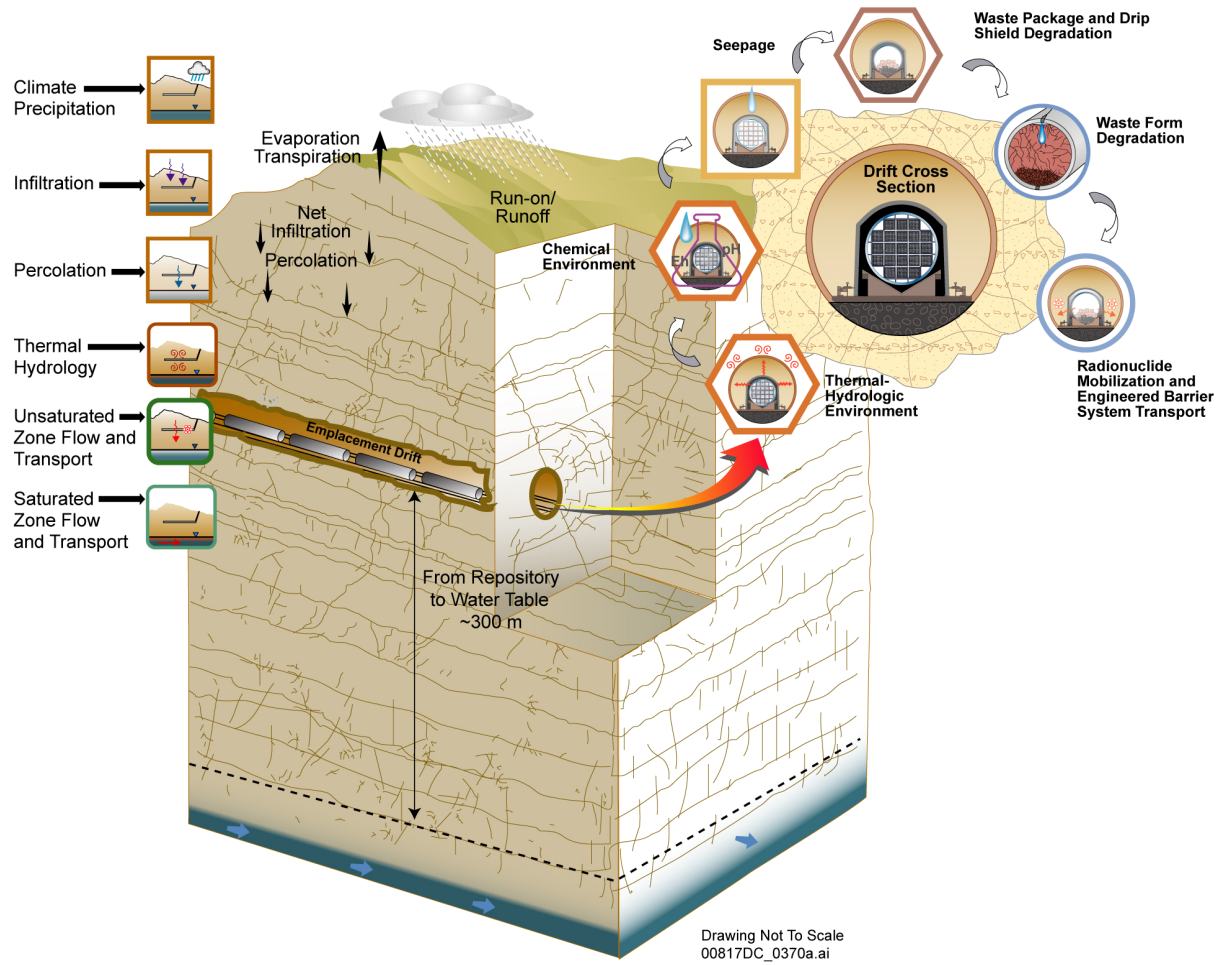
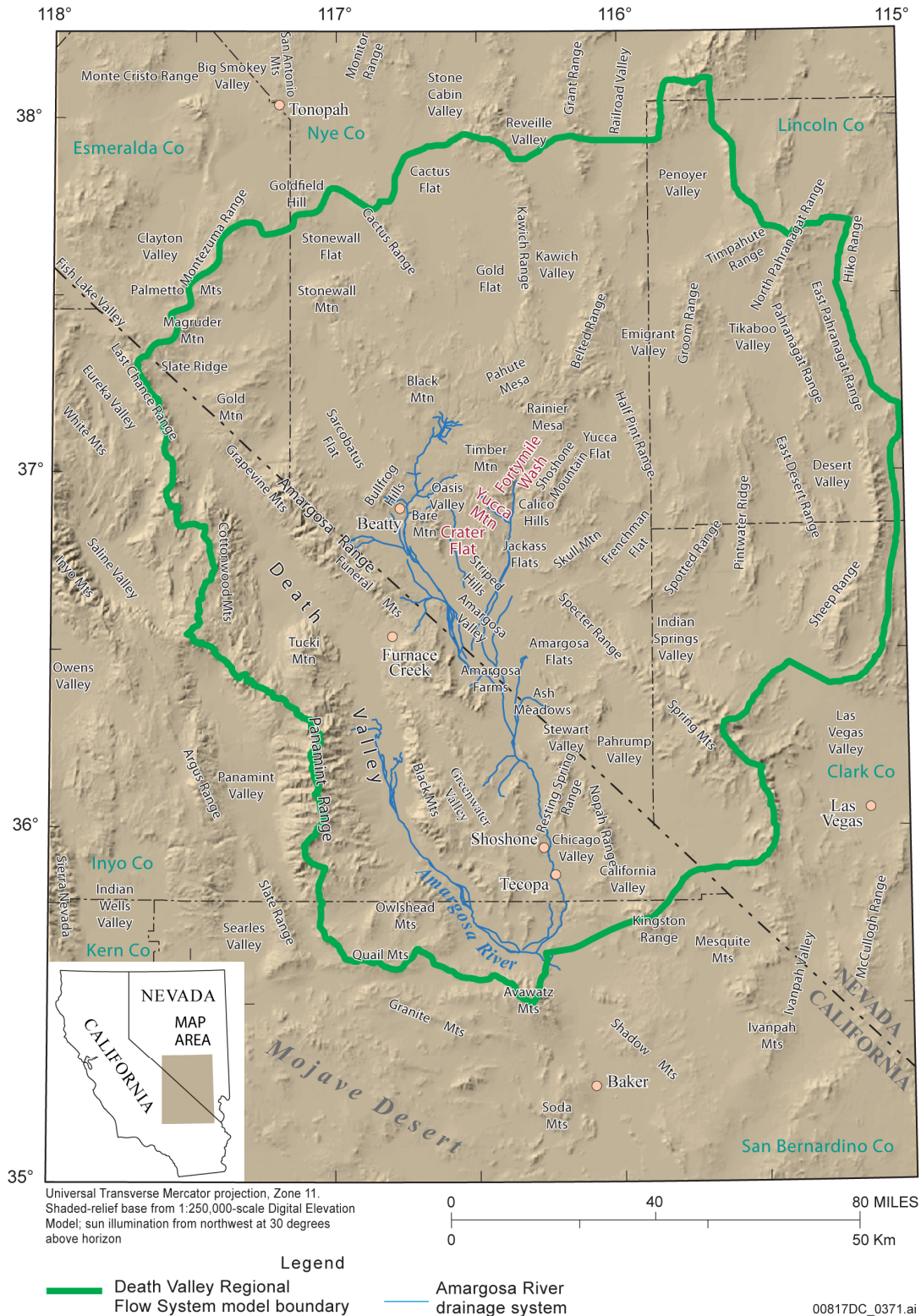
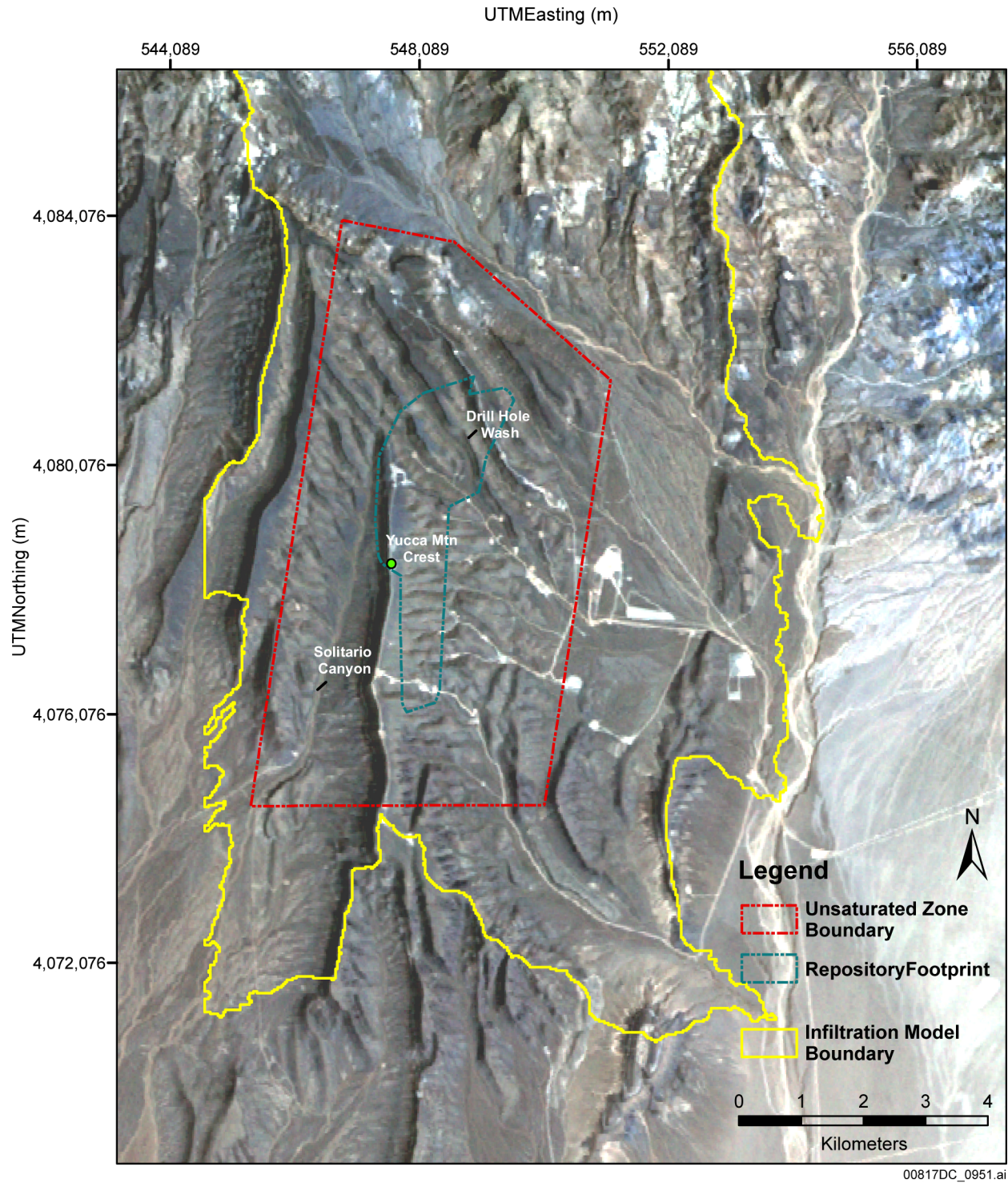


Figure ES-10. Principal Components of the Yucca Mountain Repository System



Source: Modified from BSC 2004 [DIRS 169734], Figure 8-2.

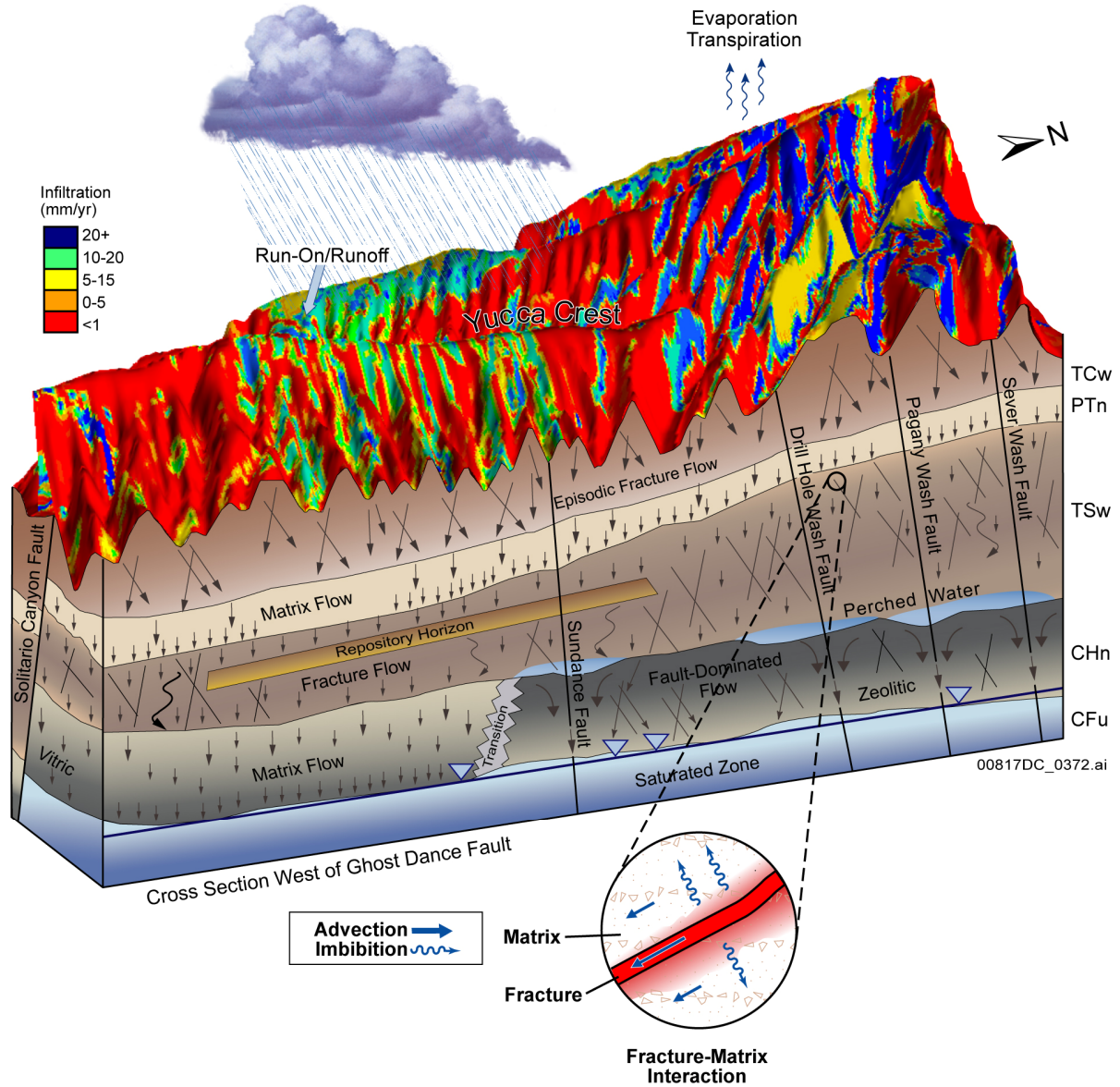
Figure ES-11. Geographic and Prominent Topographic Features of the Death Valley Region



Source: Modified from SNL 2007 [DIRS 182145], Figure 6.5.2.1-1[a].

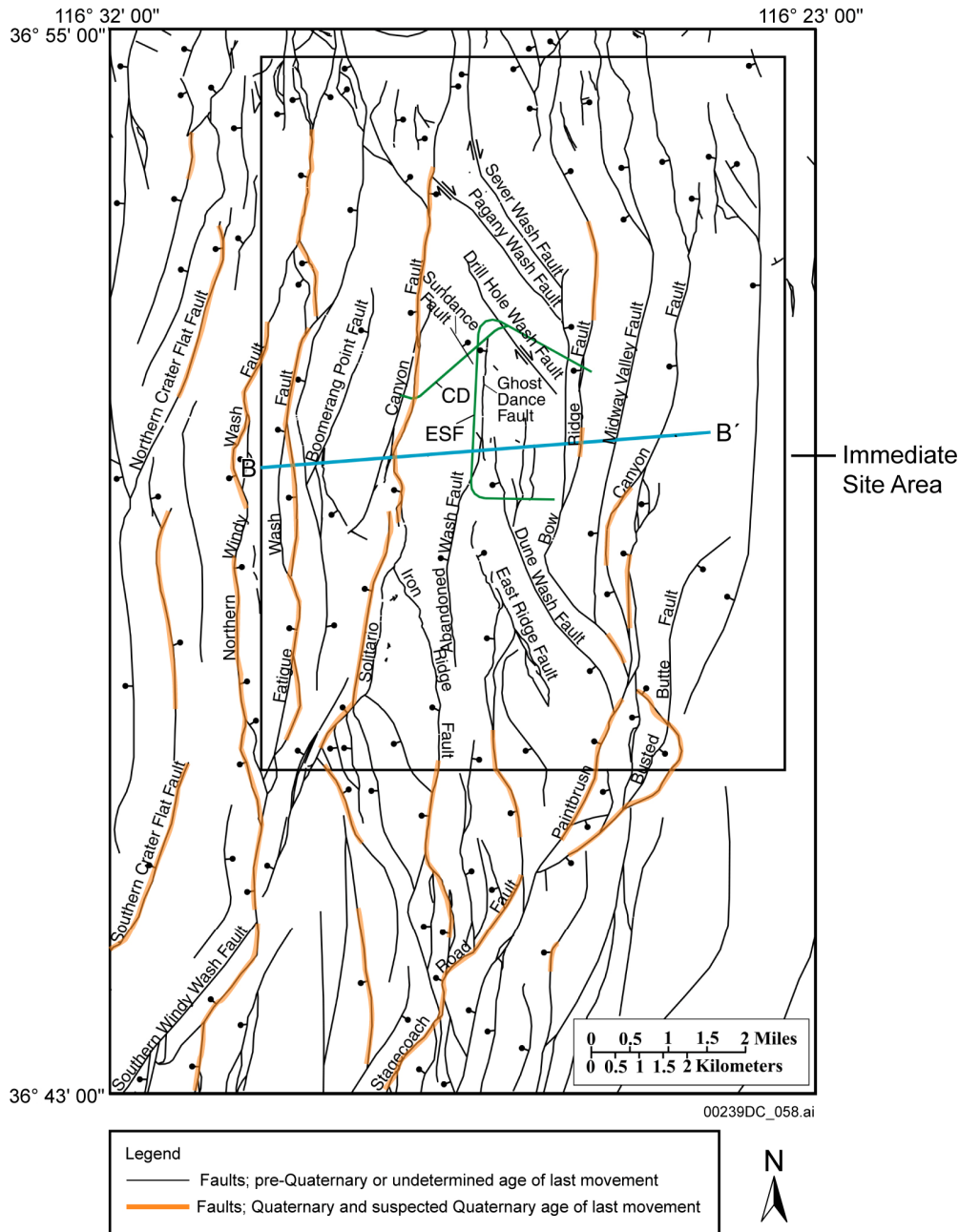
NOTE: The model boundary is the same as the 1999 unsaturated zone flow model domain of the TSPA-SR.

Figure ES-12. Topographic Map of the Yucca Mountain Site Showing in Slope Characteristics



Source: Modified from BSC 2004 [DIRS 170035], Figure 6-1.

Figure ES-13. Overall Water Flow Behavior in the Unsaturated Zone, Including the Relative Flux Magnitudes of Fracture and Matrix Flow Components in the Different Hydrogeologic Units

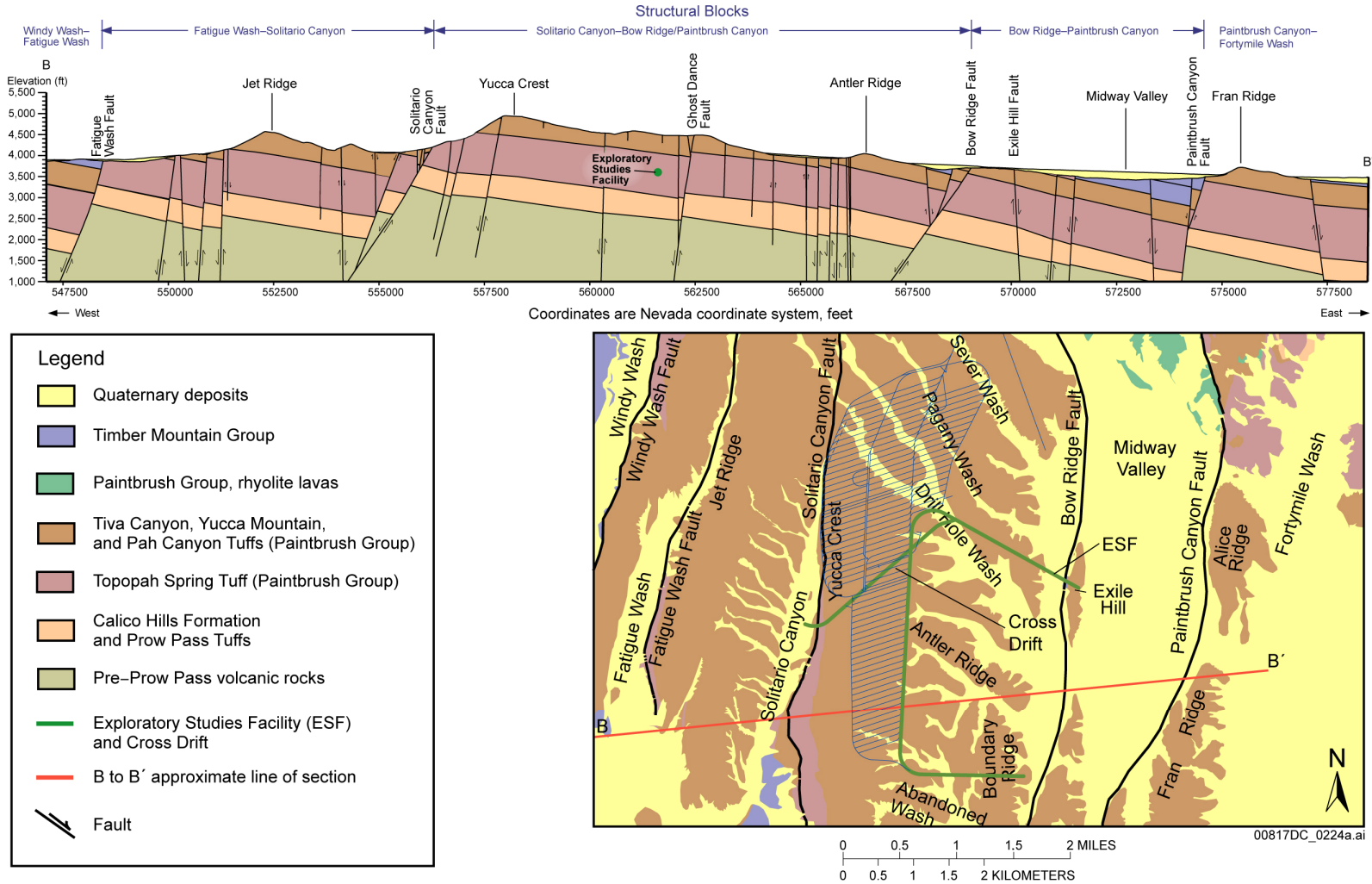


Source: Modified from BSC 2004 [DIRS 169734], Figure 3-20.

NOTES: The following faults have demonstrable Quaternary activity: Northern Crater Flat, Southern Crater Flat, Northern Windy Wash, Southern Windy Wash, Fatigue Wash, Solitario Canyon, Iron Ridge, Bow Ridge, Paintbrush Canyon, and Stagecoach Road. All faults are shown with solid lines, although many segments are concealed or inferred.

Symbols and acronyms: bar and bell: downthrown side of fault; arrows: relative direction of strike-slip movement; ESF = Exploratory Studies Facility (green line); CD = Cross-Drift; blue line: approximate location of section on Figure ES-15.

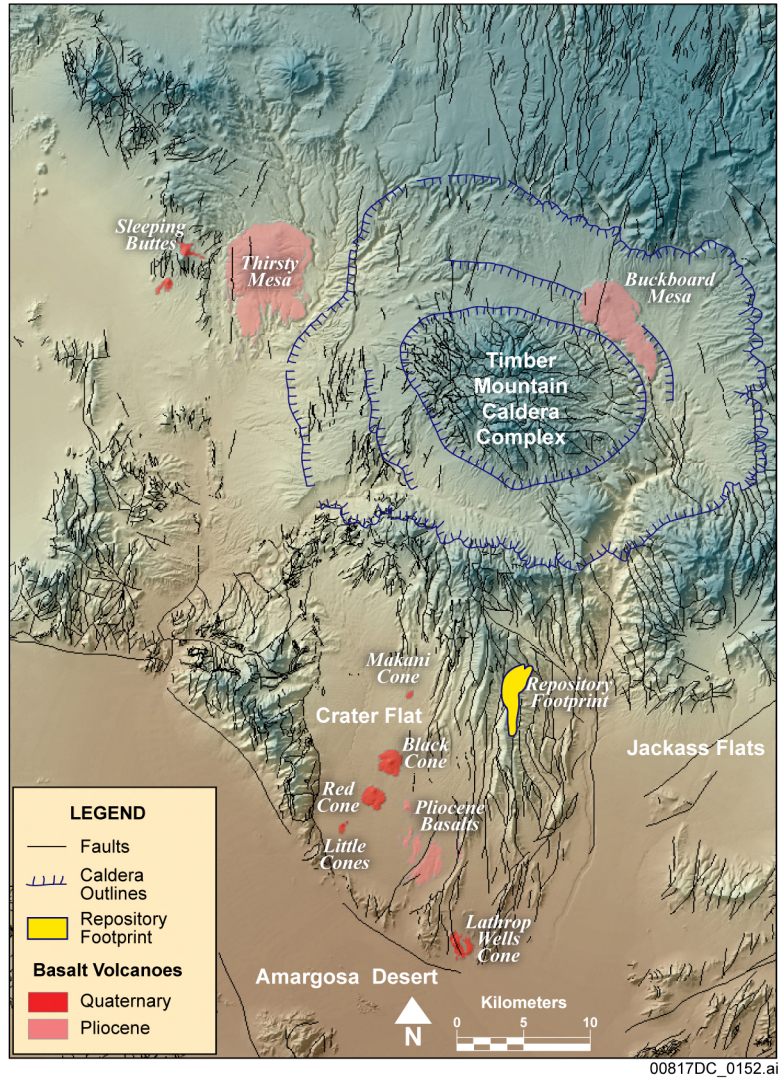
Figure ES-14. Distribution of Faults in the Yucca Mountain Site Area and Adjacent Areas to the South and West



Source: Simplified from Day et al. 1998 [DIRS 100027], Cross Section B-B'.

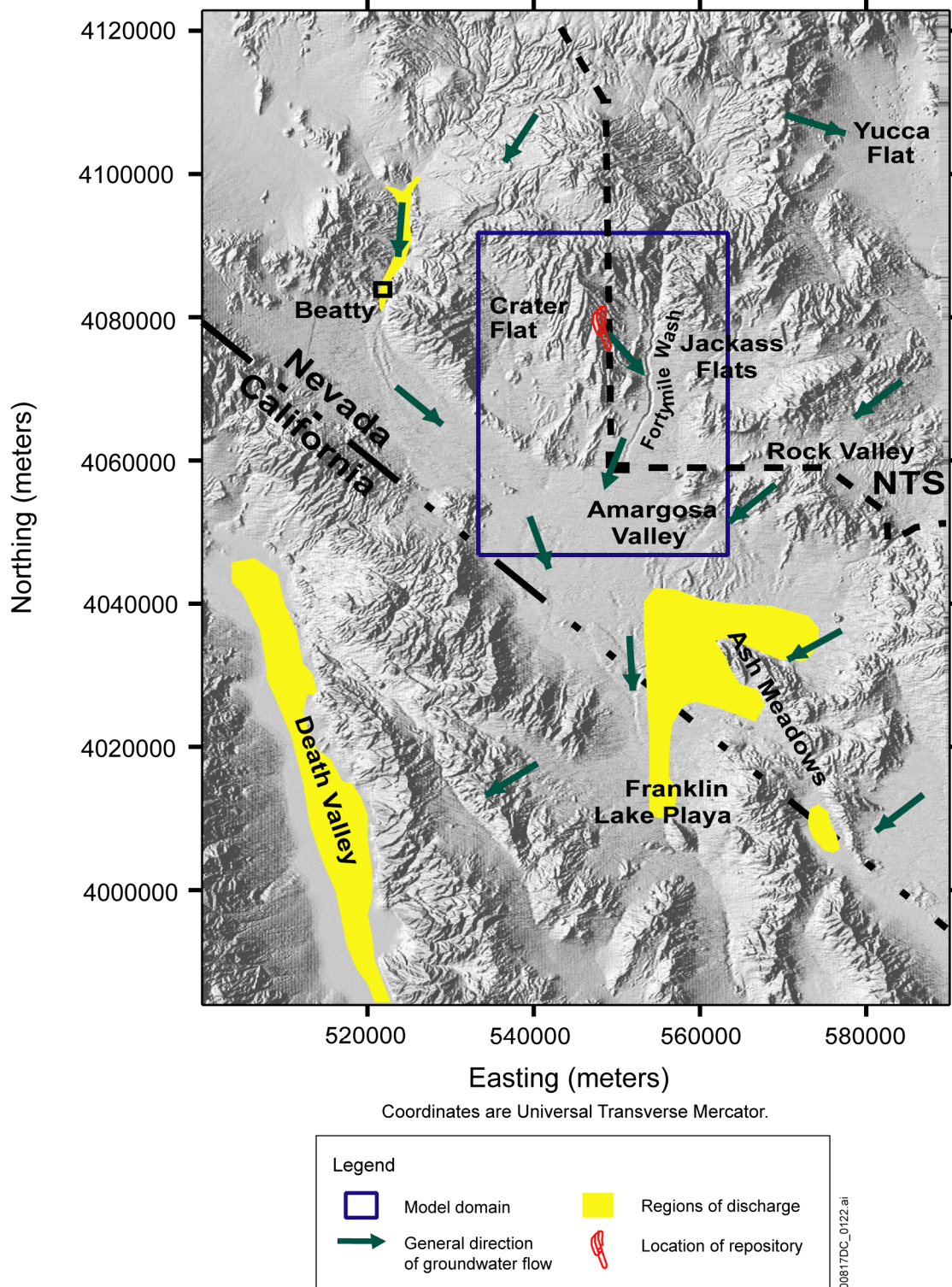
NOTE: ESF = Exploratory Studies Facility, location of intersection along the approximate line of section, also shown on Figure ES-14.

Figure ES-15. East-West Structure Section across Yucca Mountain Site Area



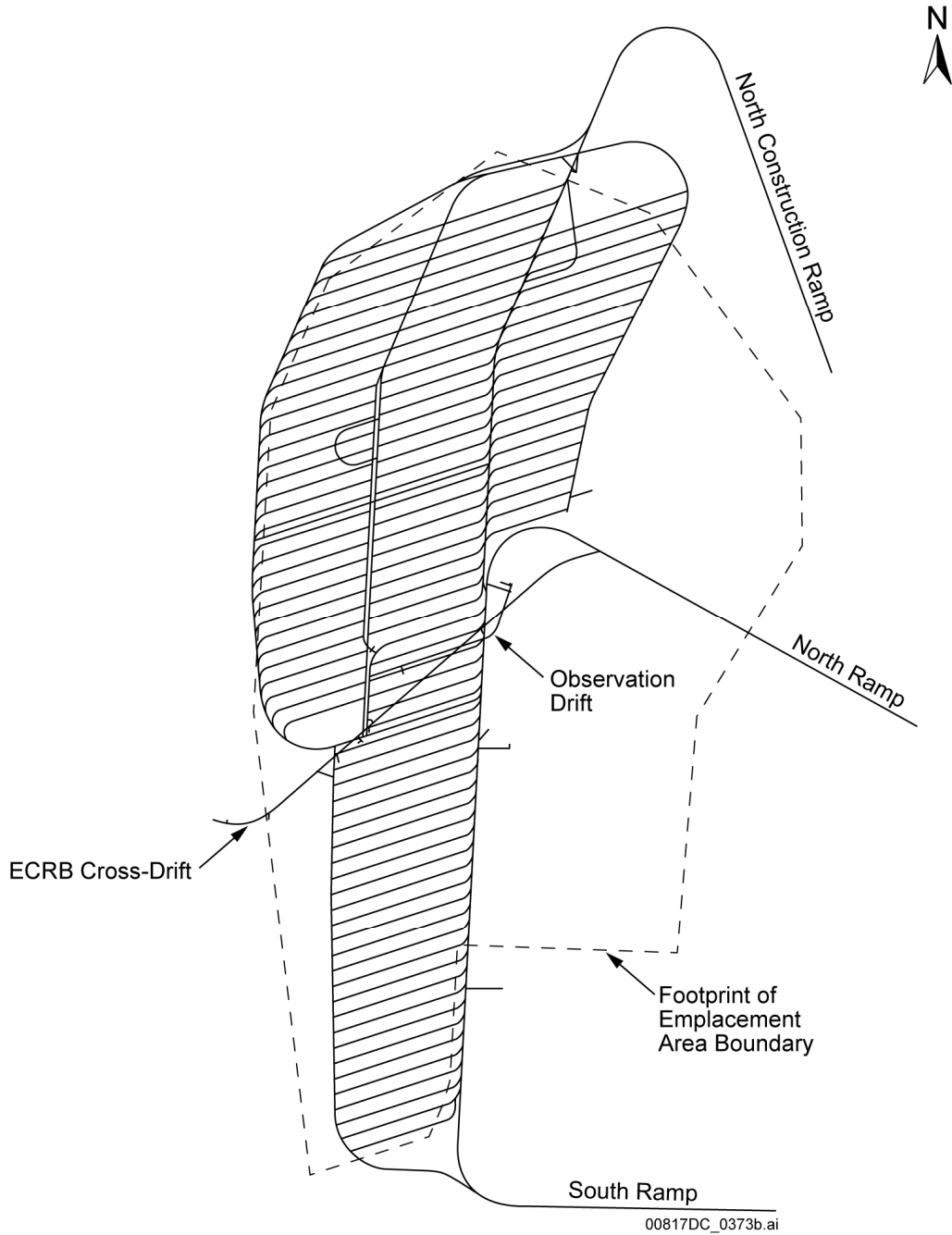
Source: Modified from CRWMS M&O 1998 [DIRS 123196], Figure 2.1.

Figure ES-16. Location and Age of Post-Miocene (less than 5.3 million years) Volcanoes (or clusters where multiple volcanoes have indistinguishable ages) in the Yucca Mountain Region



Source: Compiled from BSC 2004 [DIRS 169734], Figures 8-2, 8-5, and 8-6.

Figure ES-17. Regional Map of the Saturated Zone Flow System Showing Direction of Flow and Outline of the 3-D Saturated Zone Site-Scale Flow Model Domain



Source: Modified from SNL 2007 [DIRS 179466], Table 4-1, Parameter 01-02.

Figure ES-18. Subsurface Facility Layout